CYTOTROPHOBLAST REGULATES LIPID ESTERIFICATION AND METABOLIC ACTIVITY OF THE HUMAN TERM PLACENTA

By

Kevin S. Kolahi

A THESIS/DISSERTATION

Presented to the Department of Biomedical Engineering

and the Oregon Health & Science University

School of Medicine

in partial fulfillment of

the requirements for the degree of

Doctor of Philosophy

August 2016

Table of Contents

List of Figures

List of Tables

List of Abbreviations

AA	Arachidonic Acid
ACSL	Long Chain Acyl-CoA Synthetase
ATP	Adenosine Triphosphate
BHCG	Human Chorionic Gonadotropin- Beta subunit
BMI	Body Mass Index
BODIPY	4,4-Difluoro-5,7-Dimethyl-4-Bora-3a,4a-Diaza-s-Indacene. Chemical fluorophore used to produce fluorescent lipid analogues.
BPM	Basal Plasma Membrane
BSA	Bovine Serum Albumin
CD36	Cluster of differentiation 36, also known as Fatty Acid Translocase
CGB	National Center for Biotechnology and Informatics gene symbol for Human Chorionic Gonadotropin- Beta subunit.
CTB	Cytotrophoblast
DHA	Docosahexaenoic acid
DNA	Deoxyribonucleic Acid
EBSS	Earle's Balanced Salt Solution
ECAR	Extracellular Acidification Rate
EGF	Epidermal Growth Factor
FABP	Fatty Acid Binding Protein
FAT	Fatty Acid Translocase , also known as *CD36*
FATP	Fatty acid Transport Protein, specifically from the SLC27 gene family.
FCCP	Carbonyl cyanide 4-(trifluoromethoxy)phenylhydrazone, uncoupler of mitochondrial oxidative phosphorylation
FFA	Free Fatty Acid
GDM	Gestational Diabetes Mellitus
GPAT	Glycerol Phosphate Acyl Transferase
HBSS	Hank's Balanced Salt Solution
LCPUFA	Long Chain Polyunsaturated Fatty acid
LD	Lipid Droplet

MAPK	Mitogen-Activated Protein Kinase
MCT1	Monocarboxylate Transporter 1
MVM	Microvillous Membrane
NADPH	Nicotinamide Adenine Dinucleotide Phosphate
OA	Oleic Acid
OCR	Oxygen Consumption Rate
PA	Palmitic Acid
pFABPpm	placental plasma membrane associated Fatty Acid Binding Proteim
qPCR	Quantitative Polymerase Chain Reaction
SCT	Syncytiotrophoblast
SEM	Standard Error of the Mean
SIM	Structured Illumination Microscopy
SLC27	Gene encoding Fatty Acid Transport Protein, FATP.
TEM	Transmission Electron Microscopy

Acknowledgements

This thesis is dedicated to my mentor, Kent Thornburg, who guided and supported my growth as a scientist.

Abstract

Cytotrophoblast regulates lipid esterification and metabolic activity of the human term placenta

Kevin S. Kolahi

Department of Biomedical Engineering
School of Medicine
Oregon Health & Science University

Thesis Advisor: Kent L. Thornburg, PhD

The human placenta is the primary life-support organ for the developing fetus. It integrates the functions of a multi-organ system but is composed of only five major cell types. It is a highly metabolic organ, consuming 40% of total oxygen used by the entire conceptus while accounting for only 20% of its total mass. This high metabolic activity supports the placenta's extensive transport function, its manufacture of hormones and the biochemical processing of nutrients. The precise functions of the cells within the placenta that underlie these processes remain poorly defined. This thesis reports that some of the metabolic processes that have been traditionally assumed to be restricted to other placental cell types are primarily driven by a layer of progenitor trophoblast cells, the cytotrophoblast, which have been ignored as significant contributors to placental metabolic function. The cytotrophoblast appears to be the predominant determinant of the metabolic rate of the placenta, and serves a previously unrecognized role in placental nutrient processing and perhaps, even transport. The thesis provides experimental evidence that the current view of the regulation of nutrient transport and metabolic function in the human placenta must be

expanded to include the powerful biological actions of the heretofore ignored cytotrophoblast.

Chapter I: Introduction

Relevance of placental studies to human health

The quality of the process of development sets the resiliency of organs for an individual's life. Embryonic and fetal tissues race to balance form and function, or in more biological terms, growth and maturity. Sluggish development produces compromised organs with limited reserves and enduring maladapted physiological processes. The growth rate of a fetus is set, to a large degree, by the *in utero* environment. The fetus must be receptive to environmental cues in order to prioritize growth and maximize its chances of survival. For example, the fetus is extremely sensitive to nutrient levels and will adapt to a temporary shortage in nutrient supplies by prioritizing resources for organs that are essential for immediate survival (e.g. heart, and brain) at the expense of other organs (e.g. skeletal muscle and kidney). The fetus responds to an environmental insult by compromising the structure of its organs and by altering the epigenetic regulation of growth related genes. While some developing tissues can recover from an insult, timing is everything. If the insult occurs within a specific time window that affects a particular organ, or if the duration of insult is extended, irreversible structural changes take place. Since the resiliency of organs is dictated by developmental influences it is not surprising that fetal growth is a predictor of longevity and chronic disease risk.

The developmental origins of disease hypothesis was proposed by David JP Barker et al. based on epidemiological studies of birth records that revealed an association between ischemic heart disease and weight at birth (Barker and

Osmond, 1986; Barker et al., 1989). This conclusion was made possible by stringent record keeping in England over decades in which individuals could be longitudinally followed from birth to death. These records spanning births from 1911 to 1970s and stored to the present time, indicated that individuals born with the lowest birth weights had the highest death rates, and conversely those with the greatest birth weights and the lowest death rates (Barker et al., 1989; Barker, 1990). Barker's team found that it was specifically prenatal growth, even more than postnatal growth, that correlated best with adult death rates from heart disease and proposed that there was something about poor fetal growth *in utero* that led to chronic disease. Since the inception of this hypothesis hundreds of studies in humans and in animals have shown that insults experienced during *in utero* development can have lifelong detrimental consequences. These consequences remain poorly defined as are the mechanisms that give rise to them.

Nevertheless, a common theme from the studies is that there are critical developmental windows of exaggerated sensitivity during which each organ of the fetus is susceptible to alterations in its environment. Not all organs are equally or simultaneously susceptible and as mentioned previously, timing matters. Epidemiological studies of a Dutch cohort exposed to a famine during World War II revealed that fetal undernutrition has differing consequences depending upon the phase of development (Roseboom et al., 2001). Nutrient restriction during late gestation was associated with higher incidence of impaired glucose tolerance, but during early gestation was associated with hyperlipidemia

and coronary heart disease (Roseboom et al., 2001). The evidence strongly supports the conclusion that alterations in nutrient availability for the fetus, either through diminished maternal supplies or dysfunctional maternal to fetal transport, lead to drastic changes in fetal growth. It is unknown whether these effects are secondary to alterations in the fetal endocrine system or if low nutrient levels directly affect fetal tissue growth and maturation. A combination of these effects is likely.

Fetal growth is extremely sensitive to fluctuations in nutrient levels. Inadequate or excess nutrient delivery is common in pregnancies around the world. Conversely, fetal nutrient overload is also becoming commonplace in developed nations where obesity and diabetes are becoming the norm (Cnattingius et al., 1998; Heerwagen et al., 2010). If fetal nutrient levels are disproportionate to demand, and if the fetus survives, the resulting malnutrition usually results in permanent defects in growth and organ maturation. We are just beginning to discover the mechanisms underlying these defects. We now know that any deviation from an optimal birth weight, too large or too small, is associated with an increased risk of chronic disease, including hypertension, diabetes, and cardiovascular disease (Barker and Thornburg, 2013a; 2013b; Thornburg and Marshall, 2015). There are now numerous papers showing that the size and the shape of the placenta are important as risk factors for chronic disease in later life(Barker et al., 2011). This suggests that placental growth itself influences fetal structure and function.

The disease link may be related to the fact that fetal tissues that do not

receive adequate quantities of the required chemical components are, for undiscovered reasons, less resilient. The organ that is responsible for transporting all of the nutrients from the mother to the fetus is the placenta, an organ that develops from the early embryo. Thus, the placenta is central to fetal growth and development and is the center of the chronic disease universe (Thornburg and Marshall, 2015).

The placenta as a complex organ

The placenta functions as a life-support organ during development, and the fetus depends on the transport functions of this organ to obtain the required nutrition. Many of the nutrients transported by the placenta will be utilized as building blocks by the growing fetus, in addition to being a fuel source to generate ATP (Battaglia and Meschia, 1978; Sparks et al., 1980; Vander Heiden et al., 2009). The placenta is a relatively small organ compared to the mature fetus, but it has an extensive transport capacity which is supported by a high metabolic rate. It consumes roughly 40% of the total oxygen and 50% of the total glucose used by the entire conceptus, while only accounting for 20% of the total mass (Burd et al., 1975; Battaglia and Meschia, 1978; Sparks et al., 1983; Bonds et al., 1986; Lurie et al., 1999). The transport and metabolic function of the placenta must be attributable to at least one of its five major cell types (Benirschke et al., 2012), but the various roles of these cells during fatty acid transport and metabolism remain poorly defined (Benirschke et al., 2012).

The placenta is a specialized tissue barrier that serves as an interface

between maternal and fetal blood. It is designed to permit exchange without allowing maternal and fetal bloods to come into direct contact (Figure 1.1A). The primary tissue barrier is formed from a specialized epithelium derived early in development called trophoblast. Two trophoblast layers exist throughout pregnancy, but by term the outer maternal facing layer, the syncytiotrophoblast, which is derived from the fusion of cytotrophoblast cells found in the layer beneath it (Figure 1.1C) becomes the primary transporting layer. After crossing the syncytiotrophoblast and the second trophoblastic layer, the cytotrophoblast, nutrients must find passage across the third and final cell layer the endothelium to enter fetal blood (Figure 1.1C).

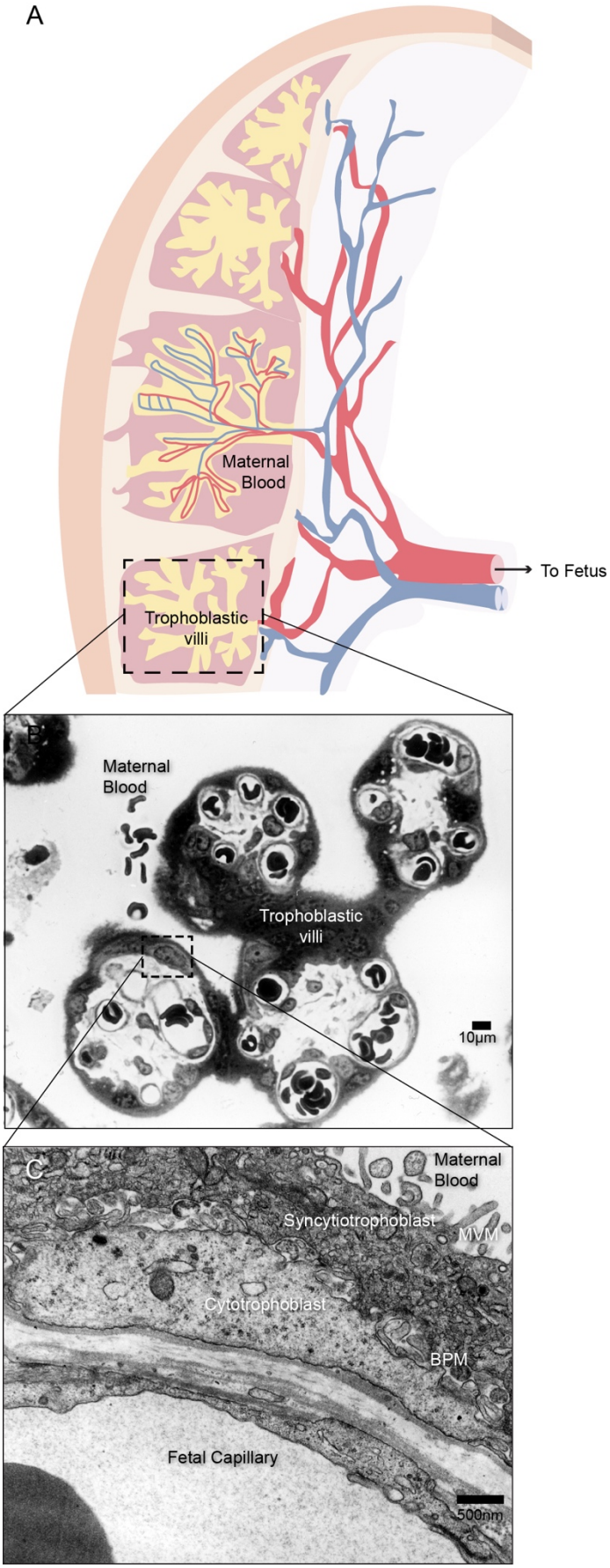

Figure 1.1. The cell layers of the mature human placenta.
(A) The placenta is established by the actions of a specialized cell type called the trophoblast. Trophoblast grows into frond-like structures called villi that serve as conduits for fetal blood vessels. A sub-population of trophoblast cells, called extravillous trophoblast invade maternal tissue and blood vessels to facilitate maternal blood flow into the placenta. (B) is a micrograph of human placenta. The four fetal villous regions shown are surrounded by maternal blood. (C) Electron micrograph of human term placental barrier. The first layer through which maternal nutrients must pass is the syncytiotrophoblast, the primary transporting layer. Deep to the syncytiotrophoblast is the cytotrophoblast layer. The latter regenerates adjacent syncytiotrophoblast when needed. The third and final cellular barrier to transport is the endothelial cell layer. MVM, syncytiotrophoblast microvillous membrane; BPM, syncytiotrophoblast basal plasma membrane. (Original electron micrographs from Thornburg).

Over the past century, a large number of biological actions have been assigned to the syncytiotrophoblast. Among those are the transport of all nutrients and the manufacturing of protein and steroid hormones along with hundreds of other molecules important to mother and fetus. This thesis reports that several important biochemical processes within the placenta that have been traditionally assumed to be restricted to the syncytiotrophoblast are instead primarily driven by the deeper cytotrophoblast cells. The cytotrophoblast layer has been ignored as a significant contributor to placental transport and metabolic function, and this thesis provides experimental evidence suggesting that cytotrophoblast plays a previously unrecognized role in placental metabolic function.

Chapter II: Background

The Placenta

Early in development, the embryo begins to outgrow its capacity to sustain itself on maternal endometrial secretions. A specialized cell layer, the trophectoderm, surrounds the inner cell mass that will become the embryo body provides nutritional support of the embryo. The trophectoderm was so-named because it is composed of the cells that provide the early stage embryo with the nourishment and protection required for survival. The word trophectoderm, derives from Greek *trophē* meaning nourishment, and ectoderm deriving from Greek *ektos*, external, and *derm*, skin. Trophectodermal cells emerge 3 days after fertilization in the form of a blastocyst and immediately forms an outer cell layer that will nurture the cells that will give rise to the fetus. In addition to protecting and nourishing the fetus, the trophectoderm also orchestrates the early invasion of the uterine endometrium which places the embryo adjacent to maternal vascular spaces within the uterine stroma. As the embryo grows and matures, the trophectoderm differentiates into a separate cell lineages, including several lines of trophoblast, which together establish a complex nutrient exchange organ, the placenta. The placenta becomes the interface between maternal and fetal bloods and serves as the life-support system for the fetus. The trophoblast protects the embryo from detrimental actions of the maternal immune system which enables uterine engraftment. The growing metabolic needs of the embryo can be met, in part, by gaining access to the mother's blood, but this is

no simple task. Maternal vascular spaces are buried behind a layer of epithelium and extracellular matrix. Even after the embryo successfully invades these barriers, maternal blood contains immunological defense systems (cells and humoral factors) to prevent invasion from foreign organisms, the embryo included. Nevertheless, the embryo must gain access to this medium in order to survive and continue growing at an exponential pace.

In fact, to facilitate embryonic growth, maternal systemic adaptations are directed by the massive secretions of steroid and protein factors manufactured within trophoblast which stimulate large increases in uterine blood flow and blood nutrient concentrations. Further increases in the exchange capacity of this interface take place at the beginning of the second trimester once fetal blood vessels, sourced from the fetal gut, begin to grow into the trophoblastic villi.

It is crucial that the interface created by the trophoblast remains intact so that maternal and fetal bloods avoid direct contact. At term in humans, three cell layers separate maternal from fetal blood. Two of these layers are derived from the trophoblast lineage, the first, in direct contact with maternal blood is the syncytiotrophoblast, and immediately underlying the syncytiotrophoblast is the second layer of trophoblast, the cytotrophoblast (See Chapter I). The syncytiotrophoblast is a terminally differentiated, syncytial cell monolayer derived from the fusion of the underlying cytotrophoblast progenitor cells. Because the syncytiotrophoblast is the first cell layer that maternal nutrients must traverse, it has been appropriately deemed the gate keeper for all nutrients acquired by the fetus.

The second layer, the cytotrophoblast, plays a well-known role in repair and regeneration of syncytiotrophoblast. The syncytiotrophoblast is incapable of proliferation and is continuously shed into the maternal circulation leaving areas of the placental villous surface denuded (Johansen et al., 1999). To regenerate these areas of denuded syncytium, the cytotrophoblast proliferates and fuses with overlying syncytium to expand and repair this layer (Figure 2.1). The rate of syncytiotrophoblast turnover *in vivo* is not known, but the rate syncytiotrophoblast fragments are shed into the maternal circulation is massive, as many as 150,000 large syncytiotrophoblast particles are shed per day (Johansen et al., 1999; Tannetta et al., 2013). The cytotrophoblast must therefore continuously proliferate to regenerate syncytium that has been lost (Simán et al., 2001).

Conveniently, since the cytotrophoblast layer is composed of numerous and discrete cells, they can be isolated from placentas and cultured (Kliman et al., 1986) (Figure 2.1). Cytotrophoblast recapitulate syncytial formation *in vitro* and form syncytiotrophoblast that secrete known markers of this cell layer *in* vitro (e.g. Human Chorionic Gonadotrophin, Progesterone) (Kliman et al., 1986). However, for reasons that are under investigation, cytotrophoblast cells are incapable of self-renewal *in vitro* (Johnstone et al., 2005). Virtually all cytotrophoblast will fuse and differentiate to syncytiotrophoblast *in vitro* by 72 hrs (Kliman et al., 1986; Johnstone et al., 2005). Studies are beginning to shed light on the pathways that regulate cytotrophoblast to syncytiotrophoblast differentiation, and novel methods to manipulate cytotrophoblast differentiation and proliferation are now becoming available (Daoud et al., 2005; Johnstone et

al., 2005).

Cytotrophoblast cells have many specialized features compared to other placental cell types. They are small and have a high nuclear to cytoplasmic ratio, features common to rapidly dividing cells (Gilbert, 2000). In addition to their proliferation, they have an inherently high metabolic rate (Bustamante et al., 2014) for reasons that we investigated in this thesis. Their nuclei contain a greater proportion of euchromatic DNA than found in syncytiotrophoblast, suggesting that these cells have more a widespread, active transcriptional program (Fogarty et al., 2015). Cytotrophoblast cells are fusogenic and as such have lipids that facilitate membrane fusion, plasmalogens, also known as ether lipids (Roels et al., 1987; Nagan and Zoeller, 2001). Plasmalogens are coincidentally enriched in long chain polyunsaturated fatty acids and are likely synthesized by specific cytotrophoblast systems (Roels et al., 1987; Nagan and Zoeller, 2001). In this thesis we investigate the cytotrophoblast's further roles in placental function.

The final cell layer that transported nutrients must cross is fetal endothelium. The endothelium is entrenched in a stroma composed of resident macrophages and fibroblasts, but the contribution of these components to the distance over which nutrients must traverse is highly variable and is a function of gestational age. As gestation advances, fetal capillaries move to oppose the basement membrane of the trophoblast, reducing the thickness of intervening stroma that would otherwise impede diffusion.

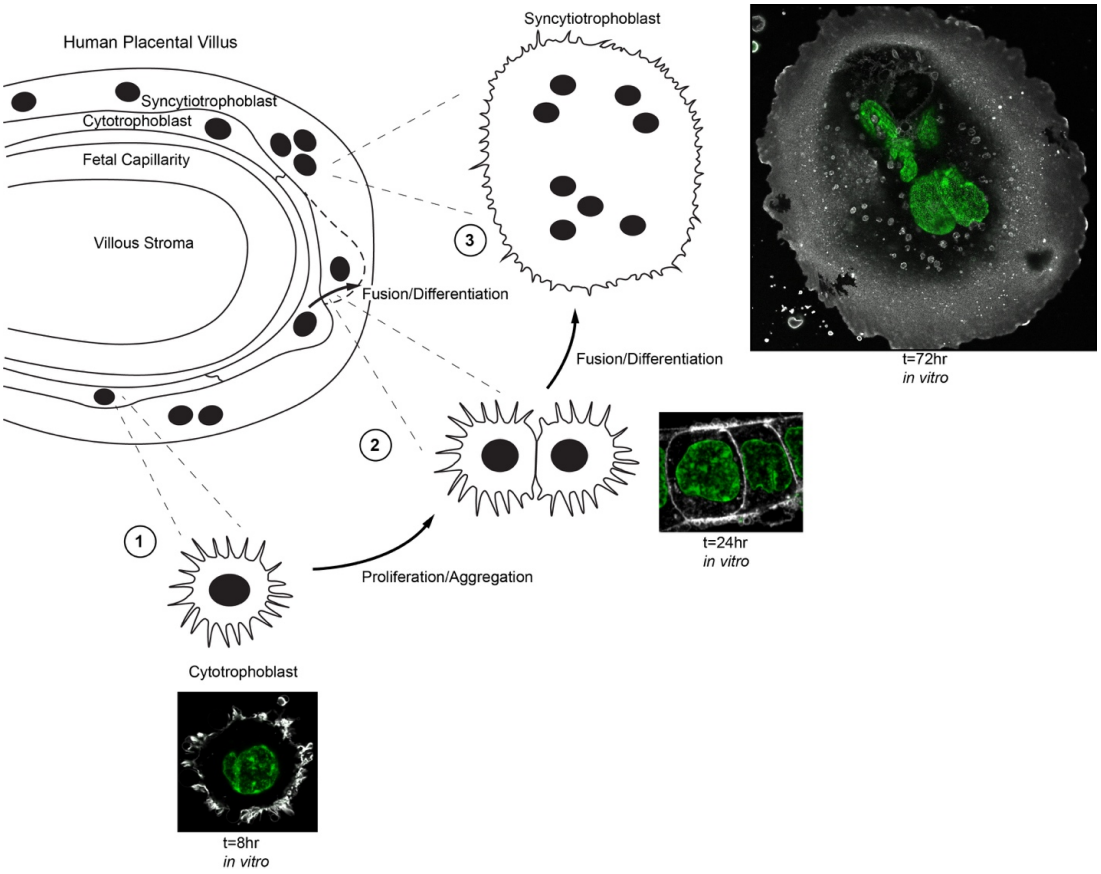

Figure 2.1 Cytotrophoblast fusion and differentiation to syncytiotrophoblast.
The functional unit of the human placenta is a trophoblast derived tissue that forms finger-like (~100μm) projections termed villi. Villi contain blood vessels (endothelium) and supportive stromal cells (e.g. fibroblasts, macrophages), which are also derived from the embryo. Placenta size and villous tissue surface area increases throughout pregnancy, but the relative proportions of placental cell types vary by gestational age. The cytotrophoblast, a progenitor epithelium which regenerates the syncytiotrophoblast continuously, can be isolated and cultured *in vitro*. The cytotrophoblast then recapitulates differentiation to become syncytiotrophoblast. (1) Cytotrophoblast are round and contain numerous filopodial extensions shortly after initial plating. (2) By 24hrs in vitro cytotrophoblast begin to aggregate and form intercellular contacts in preparation for fusion. (3) By 72hrs in culture, virtually all isolated cytotrophoblast have fused and have formed syncytium. The regeneration of syncytiotrophoblast from cytotrophoblast in cultured placental explants follows a similar time course (Simán et al., 2001).

As the interface between mother and fetus, the placenta is poised to integrate maternal and fetal signals; it balances fetal growth rate requirements with maternal needs. Some have gone so far to propose that the placenta is the central hub that regulates fetal growth (Haggarty et al., 2002; Jansson et al., 2006b; Sibley et al., 2010). It is likely that a complex interplay exists between fetal and placental growth and this is in turn regulated by the maternal environment as well. However, there is no doubt that the fetus cannot grow faster than allowed by the placental transfer of nutrients. The concept that the maternal environment can alter the course of development leading to life-long consequences requires an understanding of placental function including nutrient transport and metabolism.

Placental nutrient transport and metabolism

The combination of recent epidemiological and basic experimental evidence suggests that the role of the placenta as a rate limiting organ for fetal growth and development has been underappreciated heretofore. It is becoming increasingly clear that placental metabolism is linked to nutrient transport, as one would expect. Nutrients acquired from the mother must cross several cell layers before entrance into fetal capillaries (Figure 1.1). There have been discussions regarding the importance of the magnitude of blood flow for the transport of the major macronutrients, glucose, amino acids, and fatty acids vs. the role of transporter activity (Day et al., 2013a) vs. (Bell et al., 1999; Hay, 2006). The data supporting various views are derived from mathematical models, animal

preparations or perfused human placentas. People have not, for obvious ethical reasons, reported the kinetics for these nutrient compounds in vivo under varying conditions in human pregnancies. For those nutrients whose diffusional transport from mother to fetus is limited by blood flow, alterations in placental transporter expression would have little bearing on overall nutrient flux, but changes in the magnitude of the exchange area of the placenta would (Faber and Thornburg, 1983). While the transport systems can be mathematically modeled based on in vitro experiments, these models have not been adequately tested in vivo.

Several lines of evidence argue that the placental regulation of nutrient fluxes is required for fetal survival, and that this regulation is intimately linked to placental metabolism as an intermediate step. Nutrient transporters are differentially localized and subject to distinct mechanisms of regulation in placental tissue (Lager and Powell, 2012). In particular, transporter expression and activity at the syncytiotrophoblast's fetal facing basal plasma membrane (BPM) is more tightly regulated than the maternal facing microvillous pl asma membrane (MVM) (Lager and Powell, 2012), but the coordination of transport systems at MVM and BPMs has not been adequately studied. Using vesicles formed *in vitro* from purified plasma membrane from syncytiotrophoblast MVM and BPMs to study nutrient transport kinetics, it has been proposed that the transport of glucose, amino acids, and fatty acids is more powerfully regulated at the level of the BPM than the MVM (Kudo and Boyd, 1990; Powell et al., 1999; Lafond et al., 2000; Jansson, 2001; Baumann et al., 2002). These findings support studies indicating for many transporters of glucose, amino acid, and fatty

acids, expression is enriched at BPM and influenced by maternal physiological conditions (Gaither et al., 1999; Roos et al., 2007; Lager et al., 2016).

Experimental evidence suggests that the rate limiting step in the transport of amino acids and fatty acids is incorporation into a metabolic pool in the placenta (Szabo et al., 1973; Bianco-Miotto et al., 2015; Perazzolo et al., 2015). Amino acids taken up by the placenta are rapidly incorporated into cellular proteins, and re-released into the fetal circulation; this process represents the rate limiting step in placental amino acid transport (Bianco-Miotto et al., 2015). Some amino acids are converted to a different amino acids before transport (Wu et al., 2015). Similar to amino acids, the rate limiting step in fatty acid transport also appears to be incorporation into a metabolic pool (Perazzolo et al., 2015). Earlier studies have proposed that incorporation of fatty acids into esterified lipids, a step requiring ATP, is an intermediate step in transport (Coleman and Haynes, 1987), and the placental uptake of some essential fatty acids is ATP dependent (Lafond et al., 2000). Indeed, as will be discussed further, the selective incorporation and transport of long-chain polyunsaturated fatty acids appears to be proportional to the degree of esterification (Haggarty et al., 1997; Larqué et al., 2003).

It is not known if glucose is regulated in a similar manner. However, the placenta consumes some 50-60% of the glucose utilized by the conceptus and exports roughly a third of this glucose as lactate, a principle fuel source for fetal tissues (Burd et al., 1975; Battaglia and Meschia, 1978). In addition, the mouse placenta has specialized glycogen containing cells, spongiotrophoblasts, whose

precise roles remain to be defined but are otherwise crucial to mouse development (Rossant and Cross, 2001). Glycogen may be an important component in human placental development and function, but studies of the significance of glycogen in the placenta are limited (Yoshida, 1964).

Lastly, the alterations in fetal growth rate are associated with major changes in transporter expression and activities in placental tissue (Sibley et al., 2010; Lager and Powell, 2012). If placental metabolism and transport rates are linked, it would add complexity to understanding transport systems. In that case, nutrient transport would be regulated not only by placental tissue type (i.e. trophoblastic vs non-trophoblastic cells), but perhaps at the level of uptake and incorporation, utilization via oxidation, and efflux mechanisms. All of these steps are poorly defined in placental biology, especially in humans. We will review the mechanisms of uptake, metabolism, and efflux for the major macro nutrients individually in greater depth.

The controversy over the relative importance of maternal blood flow versus a robust transporter system for each nutrient is unworthy of debate because both are needed. A robust flow is needed for flow limited substances, including oxygen, to provide for metabolic activity that underlies placental and fetal growth. On the other hand, robust transport systems are required to ensure that nutrients pass from the maternal blood to fetal blood in an efficacious manner. Furthermore, the transplacental transport of nutrients could be compromised if the blood flow were so low that concentrations of nutrients became depleted during a single pass in the placenta.

Glucose transport and metabolism

Glucose is the principal fuel source for the fetus and placenta (Battaglia and Meschia, 1978; Sparks et al., 1982; 1983; Hay, 1995) and is essential for normal fetal growth (Hay, 2006). Placenta glucose uptake is mediated by plasma membrane glucose transporters (GLUT). Multiple members of the GLUT family exist but the primary members in placenta are GLUT1 and GLUT3 (Sciullo et al., 1997; Illsley, 2000), these isoforms are insulin independent, i.e. they do not require an insulin stimulus to be functional or to be present on the placenta membrane. GLUT transporters work via facilitated diffusion; the extracellular to intracellular gradient drives the influx of glucose. GLUT1 is the most highly expressed GLUT transporter and is localized to the syncytiotrophoblast MVM and even higher levels on the syncytiotrohpoblast BPM (Jansson et al., 1993; Ericsson et al., 2005).

Studies from chronically instrumented sheep and dually perfused human placentas have shown that the kinetics of glucose transport is determined by maternal to fetal concentration gradients (W Hay and Meznarich, 1989; Hay, 2006). In particular, maternal glucose concentrations vary dramatically and drive glucose across the placenta to the fetus (Hay et al., 1984). The maternal to fetal flux of glucose can additionally be affected by increasing or decreasing the surface area available for transport.

During the second trimester of pregnancy, an insulin resistant state begins to emerge in the mother, due to the placental production of diabetogenic

hormones, cortisol and human placental lactogen (Barbour et al., 2007). The actions of these hormones result in a systemic insulin resistance that leads to sustained elevations in maternal blood glucose and facilitates glucose transport.

The placenta removes more glucose from the mother than is transferred to the fetus (Sparks et al., 1982; Hay, 1995). Roughly 60% of the total glucose utilized by the conceptus is metabolized in the placenta (Sparks et al., 1982; Hay, 1995). A minor portion is stored as placental glycogen, its relevance to overall metabolism and transport remains unclear (Yoshida, 1964). However, roughly a third of the glucose taken up by the placenta is partially oxidized via glycolysis and converted to lactate. The lactate is exported to the fetus, and represents a major fuel source for the developing fetus. For some tissues, like the heart, lactate is the primary metabolic fuel (Battaglia and Meschia, 1978; Fisher et al., 1980; Bartelds et al., 1999). The placental production of lactate from glucose is influenced by oxygen tension, implying that placental oxygen tensions may influence the fuel mixture that the fetus sees (Kay et al., 2007). Glucose that is metabolized rapidly by the placenta via glycolysis also drives glucose across the MVM by increasing the concentration gradient for glucose.

Amino acid transport and metabolism

The placental transport systems for amino acids are among the best studied. Amino acids are required precursors to synthesized proteins and can be utilized to generate purines and pyrimidine nucleic acids *de novo*. The daily fetal acquisition of amino acids is approximately 4g/kg/day (Lemons et al., 1976).

High acquisition rates of amino acids are required to support this fetal need. In contrast to glucose the concentration of amino acids is higher in fetal blood than in maternal serum (Cetin et al., 1992). In some systems, amino acid transport is regulated by active transport processes, expending the electrochemical potential of sodium transmembrane gradient to drive amino acids intracellularly (Jansson, 2001; Lager and Powell, 2012). Efflux of amino acids from syncytiotrophoblast occurs via a separate set of exchangers that function in a facilitative diffusion manner (Jansson, 2001).

Twenty amino acid transporters in placenta have thus far been described and divided between the two major system families: System A and System L (Lager and Powell, 2012). System A transporters are sodium-cotransporters with small non-essential neutral amino acids such as alanine, glycine, and serine (Mahendran et al., 1994; Desforges et al., 2010). System A is highly polarized to the syncytiotrophoblast microvillous (maternal-facing) membrane (Jansson et al., 2002), and may serve a key role in producing the high intracellular glycine concentrations necessary for System L activity (Lager and Powell, 2012). System L transports neutral amino acids but is selective for essential amino acids such as aromatic (e.g. phenylalanine) or branched chain (e.g. leucine) amino acids (Verrey, 2003). The secondary active transport of the system L transporters expends the electrochemical potential of glycine (non-essential amino acid) to exchange with an essential amino acid. System L, like System A is localized to all plasma membranes in placenta but is highly polarized to the MVM (Okamoto et al., 2002; Gaccioli et al., 2015). As described, these amino acid transporter

families are composed of multiple isoforms and their relative expression varies across gestation and by species.

A distinguishing feature of amino acids is that they are not stored as simply as are glucose or fatty acids. For example, multiple glucose molecules can stored as a polymer, glycogen, and fatty acids can be linked to a glycerol backbone to form intracellular oil droplets called lipid droplets. Amino acids do not form storage polymers as readily as do sugars and lipids, though they do link in chains to form structural proteins in the fetus.

Maternal skeletal muscle protein turns over and releases amino acids, especially when nutrients are in short supply. Thus, they serve as an emergency storage for essential amino acids. This process may underlie the observation that liberation of amino acids from skeletal muscle in pregnancy is thought to be highly correlated with fetal growth parameters (O'Tierney-Ginn et al., 2014; Thame et al., 2015). As expected, the overall transport of individual amino acids appears to be a function of its availability in maternal plasma.

The transplacental transport of amino acids is active, requiring ATP, and linked to rates of metabolism which regulate transporter expression and ultimately the rate of amino acid transport (Bianco-Miotto et al., 2015). As with skeletal muscle, amino acids in trophoblast are largely incorporated into cellular proteins which serve as a temporary storage pools for amino acids before being released as needed (Miller, 2007; Lewis et al., 2013). Amino acids can also be used as a fuel for oxidative processes, or the nitrogen can be transferred to generate nucleic acid precursors; these processes may account for variability in

the amino acid maternal to fetal flux (Lewis et al., 2013; Day et al., 2013b). Alternatively, as is the case with other nutrients, amino acid uptake by the placenta may serve to promote growth of the placenta and increase in the surface area available for transport; this can occur along with changes in transporter expression. The regulation of amino acid transport correlates roughly with fetal growth rates. A reduction in placental amino acid transport leads to growth restriction(Jansson et al., 2006a; Avagliano et al., 2012), and although less clear, elevations in placenta amino acid transport may support fetal overgrowth (Kuruvilla et al., 1994; Lager and Powell, 2012). These biological findings fit with epidemiological data where low muscle mass at birth correlates with low muscle mass in later life (Baker et al., 2010).

Fatty acid transport and metabolism

Human fetuses accumulate more fat as a proportion of body weight by far, than any other animal (12-16% for humans vs 2-3% for other animals) (Ulijaszek, 2002). The rate of fat acquisition during human development begins to increase sharply in the mid-second trimester and reaches a maximum rate by term. Tissues that utilize fat as a structural component, such as the brain, also grow rapidly during this period. During the 25th to 36th week period of gestation, the lipid-rich fetal brain volume increases by 230%. Thus, it is essential that the placenta transports the appropriate quantities and varieties of fatty acids required for normal brain development. A disruption in fatty acid supply, either from placental dysfunction or inadequate maternal supply, leads to disproportionate

fetal growth and poor cognitive function for life (Ornoy et al., 2001; Innis, 2005; 2007).

It has become increasingly clear that each fetal organ requires specific nutrients during defined windows of development. In contrast to other mammals, the human fetus requires an increase in placental lipid transport to accommodate normal brain, membrane and fat depot requirements with advancing gestation (Martinez, 1992; Ulijaszek, 2002; Winn et al., 2007; Schaefer-Graf et al., 2008; Illsley et al., 2010). As a result, humans are born with relatively larger brains and fat reserves. Among the many organs requiring fatty acids for development, the human brain specifically requires ample long-chain polyunsaturated fatty acids (**LCPUFA**) (Clandinin et al., 1980; Farquharson et al., 1992). Since fetal production of LCPUFAs is not sufficient to meet these demands, they must be obtained from the maternal circulation (Szitanyi et al., 1999; Lapillonne and Jensen, 2009). Circulating proportions of LCPUFA are normally higher in cord blood than in maternal plasma (Crawford et al., 1976; Friedman et al., 1978; Haggarty et al., 1997), suggesting that the placenta has the capacity to selectively transfer specific fatty acid species.

Babies born to mothers with gestational diabetes mellitus (**GDM**) often exhibit delayed brain development due to inadequate placental delivery of LCPUFA, despite normal levels in maternal plasma (Pagan et al., 2013). Maternal plasma LCPUFA levels in GDM are usually within the normal range while neonatal plasma LCPUFA concentrations are depressed (Wijendran et al., 1999; 2000; Thomas et al., 2004). Lipid metabolism in both placenta and fetus

can be detrimentally altered under pathological conditions (Catalano et al., 2003; Magnusson et al., 2004; Ortega-Senovilla et al., 2009; Radaelli et al., 2009). Maternofetal transfer of docosahexaenoic acid (**DHA**, a LCPUFA) is compromised in pregnancies complicated by gestational diabetes (Pagan et al., 2013). Low circulating maternal LCPUFA levels are associated with impaired postnatal cognitive development in offspring (Strain et al., 2008) and delayed brain maturation has similarly been reported in babies born to gestational diabetic mothers (Rizzo et al., 1991; Ornoy et al., 2001). In rat models, diabetic mothers give rise to offspring with compromised cardiovascular health in adulthood (Weisinger et al., 2001). LCPUFA supplementation may have implications for at-risk pregnancies as it can increase birth weight and decrease the incidence of preterm birth (Szajewska et al., 2006; Horvath et al., 2007). With so many fetal organ systems at stake in diabetic pregnancies, it is surprising that so little is known about the mechanisms by which placental lipid transport is regulated under *normal* conditions and also in metabolic disease.

The human placenta employs a unique transport system to recognize fatty acids according to specific type. The layer that is responsible for initiating this process in the mature human placenta is the syncytiotrophoblast, an uninterrupted multinucleated single cell layer across which initial nutrient transport is accomplished. This is the layer in direct contact with maternal blood, and has specialized maternal-facing microvillus projections, much like those of the intestine, that increase the exchange area in contact with blood (Figure 1.1). Thus, the placental transfer of LCPUFA begins at the syncytiotrophoblast.

The first step of fatty acid absorption is the liberation of free fatty acids from triglyceride-rich lipoprotein particles in maternal blood (placenta) with the help of lipoprotein lipases (Magnusson et al., 2004). In general, cells contain enzymes with specificity to a narrow range in fatty acid chain length; these enzymes participate to differing degrees in the uptake and metabolism. Short- and medium chain fatty acids may diffuse into and out of some cells but they have not been well studied in placenta. LCPUFA are more non-polar and are certain to require the aid of transporters for import and export (Karmen et al., 1963; Cummings et al., 1987; Coburn et al., 2000). While many of the genes required for the differential uptake and processing of fatty acids according to chain length are expressed in the placenta, their activities have yet to be described. It is possible that a system similar to that found in other cells exists in the placenta and functions to facilitate selective LCPUFA uptake.

Several types of fatty acid transport proteins (**FATP**) and translocases are found on the MVM and fetal-facing BPM of the syncytiotrophoblast (Ibrahimi et al., 1996; Campbell et al., 1998). FATP are capable of binding fatty acids and transporting these into the cell. They work in concert with long-chain acyl-CoA synthetases (**ACSL**) that esterify entering fatty acids to Coenzyme-A (Figure 2.3). Esterification of fatty acids evidently drives fatty acid uptake as the FATP have an Acyl-CoA synthetase domain, or works in complex with separate Acyl-CoA synthetases. Fatty acid esterification is energetically expensive, requiring 2-ATP equivalents per fatty acid molecule, and thus underscoring the importance of metabolic support in this process. While there is a clear relationship between

fatty acid uptake, esterification, and ATP, there is controversy among experts as to whether fatty acid transport is active or merely facilitated. The discovery of FATPs brought into question the dogma that transplacental movement of fatty acids occurs primarily by passive diffusion alone (Baier et al., 1995). In addition to the selective nature of LCPUFA transport by the placenta, there is a net unidirectional flux from mother to fetus. This is intriguing because identical FATP proteins exist on both MVM and BM, suggesting that fatty acid transport should be, in theory, bidirectional (Campbell et al., 1996). However, others have suggested these proteins do not work in efflux and a mechanism for fatty acid efflux remains to be discovered. Thus, it appears that the directionality of LCPUFA fluxes must be regulated, but the mechanisms are not understood.

After esterification of fatty acids by FATP or ACSL to Acyl-CoA, Fatty-Acyl-CoA are bound to fatty acid binding proteins (**FABP**) whose role may include intracellular sequestration of fatty acids. FABP are diverse in function and localization, and can be selective for the types of fatty acids they bind (Ockner and Manning, 1974; Campbell et al., 1998; Levy et al., 2000; Tan et al., 2002; Bildirici et al., 2003; Montoudis et al., 2006; Mishima et al., 2011; Scifres et al., 2011). In other tissues, FABP are required for fatty acid oxidation by mitochondria and to carry fatty acids to the endoplasmic reticulum for modification and storage in lipid dropets (**LD**), sites of cholesterol and triglyceride storage (Veerkamp et al., 1990; Baier et al., 1995; Hsu and Storch, 1996; Scifres et al., 2011). FABP regulation of placental fatty acid transport is sensitive to oxygen levels, and to the milieu associated with maternal obesity (Biron-Shental

et al., 2007; Scifres et al., 2011).

A placental fatty acid binding protein (**pFABPpm**) that is exclusively associated with the MVM of the syncytiotrophoblast and selective for LCPUFA has been described (Campbell et al., 1998). The presence of pFABPpm could explain how LCPUFA are selectively transported into the cell; however, the protein is only present on the MVM of syncytiotrophoblast and does not explain how LCPUFA are transported to the fetus. One potential explanation is that LDs are organelles that participate in the transport of esterified fatty acids across the syncytiotrophoblast.

It is generally believed that fatty acids can be esterified into discrete, LD structures within the syncytiotrophoblast, the maternal facing tissue layer of the placenta. The role that LDs may play in fatty acid transport is not known. Whether intact LDs or perhaps just their contents are transferred to the fetus, or whether they are simply storage organelles, is not known. We speculate that the LD system provides an important mechanism by which the placenta regulates the transport of specific fatty acids to the fetus. Scifres et al showed a paucity of LDs in diabetic pregnancies (Scifres et al., 2011). These findings raise the question: is suppression of LD formation a factor in LCPUFA deficiency in placentas and neonates from diabetic pregnancies? Little is known about this process, but long chain acyl-CoA synthetase (**ACSL**) has been implicated to be an initial and possibly rate-limiting step in LD formation; ACSL is downregulated in trophoblasts from GDM pregnancies (Araújo et al., 2013).

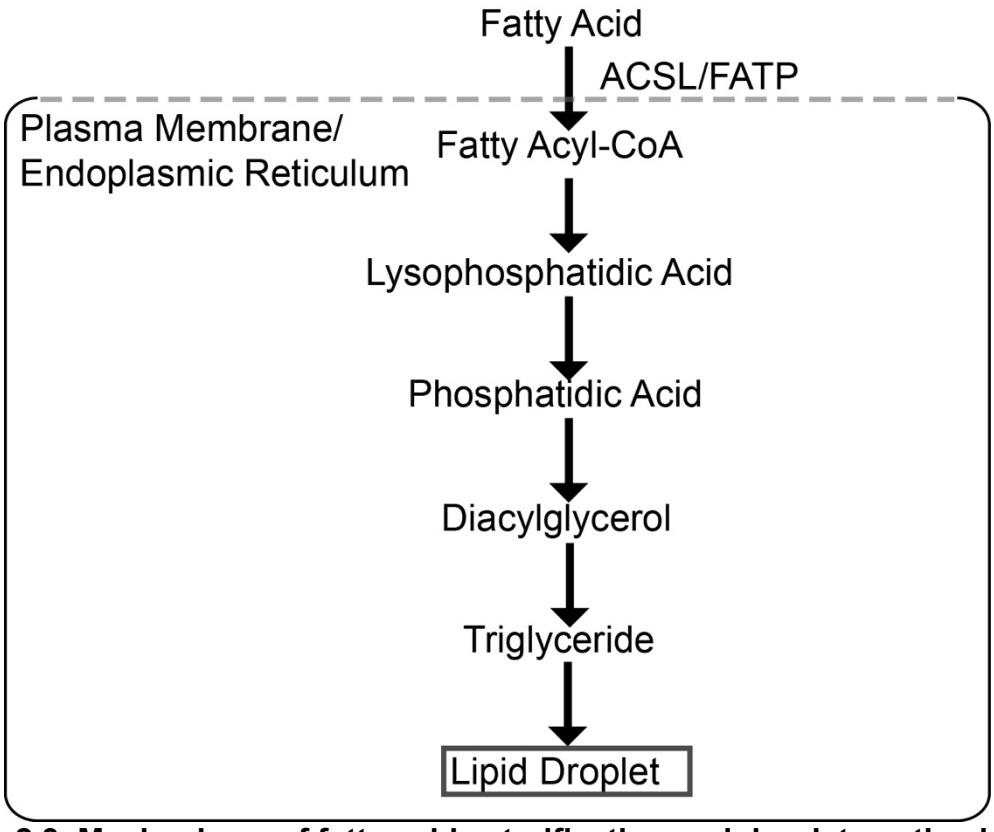

Figure 2.3. Mechanisms of fatty acid esterification and droplet synthesis
Fatty acids are first esterified to Coenzyme-A by long-chain acyl-CoA synthetase (ACSL) or by Fatty Acid Transport Proteins (FATP). At this point, the fatty acyl-CoA may be oxidized or stored. If it is stored, three fatty-acyl-CoA molecules are conjugated to a glycerol backbone in succession to form a triglyceride. These triglycerides are formed and stored in close association with the endoplasmic reticulum within an intracellular organelle, the lipid droplet.

Our laboratory has shown that fatty acid uptake in human placental explants at term differs by maternal pre-pregnancy body mass index (**BMI**) and offspring sex (Brass et al., 2013), but the mechanisms underlying these transport differences among fatty acid chains are not understood. As LCPUFA are critical building blocks for constructing the cardiovascular and nervous systems, this is a significant gap in our understanding of a key placental function.

Placental lipid metabolism: role of lipid droplets and lipoprotein metabolism comparison to the intestine.

Although little is known about placenta LDs, their roles may parallel those of intestinal LDs. In intestine, LDs are temporary triglyceride pools formed from long-chain fatty acids that will be repackaged as lipoprotein particles and exported into extracellular space for lymphatic absorption.

One way the intestine accomplishes unidirectional transport is to sequester long-chain fatty acids via esterification and storage in LDs (Redgrave, 1971; Zhu et al., 2009). Absorbed and esterified fatty acids are bound to FABP, delivered to the endoplasmic reticulum, processed into triglycerides and then stored as LDs (Murphy, 1998) (Figure 2.3). Once sequestered as LDs, intestinal cells can export triglycerides by repackaging them with specialized proteins into much smaller droplet-like structures, called apolipoprotein particles, or specific to the intestine, chylomicrons (Zhu et al., 2009; Bouchoux et al., 2011). The human placenta can also form triglyceride-rich apolipoprotein-like particles from fatty acids, but its relevance to placental fatty acid transport is unknown (Madsen et

al., 2004). The predominant forms of LCPUFA in third-trimester fetal blood and placental tissue following maternal stable isotope administration are triglycerides and phospholipids (Innis, 2005; Gil-Sanchez et al., 2010; Pagan et al., 2013). While it is thought that these lipid species in blood are produced in the fetal liver (Chambaz et al., 1985), an additional possibility is that the placenta contributes specific fatty acids in these forms (Dutta-Roy, 2000; Larqué et al., 2003).

Specific roles for proteins associated with LD membranes have been reported for intestine but not placenta. Although an essential role of intestinal LDs in regulating fatty acid absorption and metabolism has been demonstrated, the extent to which intestinal LD physiology can be extrapolated to the placenta is not clear.

Placental oxidative metabolism and oxygen consumption

All of the transport processes we have described incur an incredible metabolic cost. The placenta, accounting for only 20% of the total mass of the conceptus, consumes some 40% of the total oxygen and 60% of the total glucose utilized by the entire conceptus (Battaglia and Meschia, 1978; Sparks et al., 1983; Bonds et al., 1986; Lurie et al., 1999). This incredible metabolic rate is required to power the processes to support pregnancy and provide for a fetus that is growing at an exponential rate. It is astonishing that the placenta can serve so many diverse functions and yet is composed of only five major cell types.

The placenta operates at such an unparalleled level of efficiency and massive scale that it must be exquisitely sensitive to changes in its environment. Alterations in placental metabolism can have broad impacts on fetal growth and development. However, how the placenta normally transports the specific fats it needs, is unknown. It is surprising that so little is known about how the normal placenta functions, given the important role this organ plays in governing the future health of the baby.

Among the hundreds of large gaps in our understanding of lipid transport in the human placenta, several crucial questions remain to be addressed including those addressed in this thesis:

1. The degree to which each of the cell types is involved in fatty acid uptake and esterification.
2. How fatty acid uptake kinetics and mechanisms differ according to fatty acid chain length/species.
3. The role of various cell types in the metabolic function of the placenta. The degree to which the metabolic features of the placenta are related to nutrient transport in the placenta is also unknown.

This thesis offers new insights to our understanding of human placental biology. To that end, I offer three separate manuscripts that have been or will be submitted for publication in peer review journals.

Chapter III: Real-Time Tracking Of BODIPY-C12 Long-Chain Fatty Acid In Human Term Placenta Reveals Unique Lipid Dynamics In Cytotrophoblast Cells[1].

[1]This manuscript was originally published in the *Public Library of Science.* Kolahi K, Louey S, Varlamov O, Thornburg K. Real-Time Tracking of BODIPY-C12 Long-Chain Fatty Acid in Human Term Placenta Reveals Unique Lipid Dynamics in Cytotrophoblast Cells. PLoS ONE. 2016;11(4):e0153522. PMCID: PMC4849650

Abstract

While the human placenta must provide selected long-chain fatty acids to support the developing fetal brain, little is known about the mechanisms underlying the transport process. We tracked the movement of the fluorescently labeled long-chain fatty acid analogue, BODIPY-C_{12}, across the cell layers of living explants of human term placenta. Although all layers took up the fatty acid, rapid esterification of long-chain fatty acids and incorporation into lipid droplets was exclusive to the inner layer cytotrophoblast cells rather than the expected outer syncytiotrophoblast layer. Cytotrophoblast is a progenitor cell layer previously relegated to a repair role. As isolated cytotrophoblasts differentiated into syncytialized cells in culture, they weakened their lipid processing capacity. Syncytializing cells suppress previously active genes that regulate fatty-acid uptake (SLC27A2/FATP2, FABP4, ACSL5) and lipid metabolism (GPAT3, LPCAT3). We speculate that cytotrophoblast performs a previously unrecognized role in regulating placental fatty acid uptake and metabolism.

Introduction

The placenta, one of nature's most important inventions, enables the mammalian fetus to acquire maternal nutrients within the confines of the protective womb. In humans, the placenta is the tissue barrier that separates maternal and fetal bloods and is the gatekeeper for all nutrients acquired by the fetus. The placenta consists of a maternal facing layer of fused cells, the syncytiotrophoblast, an underlying layer of cytotrophoblast cells, a basal lamina, and a fetal capillary endothelium (Figure 3.1A).

The transport of lipids across the placental barrier is less well understood than the transport of glucose (Lager and Powell, 2012) and amino acids (Jansson, 2001). While many known lipid transport proteins are expressed in the human placenta, their roles are little studied. The once held view that all lipids cross the placenta by unregulated diffusion became untenable by reports showing that long-chain polyunsaturated fatty acids (LCPUFA) are transported preferentially (Haggarty et al., 1997) and fatty acid transporters exist on the syncytiotrophoblast MVM (Campbell et al., 1998). It is now recognized that the fetal acquisition of maternally derived long-chain fatty acids requires a placental transport system (Lafond et al., 2000; Gil-Sánchez et al., 2012). Because of our ignorance regarding lipid transport in the placenta and because disruptions in fatty acid supply have dire consequences for fetal brain development (Crawford et al., 1976; Budowski et al., 1987; Carlson et al., 1993; Crawford et al., 1997) there is a need for intense investigation into placental lipid transport mechanisms.

Long-chain fatty acid transport begins with the uptake of circulating maternal non-esterified fatty acids liberated from triglycerides in circulating lipoproteins through syncytiotrophoblast lipase activity (Waterman et al., 1998; Lindegaard et al., 2005; Gauster et al., 2007). The fatty acids are translocated into the syncytiotrophoblast by transport proteins (FATP) and fatty acid translocase (FAT/CD36) (Campbell et al., 1998) and shuttled toward the syncytiotrophoblast BPM by fatty acid specific binding proteins (FABP) or incorporated within this layer into intracellular compartments.

A large proportion of long-chain fatty acids taken up by the placenta are transformed into esterified glycerolipids (including phospholipids and triglycerides) (Klingler et al., 2003; Larqué et al., 2003; Gil-Sanchez et al., 2010). This is assumed to occur within the syncytiotrophoblast because it contains lipid droplets (LD) and several fatty acid transport proteins in that layer are coupled to an acyl-CoA synthetase enzyme or have acyl-CoA synthetase activity (Stahl et al., 2001; Duttaroy, 2009; Gil-Sánchez et al., 2012; Hernández-Albaladejo et al., 2014). The association between long-chain fatty acid uptake and acyl-CoA synthesis has led to the suggestion that the transport of long-chain fatty acids into the fetus includes an intermediate fatty acid esterification step within the syncytium (Coleman and Haynes, 1987; Desoye and Shafrir, 1994). In perfusion studies, the maternal-fetal transfer rates of long-chain fatty acids is directly proportional to degree of placental long-chain fatty acid accumulation (Haggarty et al., 1997). Reduced enrichment of LCPUFA was found in cord blood and placental tissue from gestational diabetic pregnancy *in vivo* (Pagan et al., 2013) .

Lower LCPUFA enrichment in cord blood could be due to reduced placental LCPUFA accumulation and esterification, or enhanced fetal LCPUFA uptake (Pagan et al., 2013). Nevertheless, it remains unclear whether esterification within the placenta serves as a necessary processing step for the regulation of fatty acid transport to the fetus. While the relevance of esterification to fatty acid transport and uptake is debated, it is clear that FATP expression is necessary and proportional to the degree of long-chain fatty acid cellular uptake (Sandoval et al., 2010; Krammer et al., 2011; Melton et al., 2011).

Before the availability of fluorescent tags and high resolution confocal microscopy, tracking the movement of fatty acids in placental tissue was difficult. Fatty acid uptake and transport studies relied on radiolabeled lipid (Schaiff et al., 2005; Tobin et al., 2009; Brass et al., 2013) or immunohistochemical methods which cannot localize in real time. In contrast, new confocal visualization techniques reveal that long-chain fatty acids are esterified and sequestered into lipid droplets within hepatocytes (Kassan et al., 2013; Varlamov et al., 2013). These lipid droplets are the principal storage depots for neutral lipids (e.g. triglycerides and cholesterol-esters) in cells (Coleman and Lee, 2004). Functionally, LD provides for rapid storage, as well as mobilization, of fatty acids (Rambold et al., 2015). However, such studies have not been reported in placenta.

We hypothesized that the uptake, esterification and storage of a fluorescent long-chain fatty acid analogue, BODIPY-C_{12}, occur within the syncytiotrophoblast layer of the human placenta. BODIPY-C_{12} has an overall

chain-length approximately equivalent to that of an 18-carbon fatty acid, and has been used to understand the mechanisms of long-chain fatty acid uptake and trafficking in multiple models (Stahl et al., 1999; Wang et al., 2010; Kassan et al., 2013; Varlamov et al., 2013; Rambold et al., 2015). We used real-time optical methods to quantify for the first time, the dynamic processing of BODIPY-C_{12} within the major cell layers of freshly acquired human term placental explants and in isolated cytotrophoblast before and after syncytialization in culture.

Materials and Methods

All studies were approved by the Oregon Health & Science University Institutional Review Board (IRB# 5684). Written, informed consent for tissue collection was obtained prior to cesarean section surgery.

Subject Details

Women (>37 weeks gestation, Table 3.1) scheduled for cesarean section were recruited at Oregon Health & Science University (OHSU) Labor & Delivery. Exclusion criteria included multiple gestations, fetuses with chromosomal or structural anomalies including cardiac defects, preeclampsia, maternal hypertension, and any other significant co-morbidity. Maternal data obtained from medical records included age, parity, race, gestational age at delivery, height, and weight (1st trimester). Neonatal data included birth weight, crown-heel length, and sex. Placenta weight and length and width dimensions were measured during tissue collection.

Table 3.1: Maternal Characteristics

	Mean±S.D. (n=30)	**95% Confidence Interval**
Age (yr)	31±6	[29, 33]
Body Mass Index (BMI: kg/m^2)	27±6	[24, 29]
Parity	2±1	[2 , 3]
Gestational Age (weeks)	39±1	[38, 39]
Birth Weight (g)	3500±500	[3300 , 3700]
Placenta Weight (g)	570±140	[500, 630]

Tissue overview

Thirty placentas were used for different aspects of the study. In brief, placentas were collected at the time of delivery, maternal decidua was removed, and placenta were processed within 30 min. Placental tissues were used as (i) explants for live imaging/trafficking studies, (ii) fixed tissue immunofluorescence studies, (iii) dissociated cytotrophoblast cell studies for *in vitro* live imaging/trafficking studies, or (iv) molecular analysis of mRNA expression. A subset of fresh placental explants were embedded and frozen in OCT cryoprotectant (Cryotek) for immunohistochemistry and LD analyses.

Placental explant collection

Explants (<1mm^3) were isolated as previously described (Brass et al., 2013), with some modifications. Placental tissue was isolated from two different cotyledons that appeared healthy and placed in M199-HEPES culture media (Gibco) at room temperature (<30mins). Two explants from different cotyledons were cultured per well in plastic 8-well chamber slides (Lab-Tek II, Nunc) containing 0.4mL M199-HEPES and incubated at 37°C in 5% CO_2/95% air. All explants were assayed within 2-3hrs of delivery, a known window when markers of explant health and fatty acid uptake are not compromised (Sooranna et al., 1999; Brass et al., 2013).

Primary villous cytotrophoblast isolation and culture

Cytotrophoblast cells were isolated using trypsin-DNAse I digestion followed by Percoll enrichment as previously described (Kliman et al., 1986; Morrish et al., 1997). In brief, chorion and maternal decidua were removed, and approximately ~50g of villous placenta tissue was finely minced. Villous

fragments were subjected to three sequential 30 minute (37°C) digestions in 0.25% Trypsin (Gibco) and 200 U/mL DNAse I (Roche). Cytotrophoblasts were purified by Percoll (GE Healthcare Bio-sciences AB) discontinuous density gradient centrifugation at 1200 rcf for 25 minutes (room temperature). Purity of trophoblast isolations was assessed by positive immunohistochemical staining of cyokeratin-7 (MAI-06315, Thermo Scientific), a marker of trophoblast cells. Contamination by stromal cells and syncytial fragments was determined by staining for Vimentin (PA5-27231, Thermo Scientific) and BHCG (ab9582, Abcam). Our isolations comprised at least >90% pure, viable cytotrophoblasts.

Cytotrophoblasts were plated at a density of 3.5×10^5 cells cm^{-2} on 35 mm imaging dishes (Ibidi USA) compatible with high resolution live-microscopy. Cells were cultured in Iscoves Modified Dulbecco's Medium (IMDM, Gibco) supplemented with 10% FBS (Gibco) and 100U/ml penicillin and 100µg/ml streptomycin and incubated in a 5% CO_2/95% air incubator at 37°C. Cell viability was assessed by Trypan blue exclusion. After four hours in culture, non-adherent cells were removed by washing with pre-warmed culture media, and the media was subsequently replaced every 24 hours(Morrish et al., 1997). A subset of cells was used for live imaging studies, the remainder for qPCR studies. Cells were studied at 4 hours (cytotrophoblasts) or 72 hours (maximum) when most cytotrophoblasts have fused and differentiated into multinucleated, syncytial giant cells(Kliman et al., 1986; Frendo et al., 2003).

Fluorescent fatty acid tracking and live microscopy (explants, cells).

The use of fluorescently labeled fatty acids to study uptake and LD

formation has been adapted from adipocytes (Kassan et al., 2013; Varlamov et al., 2013)and applied to placental explants and cells. BODIPY-C_{12} is a long-chain fatty acid analogue that is well established as a tool to study fatty acid uptake and esterification in multiple models (Stahl et al., 1999; Wang et al., 2010) but has not been previously used in the human placenta. BODIPY-C_{12} is a 12-carbon chain length saturated fatty acid linked to the fluorophore BODIPY (4,4-difluoro-3a,4a- diaza-s-indacene) but the BODIPY-C_{12} conjugate biologically resembles an 18-carbon fatty acid. The BODIPY fluorophore is an intensely fluorescent, intrinsically lipophilic molecule, unlike most other long-wavelength dyes. Chemists argue that probes incorporating this fluorophore are more likely to mimic the properties of natural lipids. BODIPY fatty acids analogues undergo native-like transport and metabolism in cells making it effective as a tracer for lipid trafficking(Stahl et al., 1999; Wang et al., 2010).

We prepared 10μM solutions of BODIPY-FL C_{12} (BODIPY-C_{12}) (Molecular Probes) by diluting a 2.5mM methanol stock solution (1:250) in M199-HEPES containing 0.1% defatted bovine serum albumin (BSA) (Fisher Scientific); solutions were incubated at 37°C for 30mins, protected from light, to allow for BSA conjugation. For most experiments, explants and cells were exposed to BODIPY-C_{12} for 30mins. We sought to determine if exogenously applied fluorescent lipids would be rapidly incorporated into LD within a 30 minute period in human term placenta. The use of the word “rapid” here is not to indicate that placental tissues are able to esterify fatty acids more rapidly than other cells, but to suggest that there may be esterification processes which take much longer

than the 30 minute window we studied.

Explants

2μL ethidium homodimer (LIVE/DEAD Viability/Cytotoxicity Kit; Molecular Probes) and 1μL of HCS LipidTOX Deep Red (Molecular Probes) was mixed into each well containing placental explants. After 30mins, 100μL of 10μM BODIPY-C_{12} solution was added to each well and mixed by trituration (total well volume 500μL, final concentration 2μM BODIPY-C_{12}). To immobilize explants (live or fixed) for confocal microscopy, explants were held to the bottom of the imaging chamber using 8×8 mm pieces of stainless steel mesh (40 Mesh, 0.25 mm; TWP, Inc). For live microscopy, the chamber was also placed into a stage top 37°C incubation chamber. Imaging was performed using a Nikon A1R+/Eclipse TiE resonant scanning confocal microscope equipped with a 60× High N.A. objective (N.A.=1.4; Nikon). All images were acquired using the same acquisition configurations with minimum laser intensity (0.5%) and exposure time (900ms). Images were acquired every 20 seconds for a total of 30 minutes; there is non-appreciable photobleaching under these conditions. The pixel spacing for all acquisitions was constant and chosen to reflect the Nyquist sampling frequency at 488nm for the magnification objective used. To control for the effect of tissue light scattering, all images were gathered at a consistent distance range (5-10μm) from the culture well base.

Cultured cells

Live cytotrophoblast imaging proceeded as above, with a few modifications. Cytotrophoblasts were pre-incubated with Nile Red (1μg/ml;

Molecular Probes) for 30 minutes as a counterstain for neutral lipids, and the culture medium replaced with low-fluorescence Dulbecco's Modified Eagle Medium (Fluorobrite DMEM; Gibco) supplemented with 5% FBS. 2μM BODIPY-C_{12} was added to each well and cells were imaged using a Nikon Eclipse TiE/Yokogawa CSU-W1 spinning disc confocal using a 100× objective (N.A.=1.49) with 37°C and 5%CO_2/95% air environmental control. We favored Nile Red for *in vitro* LD labeling because its excitation properties permitted simultaneous excitation of BODIPY-C_{12} and Nile Red with a single laser line, resulting in less photobleaching. We confirmed no detectable bleed-through of neither BODIPY-C_{12} and Nile Red in either channel during the time window studied; the results were similar for LipidTOX. LipidTOX was used in addition to Nile Red as a second dye to ensure interpretation of neutral lipid localization. Nuclei were identified by Hoechst 33342 (0.5μg/ml; Molecular Probes) labeling; multinucleated cells were categorized as syncytiotrophoblast. Cell viability was assessed by Trypan blue exclusion.

Quantification of total BODIPY-C_{12} uptake in cells

Total BODIPY-C_{12} uptake was determined in cytotrophoblast cultures using a plate-reader assay as described previously(Sandoval et al., 2010). Cytotrophoblast were plated at 3.5 × 10^5 cells cm^{-2} in 96-well plates (BD Falcon) and cultured as described above. Cells were pre-incubated in 80μL serum free Iscove's Modified Dulbecco's Medium (IMDM) for 60 mins (± inhibitors). After 60 minutes, 20μL of assay solution (25 μM BODIPY-C_{12}, 25 μM defatted-BSA, 10mg/ml Trypan Blue) was added to each well, mixed, and

incubated for 15 minutes at 37°C with 5% CO_2/95% air. Fluorescence (485nm excitation, 525nm emission) was measured using a BioTek Synergy H1 hybrid plate reader (BioTek). After fluorescence measurement, the assay medium was removed and cells were carefully washed with Hank's Buffer for 10min at 37°C. The cells were then lysed using RIPA buffer (EMD Millipore) to measure protein using a BCA method (Pierce).

Inhibition of fatty uptake and esterification (explants, cells)

BODIPY-C_{12} uptake and fatty acid esterification are dependent on fatty acid transporters (FATP) and long-chain acyl-CoA synthetases (ACSL), respectively. Using a pulse-chase model, explants were exposed to 2μM BODIPY-C_{12} for 2 minutes, then washed with M199-HEPES, and incubated for another 30 minutes before fixation and immunolabeling. Immunolabeling allowed us to localize the fate of the BODIPY-C_{12} pulse after 30 minutes. To test if uptake and fatty acid esterification was sensitive to inhibition of FATPs or ACSLs, explants were co-incubated with 200μM phloretin (nonspecific transporter inhibitor (Guo et al., 2006); Sigma) during BODIPY-C_{12} uptake and imaging studies, or preincubated for 1hr with 10μM (in DMSO) triacsin C (long-chain acyl-CoA synthetase inhibitor; Santa Cruz Biotech) or 1hr with specified concentrations of CB-2 (FATP2 inhibitor; EMD Millipore) (Sandoval et al., 2010). The concentrations and incubation times employed are known to block fatty acid uptake and esterification in term explants and cytotrophoblast (Rybakowski et al., 1995; Greenwood et al., 1996; Weedon-Fekjaer et al., 2010).

In explants, we inhibited both syncytiotrophoblast and cytotrophoblast fatty

acid transporters and ACSL together; thus we could not conclude whether reductions in LD production were due to inhibition of uptake or esterification in the syncytium, or solely in the cytotrophoblast. To test if the production of BODIPY-C_{12} LD in cytotrophoblast was independent from the syncytiotrophoblast we performed complementary *in vitro* experiments in primary isolated term villous cytotrophoblasts. Cells were studied at 4 hours (cytotrophoblasts) and also at 72 hours after the cells had spontaneously fused and differentiated to form syncytial giant cells (Frendo et al., 2003). Co-localization was assessed in cultured cells at 15 minutes during continuous 2μM BODIPY-C_{12} incubation with or without phloretin or triacsin C. We used live spinning disc confocal microscopy together with Nile Red to track LD (Kassan et al., 2013) to determine whether alterations in cytotrophoblast LD production are independent of changes of uptake or esterification in the syncytium.

Immunofluorescence (whole mount explants, cells)

Explants were fixed in 4% paraformaldehyde (pH 7.4) for 20 minutes at room temperature before washing 3 times in phosphate buffered saline (PBS, pH 7.4), and stored in PBS at 4°C for up to 48 hours. Samples were blocked and permeabilized in 5% normal goat serum (Life Technologies)/0.1% saponin (Sigma) for 1 hour before overnight incubation with primary antibody at 4°C. Samples were labeled with antibodies against BHCG (1:100; ab9582, Abcam), E-cadherin (1:200; ab11512, Abcam), HAI-1 (1:100; 9B10, eBioscience), FATP2 (1:50; 14048-1-AP, Proteintech), Perilipin-2 (1:100; ab52355, Abcam), and Perilipin-3 (1:100, PA5-20272, Thermo Scientific). Following primary antibody

incubation, samples were washed 3 times with 0.1% saponin in PBS and labeled with secondary antibodies (donkey F(ab')2 anti-mouse Alexa Fluor 647 (1:1000, ab150103), donkey F(ab')2 anti-rat Alexa Fluor 555 (1:1000, ab150150), donkey F(ab')2 anti-rabbit Alexa Fluor 568 (1:500, ab175694), donkey F(ab')2 anti-rabbit Alexa Fluor 647 (1:1000, ab150103), and donkey anti-rabbit Alexa Fluor 488 (1:1000, ab150069); all secondary antibodies from Abcam) for 1 hour at room temperature. After washing 3 times, the samples were counterstained with 1μg/ml Hoechst 33342 for 10 minutes and immersed in Slowfade Diamond (Molecular Probes) immediately before confocal imaging. Slowfade Diamond did not disrupt LD morphology and photobleaching resistance was substantially improved over samples imaged in PBS. Imaging was performed using a Nikon A1R+/Eclipse TiE resonant scanning confocal microscope equipped with a 60× High N.A. objective (N.A.=1.4; Nikon).

Structured Illumination Microscopy (SIM) Imaging (explants)

Our initial estimates by confocal fluorescence microscopy of LD diameter (~600nm) were near the diffraction resolution limit for light (Airy disc diameter = 560nm; wavelength =640nm, N.A.= 1.4). Thus, measurements by standard optical techniques may overestimate the true size of an LD. Hence we used structured illumination microscopy (SIM) which affords, under ideal conditions, a 2-fold increase in the lateral spatial resolution and is compatible with conventional fluorophores such as LipidTOX. Using SIM, our theoretical Airy disc diameter is 280nm (wavelength=640nm, N.A.=1.4). Since the volume of a spherical LD scales with the cube of its radius, a small increase in lateral

resolution can afford a dramatic increase in the minimum detectable volume of LDs; SIM under ideal conditions permits more accurate measurement of particles 8-fold smaller than possible using conventional confocal fluorescence microscopy.

For super-resolution microscopy of LD via SIM, explants were stained with LipidTOX Deep Red. Structured illumination microscopy was performed using an Elyra PS.1 (Zeiss) microscope equipped with a 63× objective (N.A.=1.4). Thin (0.1 μm) z-stacks of 20 high resolution images were collected in five rotations and reconstructed using Zen software (Zeiss). All processed images were analyzed using Fiji (Schindelin et al., 2012).

Image Analysis

All images obtained via confocal and SIM imaging were analyzed using Fiji software(Schindelin et al., 2012). LD were automatically segmented using the Renyi Entropy method, and quantified using consistent particle analysis parameters in Fiji and are expressed as a number (abundance) normalized to the acquired 3-D image volume of syncytiotrophoblast or cytotrophoblast. In all immunofluorescence explant experiments, replicates represent at least 2 explants, each with at least 2 independent fields of view. For live imaging of explants, 2 separate explants were imaged with one field of view that demonstrated exclusion of ethidium homodimer dead stain. On average about 90 LD were measured per replicate using SIM imaging. In live-cell imaging experiments, each time point represents the mean of a maximum-intensity projection of 20 z-slices (0.2 μm thick) representing a 3-D volume with 4μm total

thickness. With the plating density utilized, about 10 nuclei were present in a single 3-D volume on average. Co-localization analyses were performed using Imaris (Bitplane AG) and Fiji using the automatic thresholding method of Costes et al. (Costes et al., 2004) to obtain a Pearson co-localization coefficient; this coefficient indicates the degree to which BODIPY-C_{12} is being incorporated into the LD organelles identified by Nile Red or LipidTOX (Kassan et al., 2013).

qPCR gene expression

A subset of primary cytotrophoblasts was used for gene expression studies; these cells were not used for imaging studies. Total RNA from 3×10^6 cells was isolated after 4hr or 72hr of culture using Qiagen RNeasy isolation kit. RNA content was assessed by spectroscopy at 260nm/280nm and integrity via visualization of ribosomal RNA using gel-electrophoresis. Reverse transcription of 750ng of RNA to cDNA was performed using the High Capacity cDNA Reverse Transcription kit (Life Technologies). cDNA was stored at -20°C. Gene specific primers were designed for fatty acid transporter 2 (*SLC27A2*), and long-chain acyl-CoA synthetase 1 (*ACSL1*), -3 (*ACSL3*), and -5 (*ACSL5*), fatty acid binding proteins 4 (*FABP4*), -5 (*FABP5*), 1-acylglycerol-3-phosphate O-acyltransferase 9 (*GPAT3*), lysophosphatidylcholine acyltransferase 3 (*LPCAT3*), and BHCG (*CGB*) using NCBI primer-BLAST(Ye et al., 2012). Sequences for primers for GAPDH, fatty acid transporters 1 (*SLC27A1*), -4 (*SLC27A4*) and fatty acid translocase (*CD36*) were obtained from Brass et al. and Mishima et al. (Mishima et al., 2011; Brass et al., 2013). Primer sequences and gene information are shown in Table 3.2; qPCR was performed as described

previously(O'Tierney et al., 2012). PCR amplicons were detected by fluorescence of Power SYBR Green (Applied Biosystems) and following manufacturers recommendations using the Stratagene Mx3005P Thermocycler (Agilent Technologies). Cycling conditions were the same for all primer pairs with 42 amplification cycles. For each primer pair, a standard curve, no template controls and unknowns were run in triplicate. Following cycling, the melt curve of the resulting amplicon was analyzed to ensure that a single product was detected for every replicate. Efficiency of each primer set was calculated using the slope of the respective standard curves with manufacturer's software (MxPro v4.10; Stratagene) and the predicted product size for each primer pair was verified via gel-electrophoresis. The cycle threshold (Ct) was calculated for each replicate using MxPro software for detecting the amplification-based threshold. No replicates were excluded and all replicates were within 0.5 SD of the average Ct. Relative expression was quantified using comparative quantification (Pfaffl, 2001). The same sample was used as the "calibrator" in all assays. Relative expression quantities were expressed as a ratio of the gene of interest to the reference gene (*GAPDH*) in each sample; *GAPDH* expression did not differ at 4 hours versus 72 hours.

Table 3.2: Primer sequences utilized for quantitative PCR

Gene	Function	Accession	Forward (5'→3')	Reverse (5'→3')
ACSL1	Long-chain fatty acid acyl-CoA synthetase	NM_001995	GGGCAGGGAG TGGGCT	TCTAAGCTGAA TTCTCCTCCGT G
ACSL3	Long-chain fatty acid acyl-CoA synthetase	NM_004457	GGCGTAGCGGT TTTGACAC	CCAGTCCTTCC CAACAACG
ACSL5	Long-chain fatty acid acyl-CoA synthetase	NM_016234	CTGAAGCCACC CTGTCTCTG	AGGAAATTCAG ACCCTGCGA
GAPDH	Reference gene	NM_002046	AGGTGGTCTCC TCTGACTTC	TACTCCTTGGA GGCCATGTG
GPAT3	*De novo* glycerolipid synthesis	NM_001256421	GAGGGCCTCCA GGTGAGT	AGAGACACTCC GAAGACCGA
CD36	Fatty acid transporter	NM_001001548	AAACCTCCTTG GCCTGATAG	GAATTGGCCAC CCAGAAACC
BHCG (CGB)	Marker for cytotrophoblast syncytialization	NM_00737	ACCCCAGCATC CTATCACCT	CACGCGGGTCA TGGTG
CPT1A	Fatty acid transporter located on mitochondrial outer membrane	NM_001876	ATTACGTGAGC GACTGGTGG	TGTGCTGGATG GTGTCTGTC
FABP4	Fatty acid binding protein	NM_001442	AAACTGGTGGT GGAATGCGT	GCGAACTTCAG TCCAGGTCA
FABP5	Fatty acid binding protein	NM_001444	TGAAGGAGCTA GGAGTGGGAA	TCTGCCATCAG CTGTGGTTT
LPCAT3	Glycerophospholipid synthesis	NM_005768	TTCCTGGGTTA CCCCTTTGC	GCCGGTGGCA GTGTAATAGT
SLC27A1	Fatty acid transporter	NM_198580	CCGGAATTGAC TGTGACCACTT	CACGCAGTGCA GGGTTCA

SLC27A2	Fatty acid transporter	NM_003645	TGCTGCACTAC TGATTGGCA	TTGGTTTCTGT GGTGAGTTGC
SLC27A4	Fatty acid transporter	NM_005094	GCTGCCCTGGT GTACTATGG	GGAGGCTGAAG AACTTCTTCC

Electron Microscopy

Electron microscopy of term placental tissue was performed as previously described (Thornburg and Faber, 1976). Placental pieces were fixed in 2.5% glutaraldehyde/2% formalin in 0.1 M phosphate buffer for 45 minutes. The tissue was then sliced into thinner pieces and allowed to fix for an additional 30 minutes. Lastly, the tissue was cut to embedding size and fixed for 30 minutes before being placed in 0.1 M phosphate buffer, pH 7.3, 4°C overnight. The next day, the tissue blocks were post fixed for 90min in 2% osmium tetroxide, dehydrated in ethanol series and embedded in Epon resin. Electron micrographs were made on JEOL electron microscopes.

Lipid Extraction and Thin Layer Chromatography

The incorporation of BODIPY-C_{12} into lipid classes was characterized as described previously (Wang et al., 2010). Cells were incubated with 5μM BODIPY-C_{12} in 6-well dishes and were collected and washed with HBSS containing 0.1% BSA at specified time points. Lipids were extracted using chloroform and the lipid phase was collected and evaporated using a vacuum concentrator (SpeedVac). Lipid residues were dissolved in 100μL of chloroform and applied onto silica gel 60G TLC plates (EMD Millipore). Neutral lipids were separated on TLC plates using heptane/isopropyl ether/acetic acid, 60:40:4, vol/vol/vol). Developed plates were visualized under UV light (365nm) using an emission filter (515-570nm) and images were captured using a digital camera.

Statistics

ANOVA with Bonferroni post-hoc testing was used to test for differences in

LD abundance via SIM in LD analyses (one-way) and BODIPY-C_{12} LD accumulation in each cell type (2-way). Total BODIPY-C_{12} uptake and qPCR were analyzed by a paired t-test. A four parameter, nonlinear regression analysis was used to calculate IC_{50} values for CB-2 FATP2 inhibitor. All data were analyzed using GraphPad Prism 6 and are presented as mean ± SEM unless noted otherwise. P-values <0.05 were considered statistically significant.

Study Approval

Studies were approved by the Institutional Review Board (IRB # 5684). Written, informed consent for tissue collection was obtained prior to cesarean section surgery.

Results

Lipid droplet (LD) analysis in explants

The existence and localization of LDs in human term placenta was confirmed in all 30 placentas using several modalities of microscopy and multiple staining methods (Figure 3.1B-E). LDs were visible in the syncytiotrophoblast, cytotrophoblast and fetal endothelium. LD volumes in cytotrophoblast ($0.047 \pm 0.006\ \mu m^3$) were similar to syncytiotrophoblast ($0.038 \pm 0.003\ \mu m^3$) (Figure 3.1F, N.S.). Likewise, LD abundance was not different between cytotrophoblast ($3 \times 10^7 \pm 4 \times 10^6$ LD mm^{-3}) and syncytiotrophoblast ($3 \times 10^7 \pm 5 \times 10^6$ LD mm^{-3}). We found no associations between LD volume or abundance with fetal sex in syncytiotrophoblast or cytotrophoblast. These data suggest that LD are a normal feature of all human term placentas. The presence of LD in normal placenta, led us to speculate that the syncytiotrophoblast was capable of free fatty acid esterification and that LD in cytotrophoblast originated from those manufactured in the syncytium. We also supposed that the transfer of LD from syncytial tissue to deeper layers in the placenta could be visualized in real-time using microscopic methods.

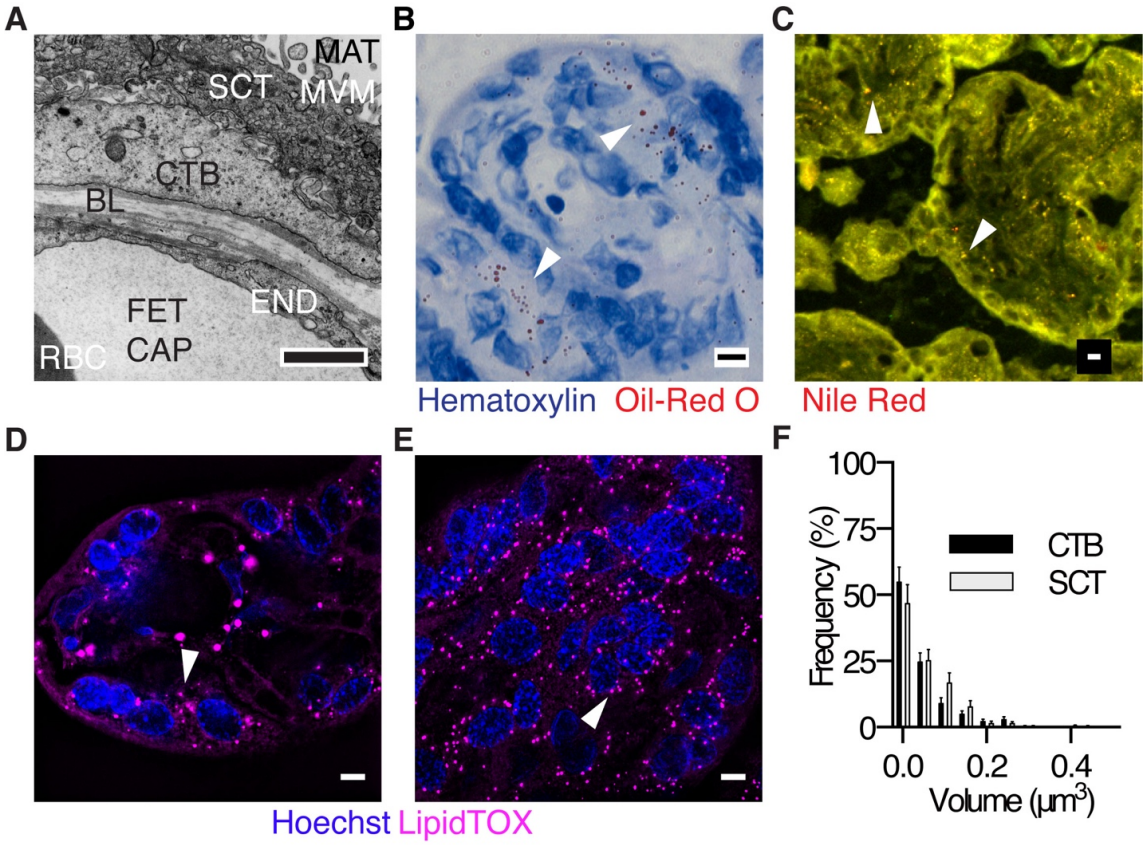

Figure 3.1 The layers of the human placenta at term and resident lipid droplets.

(A) TEM of human placenta at term. MAT, maternal blood space; MVM, microvillous membrane; SCT, syncytiotrophoblast; CTB, cytotrophoblast; END, endothelium; FET CAP, fetal capillary; RBC, red blood cell; BL, basal lamina. Scale Bar: 1μm. (B-E) Lipid droplets (LD, arrow heads) in the human placenta can be detected by multiple staining methodologies. (B) Oil-Red O (C) Nile Red (D-E) Structured illumination microscopy (SIM, a super-resolution technique). Only the syncytiotrophoblast is imaged in (E). (F) The LD volume distribution in freshly delivered placenta is not different (One-way ANOVA) between cytotrophoblast (CTB) and syncytiotrophoblast (SCT) layers, as measured by SIM. (Data are mean ± SEM, n=7, unpaired t-test). Scale Bar (B-E): 5μm.

BODIPY-C_{12} uptake in live and fixed explants

We sought to determine whether exogenous fluorescent-labeled BODIPY-C_{12}, a long-chain fatty acid analogue, would be incorporated into syncytiotrophoblast LD of living explants within 30 minutes, a technique and time period that has been used in other tissues including white adipose tissue (Varlamov et al., 2013). Uptake and distinct localization patterns of BODIPY-C_{12}became evident within 30 min. BODIPY-C_{12} appeared both diffusely and as punctate structures within the cytoplasm of placental tissue, which we surmised to be the syncytium and the cytotrophoblast (Figure 3.2A). LDs are composed of endogenous neutral lipids (triglycerides and cholesterol-esters) (Coleman and Lee, 2004) that can be visualized by LipidTOX staining (Figure 3.2B). As indicated by merged staining, BODIPY-C_{12} was incorporated into preexisting LipidTOX positive LD within 20 minutes, signifying that (Figure 3.2C) it was being esterified, a requirement for LD incorporation (Wang et al., 2010). Surprisingly, esterification was consistently associated with the cell layer beneath the syncytiotrophoblast, which appeared to be cytotrophoblast (Figure 3.2C,D). To test this, placental tissues were stained with hepatocyte growth factor inhibitor type 1 (HAI-1), a cytotrophoblast-specific marker (Mori et al., 2007). It confirmed that the cells containing newly esterified BODIPY-C12 were cytotrophoblasts (Figure 3.2E). The cytotrophoblast layer appeared to be rarely interrupted under our microscopic conditions and was the layer that rapidly accumulated esterified BODIPY-C_{12} (Figure 3.2G). In separate experiments, explants fixed after 30 min also confirmed co-localization of BODIPY-C_{12} with LipidTOX in LD organelles

within the cytotrophoblast, but not within the syncytiotrophoblast (Figure 3.2D-F), in which there was little co-localization between the markers even by 60 minutes (not shown). In a separate set of experiments, placental tissues were exposed to a 2 minute pulse of BODIPY-C_{12}, followed by washout, to determine the fate of fatty acids initially absorbed by the syncytiotrophoblast. From previous experiments, we determined that incorporation of BODIP-C_{12} into LD required 30 minutes. We measured LD production after initial uptake using this time point. Thirty minutes after the 2 minute pulse, the abundance of BODIPY-C_{12} labeled LD was higher in cytotrophoblast than syncytiotrophoblast ($2\times10^{7} \pm 3\times10^{6}$ LD mm^{-3} versus $6\times10^{4} \pm 2\times10^{4}$ LD mm^{-3}; $p<0.001$, Figure 3.2J). The number of BODIPY-C_{12} LD in cytotrophoblast was dramatically reduced following treatment with the nonspecific transporter inhibitor, phloretin, ($1\times10^{5} \pm 8\times10^{4}$ LD mm^{-3}; $p<0.001$, Figure 3.2H,J) and the long-chain acyl-CoA synthetase inhibitor, triacsin C ($1\times10^{6} \pm 3\times10^{5}$ LD mm^{-3}; $p<0.05$, Figure 3.2I,J), implying both FATP and ACSL are involved in the rapid production of BODIPY-C_{12} LD. In contrast, LD abundance in the syncytiotrophoblast was not altered by phloretin ($5\times10^{3} \pm 4\times10^{3}$ LD mm^{-3}) or triacsin C ($5\times10^{3} \pm 5\times10^{3}$ LD mm^{-3}, Figure 3.2J).

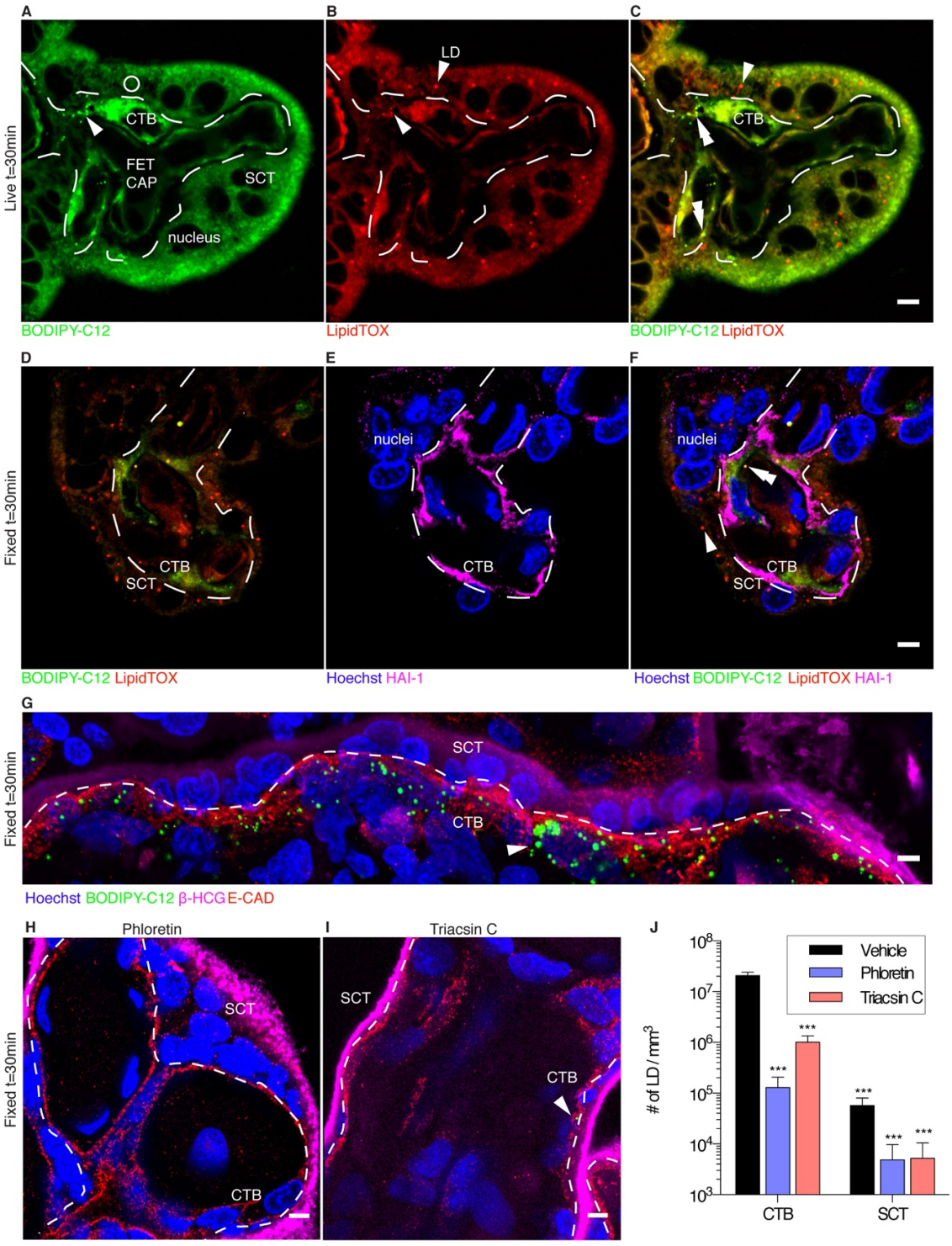

Figure 3.2 BODIPY-C_{12} fatty acid uptake in human term placental explants (30 min exposure).

Dashed line represents the syncytiotrophoblast-cytotrophoblast interface. Co-localized BODIPY-C_{12} and LipidTOX forms yellow LD, indicating esterified BODIPY-C_{12}. (A) BODIPY-C_{12} (green) is localized to punctate structures (arrow heads) and diffuse areas in syncytiotrophoblasts (SCT) and cytotrophoblasts

(CTB). Dark “holes” are unstained nuclei. (B) Pre-existing neutral lipids (LipidTOX, red) are found in punctate structures which are lipid droplets (LD) (arrow head); (C) LipidTOX co-localizes with BODIPY-C_{12} (double arrowhead) predominantly in CTB, providing evidence that BODIPY-C_{12} is esterified and localized within LD. Conversely, in SCT, LD (arrowhead) contains little BODIPY-C12 (corresponding region 2A open circle). (D-F) images of explants after fixation showing BODIPY-C_{12} (green) and LipidTOX (red). (D) LD are present in both SCT and CTB, but BODIPY-C_{12} seen in (A) has mostly washed out in processing but some remain in sequestered organelles. (E) Hoechst (blue) marks nuclei and HAI-1 (magenta) marks CTB, (F) BODIPY-C_{12} (green) is found primarily in CTB (magenta) but not in SCT (see double arrow head). (G) BODIPY-C_{12} containing lipid droplets (arrow heads) are found extensively in the CTB layer (e-cadherin, red) but are sparse in the SCT layer. (H) phloretin (a blocker of protein mediated transport), and (I) triacsin C (a blocker of long-chain fatty acyl-CoA synthetases) reduces the population of lipid droplet containing BODIPY-C_{12} in CTB. These experiments suggest that transporters and acyl-CoA synthetases are required for production of LD. (J) Quantification of lipid droplets synthesized in explants illustrating the effects of chemical inhibitors and shows under control conditions BODIPY-C_{12} LD accumulation is higher in 30 min in the CTB vs. SCT; (I): Data are mean ± SEM; n=6 control, n=5 phloretin, and n=4 triacsin C. 2-way ANOVA, ***= $p<0.001$ vs CTB vehicle; VS, villous stroma; FET CAP, fetal capillary; Scale Bar: 5μm.

BODIPY-C_{12} uptake in live, isolated undifferentiated cytotrophoblast

Cytotrophoblasts are unique in that they are isolated in their immature undifferentiated form but become mature over time in culture to form multinucleated syncytialized giant cells, presumably as *in vivo*. We used the differentiation process to determine whether the capacity to esterify fatty acids was lost during differentiation and syncytialization. To test if esterification was taking place within cytotrophoblast, we analyzed BODIPY- C_{12} incorporation into lipid subclasses via thin-layer chromatography in isolated primary cytotrophoblast. We found that BODIPY-labeled neutral lipids were present within 30 minutes (Figure 3.3A), and that differentiation of cytotrophoblast (4hr) to syncytiotrophoblast (72hr) led to a pronounced decrease in esterified BODIPY-C_{12} esterification products (Figure 3.3B). This finding is consistent with the observation that BODIPY-C_{12} is esterified during integration into cytotrophoblastic LDs and that differentiation results in a switch in lipid metabolic phenotype.

We measured total uptake of BODIPY-C_{12}, using a plate reader before and after cytotrophoblast differentiation/syncytialization. BODIPY-C_{12} Uptake was approximately 2-fold greater in cytotrophoblast at 4hr (1.8×10^3 ± 37 RFU /μg protein) than in syncytial giant cells at 72hr (7×10^2 ± 74 RFU /μg protein; $p<0.01$, Figure 3.3J). We also tested the degree to which BODIPY- C_{12} uptake in cultured trophoblast was sensitive to CB-2, an inhibitor of FATP2. FATP2 is the most highly expressed fatty acid transporter in the placenta (Weedon-Fekjaer et al., 2010). The similar efficacies and estimates of IC_{50}s of CB-2 indicates 4hr cytotrophoblast and 72hr syncytial giant cells are not differentially sensitive to

CB-2 (4hr, 13 ± 2.4 μM) vs (72hr, 8 ± 1.6 μM; Figure 3.3K) and thus both of these cell types are likely dependent on FATP2 for the uptake of BODIPY-C_{12} long-chain fatty acid.

Primary villous trophoblast accumulates BODIPY-C_{12} LD at different rates depending on the degree of maturation. Cytotrophoblasts (4hrs, Figure 3.3C-E) had greater abundance of BODIPY-C_{12} LD than syncytialized cells (72hrs, Figure 3.3F-H) ($1\times10^6 \pm 0.3\times10^6$ LD mm^{-3} vs $4\times10^4 \pm 1\times10^5$ LD mm^{-3}; $p<0.01$, Figure 3.3I). Consistent with our explant experiments, BODIPY-C_{12} LD abundance was reduced by phloretin ($5\times10^4 \pm 6\times10^4$ LD mm^{-3}; $p<0.01$) and triacsin C ($1\times10^4 \pm 3\times10^4$ LD mm^{-3}; $p<0.01$) in cytotrophoblasts (Figure 3.3I) and with minimal effect on syncytial giant cells (Figure 3.3G).

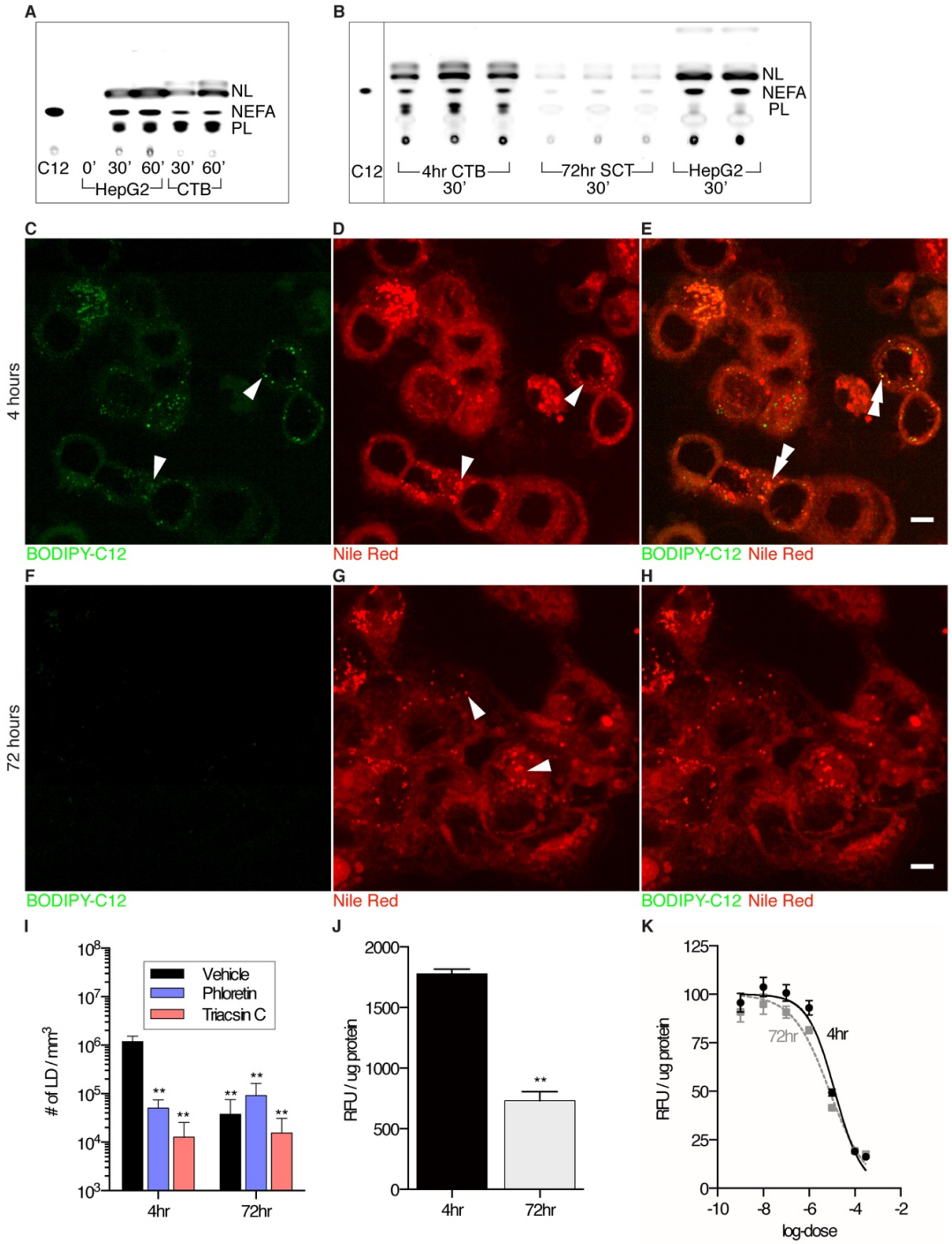

Figure 3.3 BODIPY-C_{12} incorporation into lipid droplets in primary cytotrophoblasts incubated for 15 or 30 min.

Cytotrophoblasts (CTB) were in two states of maturation after being in culture for 4hr(A,C-E) or 72hr which leads to syncytialization (SCT) (B,F-H). (A,B) Analyses of BODIPY- C_{12} incorporation into lipid subclasses via thin-layer chromatography in CTB and SCT *in vitro* (A) Time course of HepG2 cells (positive control) and primary cytotrophoblast incubated continuously with BODIPY-C_{12}. BODIPY-C_{12} is incorporated into neutral lipids (NL) and phospholipids (PL) within 30 minutes

indicating esterification of this long-chain fatty acid analogue. NEFA, non-esterified fatty acid. (B) CTB incorporate more BODIPY-C_{12} into esterified lipid subclasses than SCT *in vitro* within 30 minutes. (D) Cultures (D,E and G,H) were stained with Nile Red to visualize neutral lipid droplets (LD). Images (C,F) shows that BODIPY-C_{12} incorporation is greater among CTB than among SCT. (E) In CTB, BODIPY-C_{12} merges with Nile-Red in LD. (H) When CTB have undergone syncytialization, they incorporate very little BODIPY-C_{12} in LD. (I) Quantification of lipid droplets shows that cultured (4 hours) cells accumulate more BODIPY-C_{12} LD than those that have syncytialized (72hrs). Phloretin and triacsin C significantly reduce BODIPY-C_{12} LD accumulation in cytotrophoblasts but not in syncytialized cells. (J) The uptake of BODIPY-C_{12} using a 96-well plate-reader indicates that uptake is higher in cytotrophoblast before syncytialization (K) The log-dose response curve of CB-2, a FATP2 inhibitor, supports that both cytotrophoblast and syncytialized cells are equally sensitive to inhibition of BODIPY-C12 uptake by CB-2. The efficacy of this inhibition of BODIPY-C_{12} uptake suggests that FATP2 largely mediates long-chain fatty acid uptake in these cells. TLC plates are representative of 3 technical replicates. (C-H): Scale Bar: 5μm, LD (arrow heads), co-localization (double arrowhead). Image intensity ranges are the same in all panels (I-K): Data are mean ± SEM; (I) n=6 for each group. 2-way ANOVA, (J,K) n=4. Paired t-test. *= $p<0.05$, **=$p<0.01$ vs CTB vehicle.

To test if the BODIPY-C_{12} LD are labeled by LD-associated proteins, we fixed and immunolabeled 4hr CTB after 30 minutes of incubation with BODIPY-C_{12}. We found all BODIPY-C_{12} LD in CTB contained some degree of LD associated Perilipin-2 or Perilipin-3 (Figure 3.4). We detected little BODIPY-C_{12} LD synthesis in 72hr syncytialized cells.

Lipid transporter gene expression in cultured cytotrophoblasts

After 72hrs, *BHCG* mRNA expression in cultured cytotrophoblasts was >4500% higher ($p<0.05$), indicating differentiation into syncytial giant cells; *BHCG* is a specific marker of syncytialization. We also looked for the presence of desmoplakin, which disappears from intercellular junctions with syncytialization. Junctional complexes were absent in syncytial giant cells as indicated by the loss of desmoplakin concomitant with cytotrophoblast syncytialization, there was a pronounced decrease in *SLC27A2* expression, the gene encoding FATP2 (-88%, $p<0.001$). Genes regulating glycerolipid metabolism were downregulated during syncytialization: *GPAT3* (-75%, $p<0.05$), *ACSL5* (-60%, $p=0.002$), *FABP4* (-38%, $p<0.05$), and *LPCAT3* (-66%, $p<0.001$). In contrast, mRNA levels of *SLC27A4* (FATP4; +133%, $p<0.1$), *CD36/FAT* (+349%, $p<0.001$), and *SLC27A1* (FATP1; +129%, $p<0.01$) increased during syncytialization. We did not detect differences in of *FABP5*, *ACSL1*, *ACSL3*, or *CPT1A* expression (data not shown). FATP2 (*SLC27A2*) is highly expressed in the placenta and we found it is distinctly localized to the cytotrophoblast (Figure 3.5J,K) perhaps within a discrete subcellular compartment.

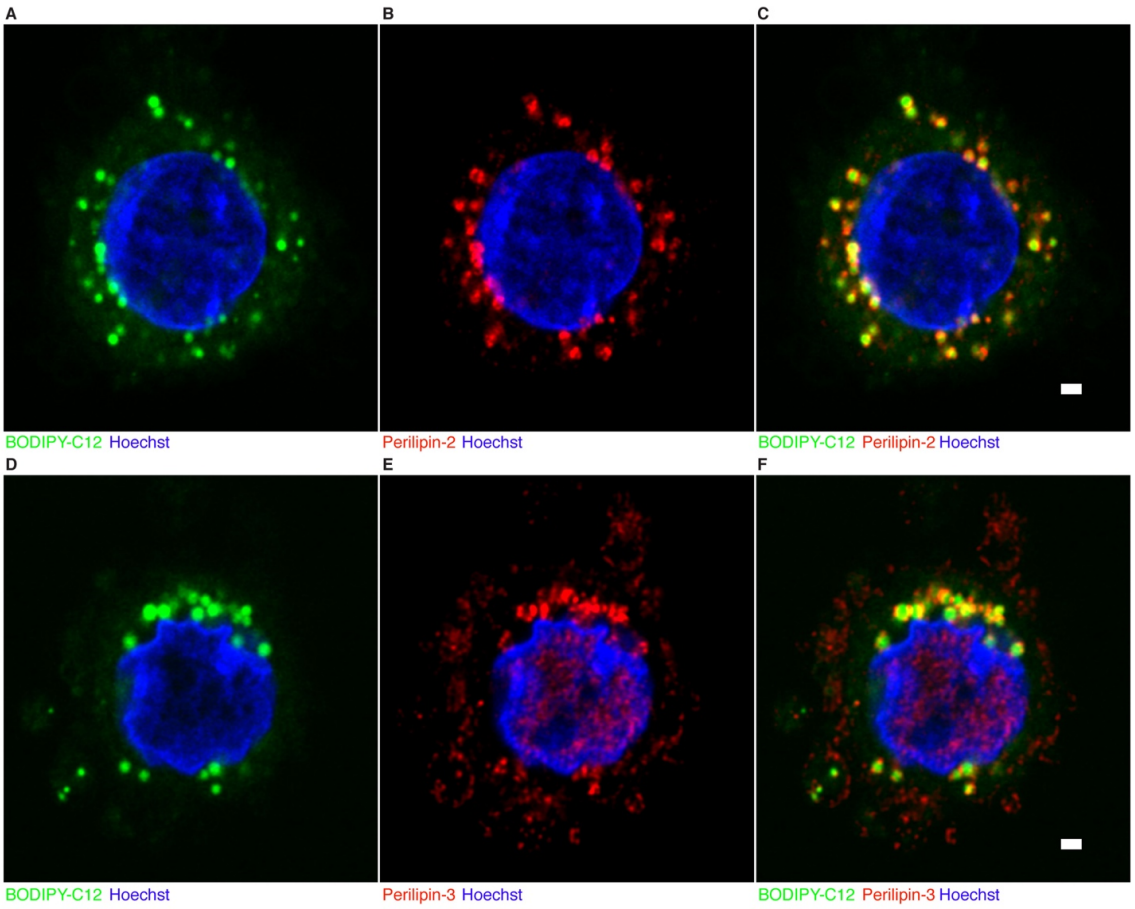

Figure 3.4 BODIPY-C_{12} incorporates into Perilipin-2 and Perilipin-3 labeled cytotrophoblast lipid droplets.
Cytotrophoblast plated for 4hr onto glass coverslips were incubated with 2μM BODIPY-C_{12} for 30 minutes and fixed as described in the methods section. Cells were immunolabeled with Perilipin-2 or Perilipin-3. Nuclei are labeled using Hoechst dye. All BODIPY-C_{12} cytotrophoblast lipid droplets contain some degree of Perilipin-2 (A-C) or Perilipin-3 (D-F) on the surface. In addition to the presence of Perilipin-3 on lipid droplets, Perilipin-3 is also distributed on the plasma membrane of cytotrophoblast (E). n=5. Scale Bar: 1μm.

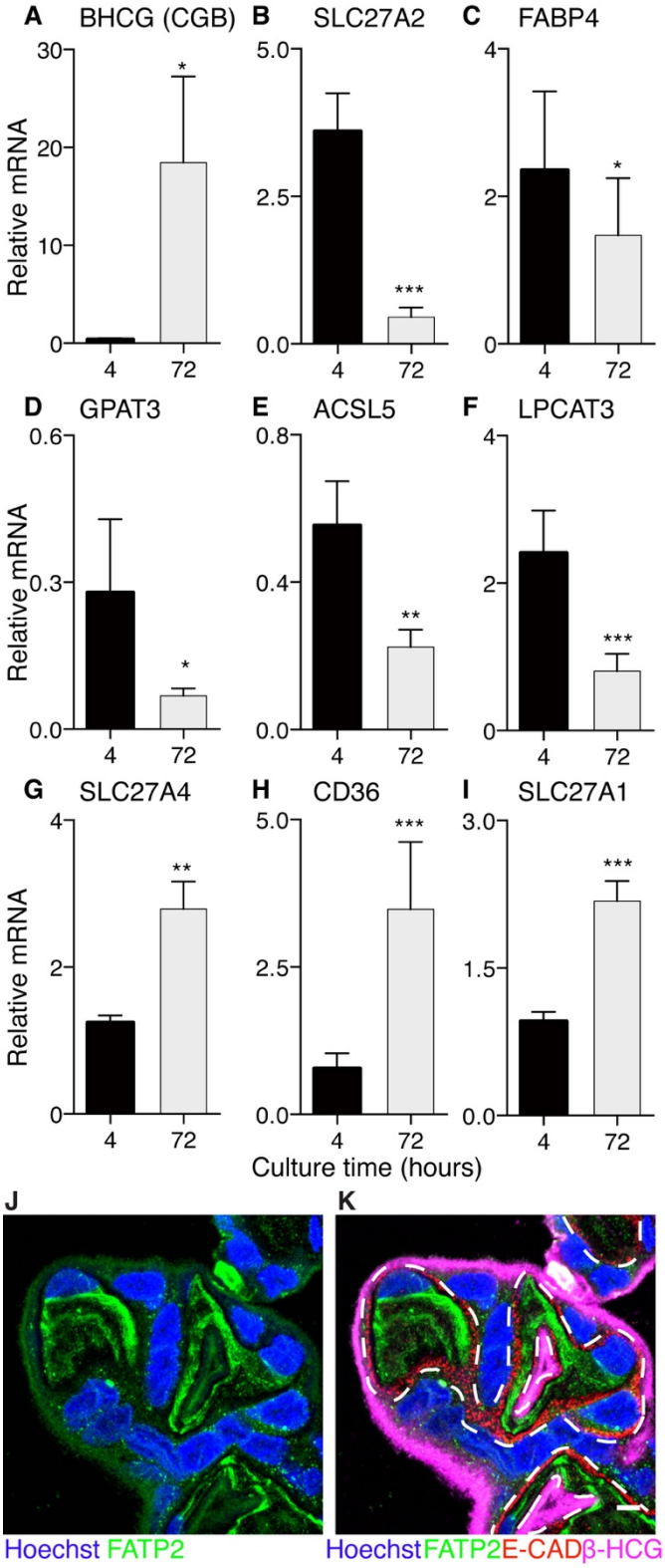

Figure 3.5 mRNA expression of key lipid processing genes before and after cytotrophoblast syncytialization. (A) In 72hr syncytia, the expression of *BHCG* is significantly higher compared to cytotrophoblast at 4hrs, indicating differentiation. (B-I) By 72 hours, there are significant changes in expression of several fatty acid uptake and processing genes. (B) *SLC27A2* (FATP2, the most highly expressed fatty acid transport protein in placenta). (C) *FABP4* (fatty acid binding protein). (D) *GPAT3* (glycerol-3-phosphate acyltransferase). (E) *ACSL5* (Acyl-CoA synthetase, long-chain). (F) *LPCAT3* (lysophosphatidylcholine acyl transferase). (G) *SLC27A4* (FATP4, fatty acid transport protein). (H) *CD36* (FAT, fatty acid translocase). (I) *SLC27A1* (FATP1, fatty acid transport protein). Data are mean ± SEM, n=6 for all groups. Expression is relative to GAPDH, which is not significantly different between groups. Paired t-test *= p<0.05, **=p<0.01, ***=p<0.001. (J) Immunofluorescence of FATP2 (green), nuclei are blue (Hoechst). (K) Merged immunofluorescence illustrating cytotrophoblast (E-cadherin, red), syncytiotrophoblast (BHCG, magenta) with FATP2/SLC27A2 (green). FATP2 can be found in both cytotrophoblast and syncytiotrophoblast,

but appears to be more strongly expressed in cytotrophoblast which fits gene expression data in panel (B). Dashed line represents the syncytiotrophoblast-cytotrophoblast interface. Scale Bar: 5μm.

Discussion

We tested the hypothesis that BODIPY-C_{12} would be incorporated into esterified lipid pools within syncytiotrophoblast. We chose BODIPY-C_{12} as a tracer because it is well-established tool to investigate long-chain fatty acid uptake and esterification in many cell types (Stahl et al., 1999; Wang et al., 2010). The strength of the method is that fatty acid uptake can be tracked in real-time within different cell layers and sub-cellular compartments of the placenta.

Contrary to our hypothesis, the syncytiotrophoblast was not the primary site of esterification of this synthetic long-chain fatty acid. Rather, BODIPY-C_{12} esterification occurred almost exclusively in the cytotrophoblast. We were surprised to find that the syncytiotrophoblast seemed to be incapable of esterifying BODIPY-C_{12}. We were forced to conclude that the cytotrophoblast plays a previously unsuspected role in placental lipid metabolism.

It has been previously reported that the cytotrophoblast layer, found beneath the syncytial layer becomes increasingly interrupted as gestation proceeds (Benirschke et al., 2012). This view contributed to the conclusion that cytotrophoblast plays an insignificant role in transport processes as term approaches. In contrast, Mori et al. suggested that the cytotrophoblast cell layer is nearly continuous over most of the villous placental surface until term (Mori et al., 2007). Furthermore, although the layer gets thinner toward term, the total number of cytotrophoblast cells increases, by approximately 6 fold, between the first and third trimester (Simpson et al., 1992).

Lipid droplets have been biochemically detected in placenta and isolated

by others (Hernández-Albaladejo et al., 2014). In our study, we were able to visualize LD in all term human placentas examined using an array of microscopic techniques (Figure 3.1). Because high concentrations of non-esterified fatty acids can be cytotoxic, incorporation into LD offers safe storage and a way to regulate fatty acid trafficking (Listenberger et al., 2003). We did observe a portion of exogenous BODIPY-C_{12} that was taken up by cytotrophoblast but not incorporated into pre-existing LD within the time frame of our experiments. The fate of the unincorporated fatty acid fraction is not known. In similar experiments performed in hepatocytes, there are pre-existing LDs that immediately incorporate BODIPY-C_{12} akin to our neutral LDs in placenta, but these cells also contain a secondary LD population that arises within minutes after being incubated with BODIPY-C_{12} (Kassan et al., 2013). Like the hepatocyte experiments, we found new lipid droplets in cytotrophoblast within minutes of exposure to BODIPY-$C_{12.}$ Our live imaging studies were limited to 30-60 minute windows to ensure that tissues were metabolically stable (Kassan et al., 2013). Alternatively these structures may represent sites of phospholipids incorporating BODIPY-C_{12}, as we have observed BODIPY-C_{12} incorporation into CTB phospholipid pools during esterification (Figure 3.3).

BODIPY-C_{12} may approximate some features of long-chain fatty acids, but further tests are warranted to delineate how these results translate to the esterification of natural long-chain fatty acids in trophoblast. Primary cultured human cytotrophoblast cells are highly active in esterification and lipolysis of ^{14}C radiolabeled oleic acid (Coleman and Haynes, 1987) but show a 2-3 fold

decrease in fat esterification and glycerolipid synthesis after 72 hours in culture (Coleman and Haynes, 1987). Our findings point to a decline in esterification occurring concurrently with syncytialization.

Although LD are present in the syncytium, we did not find evidence that the esterification took place within the syncytiotrophoblast. Thus, we speculate that the syncytiotrophoblast acquires LD manufactured in the cytotrophoblast. The transfer could occur by fusion of cyto- to syncytio-trophoblast under repair conditions. It is well known that cytotrophoblasts are incorporated into areas of syncytium to replace damaged regions of syncytiotrophoblast (Benirschke et al., 2012). In addition, the LD could be transported directly from the cytotrophoblast to the syncytial layer, an attractive but untested explanation for the large numbers of LD in syncytiotrophoblast.

SLC27A2 (FATP2) is the most highly expressed fatty acid transporter (FATP) in the human term placenta (Weedon-Fekjaer et al., 2010). The uptake and processing of BODIPY-C_{12} correlates more with its expression, than with *SLC27A4* (FATP4) or *ACSL1* (Krammer et al., 2011). FATP2 is found within multiple subcellular locations including peroxisomal membranes, cytosolic plasma membrane, and endoplasmic reticulum, and serves a variety of roles in lipid metabolism including mediating LCPUFA uptake (Melton et al., 2011). In culture, *SLC27A2* had higher levels of mRNA expression and higher staining intensity in cytotrophoblasts at stages than after the cells became syncytialized. However, the expression level of transporters may or may not directly equate to to transporter activity levels, and the role of post-translational FATP modifications

in placental fatty acid uptake is unknown (Glatz et al., 2010).

We blocked FATP2 function with CB-2 to determine the degree to which FATP2 was responsible for transporting BODIPY-C_{12} into trophoblast whereupon BODIPY-C_{12} uptake was reduced by ~80%. We determined that IC_{50} values for CB-2 in trophoblast were comparable to those reported for cells expressing high levels of FATP2, Caco-2 and HepG2 (IC_{50}~10μM) (Sandoval et al., 2010) but were much lower (20-fold) than for 3T3-L1 adipocytes that primarily express FATP1 (Sandoval et al., 2010). The potency and efficacy of CB-2 on uptake suggests FATP2 may be largely responsible for driving BODIPY-C_{12} uptake in trophoblast. FATP2 can drive long-chain fatty acid uptake via its acyl-CoA synthetase activity (Melton et al., 2011). This process displays selectivity for LCPUFA and is known to channel fatty acids into esterified lipid pools (Melton et al., 2011). The low level of FATP2 expression in syncytiotrophoblast suggests that it is not well suited for long-chain fatty acid acylation.

A number of other key fatty acid transporters and glycerolipid metabolic genes were more highly expressed before syncytialization than after. These patterns of expression may be tied to the differing roles of cytotrophoblast and syncytiotrophoblast. Glycerol-phosphate acyl transferase-3, encoded by the *GPAT3* gene, catalyzes the initial and rate limiting step in the *de novo* formation of triglycerides (Wendel et al., 2009); *ACSL5* is expressed in tissues with high rates of triglyceride synthesis (Bu and Mashek, 2010). Thus higher expression of these genes in cytotrophoblast is consistent with greater neutral lipid and LD synthetic capacity. *LPCAT3* preferentially channels LCPUFA, including omega-3

fatty acids, into cellular phospholipids (Hashidate-Yoshida et al., 2015). Higher levels of all of these genes support the observation that there is greater capacity for fatty acid esterification in cytotrophoblast. Alternatively, differential esterification in cytotrophoblast may be accounted for by greater availability of other glycerolipid precursors (e.g. glycerol, acyl-glycerols, and phospholipids) which we did not measure.

Cytotrophoblast LD incorporation of BODIPY-C_{12} could be disrupted by triacsin C and phloretin. Reductions in LD production due to Triacsin C may indicate ACSL (1,3,4, or 5) involvement(Kim et al., 2001; Van Horn et al., 2005; Kaemmerer et al., 2011), while phloretin sensitivity may indicate a role for protein mediated transporters or a requirement for ATP, since phloretin disrupts multiple cellular transporters including GLUT1 (Afzal et al., 2002).

Our study was not designed to address the relevance of esterification in regulating the transplacental transport of free fatty acids. However, long-chain fatty acids taken up by the placenta are found predominantly incorporated into esterified lipids, and esterification is hypothesized to be an intermediate step during fatty acid transport in the placenta (Coleman and Haynes, 1987; Desoye and Shafrir, 1994). Our study does illustrate differing lipid dynamics between the cytotrophoblast and syncytiotrophoblast and suggests that future considerations of placental fatty acid transport include studies on the role of cytotrophoblast in addition to syncytiotrophoblast. In fact, the LD in the cytotrophoblast may represent the metabolically active lipid pool that was hypothesized to exist in a recent model of human placental fatty acid transfer (Perazzolo et al., 2015).

Esterified fatty acids in trophoblast can be re-released via lipolysis or exported after incorporation into apolipoprotein particles (Madsen et al., 2004), but the mechanisms by which these processes occur have not been described in placenta. Our BODIPY-C_{12} uptake and FATP-2 expression data are also consistent with the idea that long-chain fatty acids are more highly sequestered in and permeable to cytotrophoblast than the syncytiotrophoblast. Transplacental movement of fatty acids likely involves an interplay between these two cell layers.

Understanding the fundamentals of fatty acid transport and storage in the placenta is highly important because the human fetus must acquire large amounts of fat to provide for its developing brain; inadequate amounts of omega-3 LCPUFAs result in cognitive deficits in offspring (Rizzo et al., 1991; Pagan et al., 2013). The prevalence of obesity, gestational diabetes mellitus and pre-eclampsia is increasing in the US, conditions associated with dysregulation of LCPUFA uptake, esterification and transfer, and altered fusion and viability of cytotrophoblasts (Langbein et al., 2008; Kulkarni et al., 2011; Araújo et al., 2013; Pagan et al., 2013). Understanding the mechanisms that underlie these dysfunctions and developing interventions to prevent them will require a robust understanding of normal fatty acid transport in the placenta.

Conclusions

Using novel optical methods we have found differential localization of LD synthetic activity in the two trophoblast layers of the term human placenta. Based on these new findings we propose a modified model of lipid uptake and storage

in the placenta (Figure 3.6). The cytotrophoblast had not previously been reported to play a significant role in long-chain fatty acid processing. Differential rates of esterification may due to inherent differences in expression of FATPs and ACSLs in the two cell types. During syncytialization of the cytotrophoblast, multiple genes involved in esterification and glycerolipid processing are significantly downregulated, which supports the observed differences in LD production in cytotrophoblast compared to syncytiotrophoblast.

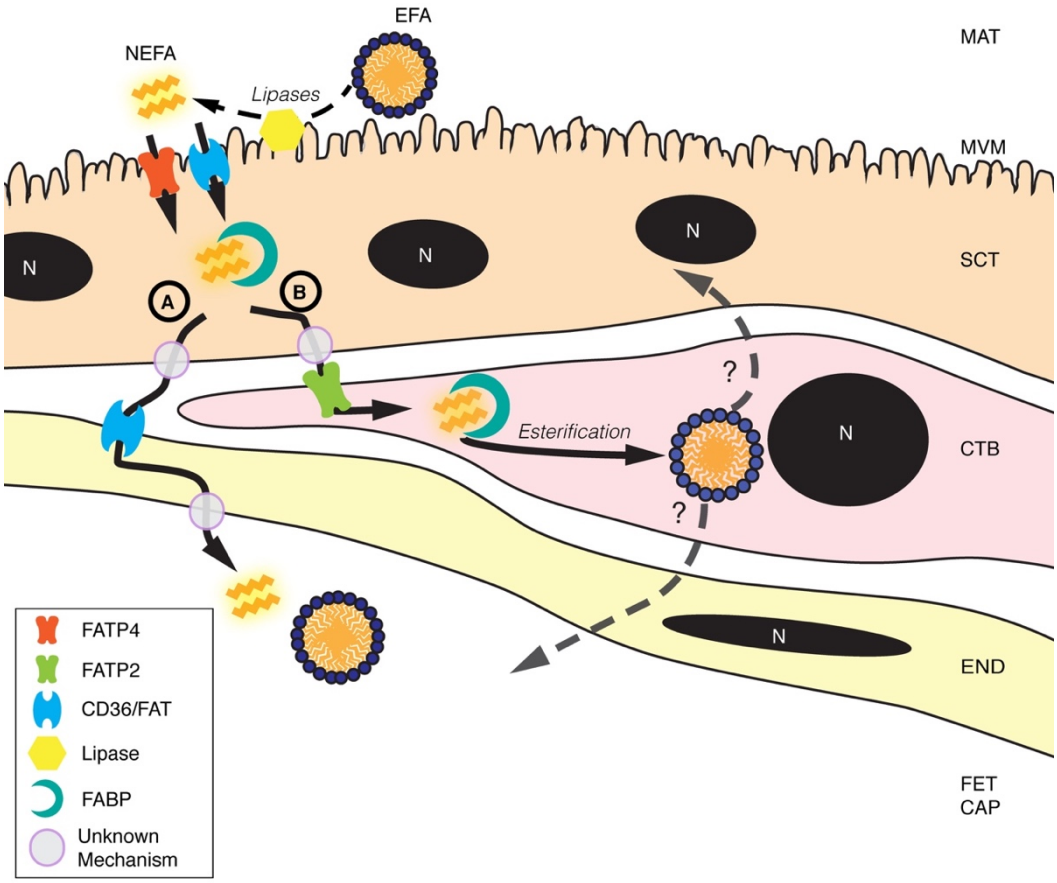

Figure 3.6 Hypothetical simplified model of placental transport of fatty acids.
Long-chain fatty acids are rapidly absorbed into villous tissue after lipolytic activity by lipases on triglycerides at the microvillous membrane. Fatty acid transporters/translocases (FATP, CD36) appear to facilitate the uptake of long-chain fatty acids, but the importance of fatty acid activation and conjugation to Acyl-CoA during transport is not known. Intracellular fatty acids or fatty Acyl-CoAs are held by fatty acid binding proteins (FABP). The mechanism of fatty acid efflux is unclear, but free fatty acids may proceed through may proceed to fetal capillaries (FET CAP) in a manner resembling facilitated diffusion. This route (Route A) does not involve esterification. Unlike previous explanations of long-chain fatty acid transport, our data suggest an additional route B. Non-esterified fatty acids on Route B are transported across the syncytial layer and taken up by cytotrophoblast where they are rapidly esterified and incorporated into lipid droplets. LD in SCT may derive from CTB. The mechanisms by which the long-chain polyunsaturated fats versus saturated fats are differentially transported are unknown. Nevertheless, long-chain fatty acid transport processes are dependent upon a number of lipases and transport proteins, including FATP2, FATP4, FABP, and CD36. MAT, maternal blood space; MVM, microvillous membrane;

SCT, syncytiotrophoblast; CTB, cytotrophoblast; END, endothelium; FET CAP, fetal capillary.

Acknowledgements

This research was supported by the M. Lowell Edwards Endowment and NICHD P01HD034430 (KT). Additional funding provided by Oregon Health and Science University School of Medicine Faculty Innovation Program (KT), the Tartar Trust Fellowship (KK). KK was funded by the Charles Patrick Memorial Fund and a Ruth L. Kirchstein National Research Service Award F30 HD084095-01. The authors thank Amy Valent for proofreading the manuscript.

Chapter IV: Real-Time Assessment of Fatty Acid Uptake Kinetics in The Human Term Placenta.

Abstract

Fatty acids (FA) are essential for normal fetal development. Omega-3 FA are especially important for the heart and brain. Nevertheless, the molecular mechanisms underlying normal placental lipid uptake and transport are not well understood. We employed BODIPY fluorophore conjugated FA analogues of three chain lengths, medium chain- (BODIPY-C5), long chain- (BODIPY-C12), and very long chain- (BODIPY-C16), to study fatty acid trafficking in living tissues and isolated trophoblast cells using confocal microscopy. BODIPY-labeled fatty acids were added to freshly isolated explants of term human placenta obtained from caesarean section and tracked for up to 30 minutes at 37°C in Hank's buffer exposed to ambient air. Fatty acid uptake kinetics were quantified in each tissue layer. Our data suggest that accumulation in the fetal capillary spaces is inversely proportional to FA chain length. For BODIPY-C5 the mean fetal capillary accumulation rate was 110 ± 13 Fluorescence units (FU) per minute ($FU \bullet min^{-1}$), compared to 50 ± 2.5 $\%min^{-1}$, for BODIPY-C12 and 6.1 ± 0.46 $\%min^{-1}$, for BODIPY-C16 (Mean± S.E.M. $p<0.0001$). However, fatty acid uptake by cytotrophoblast, but not syncytiotrophoblast, appears to be transporter and esterification dependent. Using isolated primary human trophoblasts from term placentas we quantified the total uptake of BODIPY-C12 into cytotrophoblast and syncytiotrophoblast. Cytotrophoblast BODIPY-C12 uptake by 15 minutes was 556±128 $FU \cdot \mu g\ protein^{-1}$, and uptake was inhibited by fetal bovine serum (165±42.3 $FU \cdot \mu g\ protein^{-1}$, Mean± S.E.M. $p<0.0001$), Acyl-CoA Synthetase inhibitor triacsin C (394±81.2 $FU \cdot \mu g\ protein^{-1}$, $p<0.05$), and fatty acid transporter

type 2 inhibitor CB-2 (339±91.2 FU·μg protein^{-1} , p<0.01). The uptake of BODIPY-C12 into syncytiotrophoblast by 15 minutes was significantly less than cytotrophoblast (131±10.6 FU·μg protein^{-1} p<0.0001 vs cytotrophoblast), and was not inhibited by serum (57.5±3.62 FU·μg protein^{-1}, p=n.s.), triacsin C (142±39.5 FU·μg protein^{-1}, p=n.s.), CB-2 (114±10.8 FU·μg protein^{-1}, p=n.s.). Our observations are consistent with studies using radiolabeled long-chain fatty acids and the incorporation into glycerophospholipids in human placenta tissue. Taken together, these studies provide more evidence that the placenta is selective for the types of fatty acids it transfers to the developing fetus. We conclude that the transport and processing of lipid molecules is carefully regulated by the placenta.

Introduction

A central function of the human placenta is the transport of fatty acids. The high level of placental fat transport in humans reflects the needs of the growing brain and the deposition of body fat at birth which is larger than for any other mammal, 12-16%, compared to 2-3% body fat for other mammals (Widdowson, 1950; Ulijaszek, 2002). Fatty acids, in addition to their serving as a source of metabolic fuel, are crucial building blocks for the developing organs including the lipid rich brain and cardiovascular systems (Clandinin et al., 1980; Martinez, 1992; Weisinger et al., 2001). In particular, the omega-3 fatty acids along with other long- and very-long chain polyunsaturated fatty acids are central structural components of myelin sheaths in white matter that form in the second and third trimesters of development (Farquharson et al., 1992; Innis, 2005). Specific fatty acids must be constantly delivered to developing tissues of the fetus upon demand else growth and maturation become restricted (Barker and Thornburg, 2013b).

Placental fat transport accounts for some 90% of the total calories used by the conceptus in the third trimester (Sparks et al., 1980). The fetus requires a higher composition of long-chain polyunsaturated fatty acids than what is normally present in the mother's blood (Cetin et al., 2009). Through unknown mechanisms, the human placenta selectively acquires the fatty acids to meet fetal demands (Haggarty, 2002; 2010). Should these demands not be met - either through in adequate maternal resources or dysfunctional placenta transport, offspring suffer permanent developmental defects such as cognitive

impairment and delayed brain maturation (Rizzo et al., 1991; Strain et al., 2008). Despite how important placental fat transport processes are to normal development and subsequent lifelong health it is surprising the cellular mechanisms of placental fatty acid uptake and transport are ill defined.

In the past, the transport of fatty acids across the placenta was believed to be by diffusion because of the lipophilic nature of the molecule as described in studies using the dually perfused human placenta. Recent evidence does not support this view. For example, it has been suggested that fatty acid transport requires an intermediate metabolic step, esterification, that requires 2-ATP equivalents per fatty acid molecule (Szabo et al., 1973; Coleman and Haynes, 1987; Perazzolo et al., 2015; Kolahi et al., 2016). Thus, esterification would likely occur during the uptake step in the placental microvillous membrane since the majority of the members of the Fatty Acid Transporter family (FATP/SLC27A) contain an Acyl-CoA synthetase domain that catalyzes the initial esterification of fatty acids to fatty-acyl CoA (Stahl et al., 2001).

Two recent studies have illustrated that fatty acid esterification takes place within minutes of uptake in the human placenta (Perazzolo et al., 2015; Kolahi et al., 2016). Perazzolo et al. have proposed that the rate limiting transport step is incorporation of the fatty acids into a metabolic pool (Perazzolo et al., 2015), presumably representing esterified fatty acids. It is unclear how esterification might play a role in placental lipid transport since the mechanisms of fatty acid efflux are unknown (Henkin et al., 2012). Esterification may underlie the selectivity of fatty acid uptake in placenta, since esterification is selective by fatty

acid chain length and degree of unsaturation (Mashek et al., 2007; Melton et al., 2011). In addition, the majority (80%) of long and very long chain fatty acids taken up by the placenta are incorporated into esterified lipids (Klingler et al., 2003; Larqué et al., 2003; Gil-Sanchez et al., 2010). These esterified fatty acids may be re-released via subsequent lipolysis or lipoprotein export (Madsen et al., 2004) a step that may also select for particular fatty acids (Henkin et al., 2012). These processes are also poorly defined in placenta.

We set out to investigate the rates at which the human placenta takes up fatty acids as a function of fatty acid chain length. We hypothesized that fatty acid fluxes into the fetal capillary would depend on chain length and that esterification would be directly proportional to fatty acid chain length. We employ BODIPY-labeled fatty acid analogues to track and quantify fatty acid uptake and processing in human placenta and isolated trophoblast.

Materials and Methods

All studies were approved by the Oregon Health & Science University Institutional Review Board (IRB# 5684). All study subjects provided written, informed consent for tissue collection before cesarean section surgery.

Subject Details

Women (>37 weeks gestation, Table 1) scheduled for cesarean section were recruited at Oregon Health & Science University (OHSU) Labor & Delivery. Exclusion criteria included multiple gestations, fetuses with chromosomal or structural anomalies including cardiac defects, preeclampsia, maternal hypertension, and any other significant co-morbidity. Maternal data obtained from medical records included age, parity, race, gestational age at delivery, height, and weight (1st trimester). Neonatal data included birth weight, crown-heel length, and sex. Placenta weight and length and width dimensions were measured during tissue collection.

Table 4.1: Maternal Characteristics

	Mean±S.D. (n=28)	**95% Confidence Interval**
Age (yr)	31±5	[29, 33]
Body Mass Index (BMI: kg/m^2)	27±8	[24, 30]
Parity	2±1	[1 , 3]
Gestational Age (weeks)	39±1	[38, 39]
Birth Weight (g)	3400±500	[3200 , 3600]
Placenta Weight (g)	546±120	[500, 590]

Tissue overview

We used twenty-eight placentas for different aspects of the study. In brief, placentas were collected at the time of delivery, maternal decidua was removed, and placenta was processed within 30 min. Placental tissues were used as (i) explants for live imaging/trafficking studies, (ii) dissociated cytotrophoblast cell studies for *in vitro* studies and Western Blotting.

Placental explant collection

Explants (<1mm^3) were isolated as previously described (Brass et al., 2013; Kolahi et al., 2016). Placental tissue was isolated from two different cotyledons that appeared healthy and placed in M199-HEPES culture media (Gibco) at room temperature (<30mins). Two explants from different cotyledons were cultured per well in plastic 8-well chamber slides (Lab-Tek II, Nunc) containing 0.4mL M199-HEPES and incubated at 37°C in 5% CO_2/95% air. All explants were assayed within 2-3hrs of delivery, a known window when markers of explant health and fatty acid uptake are not compromised (Brass et al., 2013).

Primary villous cytotrophoblast isolation and culture

Cytotrophoblast cells were isolated using trypsin-DNAse I digestion followed by Percoll enrichment as previously described (Morrish et al., 1997). In brief, chorion and maternal decidua were removed, and approximately ~40g of villous placenta tissue was finely minced. Villous fragments were subjected to five sequential 10 minute (37°C) digestions in 0.25% Trypsin (Gibco) and 200 U/mL DNAse I (Roche). Cytotrophoblasts were purified by Percoll (GE

Healthcare Bio-sciences AB) discontinuous density gradient centrifugation at 1200 rcf for 25 minutes (room temperature). The purity of trophoblast isolations was assessed by positive immunohistochemical staining of cyokeratin-7 (MAI-06315, Thermo Scientific), a marker of trophoblast cells. Contamination by stromal cells and syncytial fragments was determined by staining for Vimentin (PA5-27231, Thermo Scientific) and BHCG (ab9582, Abcam). Our isolations comprised at least >90% pure, viable cytotrophoblasts.

Cytotrophoblasts were plated at a density of 3.0×10^5 cells cm^{-2} on tissue culture dishes or glass coverslips. Cells were cultured in Iscoves Modified Dulbecco's Medium (IMDM, ATCC) supplemented with 10% Fetal Bovine Serum (FBS) (Gibco) and 100U/ml penicillin and 100µg/ml streptomycin and incubated in a 5% CO_2/95% air incubator at 37°C. Cell viability was assessed by Trypan blue exclusion. After eight hours in culture, non-adherent cells were removed by washing with pre-warmed culture media, and the media was subsequently replaced every 24 hours (Morrish et al., 1997). A subset of cells was used for fatty acid uptake studies, and the remainder for Western Blot analyses. Cells were studied at 8 hours (cytotrophoblasts) or 72 hours (maximum) when most cytotrophoblasts have fused and differentiated into multinucleated, syncytial giant cells (Douglas and King, 1990).

Fluorescent fatty acid tracking and microscopy (explants, cells).

The BODIPY fluorophore (4,4-Difluoro-5,7-Dimethyl-4-Bora-3a,4a-Diaza-s-Indacene) is an intensely fluorescent, photostable, intrinsically lipophilic molecule, unlike most other long-wavelength dyes. BODIPY conjugated fatty

acids analogues undergo native-like transport and metabolism in cells making it effective as a tracer for lipid trafficking (Stahl et al., 1999). The BODIPY- moiety effectively adds some 4-6 carbons to the conjugated fatty acid (e.g. BODIPY-C12 is most similar to C-16 and C-18 natural fatty acids) (Rambold et al., 2015). BODIPY-C16 is similar to very-long chain fatty acids C-20 and C-22. BODIPY-C_{12}, C_{16}, C_5 are well established as tools to study fatty acid uptake and esterification in multiple models (Stahl et al., 1999).

We prepared 10μM solutions of BODIPY fatty acids (Molecular Probes) by diluting a 2.5mM DMSO stock solution (1:250) in M199-HEPES containing 0.1% defatted bovine serum albumin (BSA) (Fisher Scientific); solutions were incubated at 37°C for 30mins, protected from light, to allow for BSA conjugation. Explants and cells were exposed to 2μM BODIPY- fatty acids for 30mins for most experiments because the uptake reached a plateau by 15mins.

Explants: To assess explant viability, 2μL ethidium homodimer (LIVE/DEAD Viability/Cytotoxicity Kit; Molecular Probes) was added to each well containing explants to distinguish dead regions of tissue. Imaging was restricted to regions with no evidence of ethidium homodimer uptake. For lipid droplet labeling, 1μL of HCS LipidTOX Deep Red (Molecular Probes) was mixed into each well containing placental explants. After 30mins, 100μL of 10μM BODIPY fatty acid solution was added to each well and mixed by trituration (total well volume 500μL, final concentration 2μM BODIPY- fatty acid). Explants in imaging chambers were immobilized for confocal microscopy using 8×8 mm pieces of stainless steel mesh (40 Mesh, 0.25 mm; TWP, Inc). The chamber was then

placed on a stage top 37°C incubation chamber (Okolab). A Nikon A1R+/Eclipse TiE resonant scanning confocal microscope equipped with a 60× High N.A. objective (N.A.=1.4; Nikon) was used for imaging. All images were acquired using the same acquisition configurations with minimum laser intensity (0.5%) and exposure time (900ms). Images were acquired every 20 seconds for a total of 30 minutes; there is non-appreciable photobleaching under these conditions. All images were gathered at a consistent distance range (5-10μm) from the culture well base.

Quantification of total BODIPY C12 fatty acid uptake in cells

Total BODIPY-C_{12} uptake was determined in cytotrophoblast cultures using a plate-reader assay as described previously (Sandoval et al., 2010). Cytotrophoblast were plated at 3.0×10^5 cells cm^{-2} in 96-well plates (BD Falcon) and cultured as described above. Cells were studied at 8 hours (cytotrophoblasts) and also at 72 hours after the cells had spontaneously fused and differentiated to form syncytial giant cells (Frendo et al., 2003). Cells were pre-incubated in 80μL serum free Iscove's Modified Dulbecco's Medium (IMDM) for 60 mins (± inhibitors). The inhibitors used were: 10% FBS to include natural fatty acids as competitive inhibitors, Triacsin C to inhibit Long chain Acyl-CoA Synthetase (Santa Cruz Biotech), and the FATP2 inhibitor, CB-2 (EMD Millipore). After 60 minutes, 20μL of assay solution (25 μM BODIPY-C_{12}, 25 μM defatted-BSA, 10mg/ml Trypan Blue) was added to each well, mixed, and incubated for 20 minutes at 37°C with 5% CO_2/95% air. Fluorescence (485nm excitation, 525nm emission) was measured using a BioTek Synergy H1 hybrid plate reader

(BioTek). After fluorescence measurement, the assay medium was removed, and cells were carefully washed with Hank's Buffer for 10min at 37°C. The cells were then lysed using RIPA buffer (EMD Millipore) to measure protein using a BCA method (Thermo Pierce).

Immunofluorescence

Cells plated on glass coverslips were incubated with BODIPY-C_{12} for 30 minutes as described above and fixed in 4% paraformaldehyde (pH 7.4) for 20 minutes at room temperature. Fixed cells were processed immediately. Samples were blocked and permeabilized in Block-aid (Life Technologies)/0.1% saponin (Sigma) for 1 hour before overnight incubation with primary antibody at 4°C. Samples were labeled with antibodies against desmoplakin (1:200, ab16434, Abcam). Following primary antibody incubation, samples were washed with PBS and labeled with secondary antibodies (donkey F(ab')2 anti-mouse Alexa Fluor 647 (1:500, ab150103), for 1 hour at room temperature. After washing, the samples were counterstained with 1µg/ml Hoechst 33342 for 10 minutes and immersed in Slowfade Diamond (Molecular Probes) immediately before confocal imaging. Imaging was performed using a Zeiss 880 LSM Confocal with Airyscan with 63x objective (N.A. = 1.4).

Image Analysis

For live imaging of explants, 2 separate explants were imaged with one field of view that demonstrated exclusion of ethidium homodimer dead stain. All images obtained via confocal imaging were analyzed using Fiji software (Schindelin et al., 2012). To measure mean fluorescence intensity versus time for

a region of interest, the image series' was first stabilized using automatic registration. The mean fluorescence intensity was measured in two region of interests, the syncytiotrophoblast cytosol, and fetal capillary lumen. The intensity values were plotted as versus time and the initial, linear portion of the curve (0-15 min) was utilized for regression analysis. Co-localization analyses were performed using Imaris (Bitplane AG) and Fiji using the automatic thresholding method of Costes et al. (Costes et al., 2004) to obtain a Pearson co-localization coefficient; this coefficient indicates the degree to which BODIPY-C_{12} is being incorporated into the LD organelles identified by LipidTOX (Kassan et al., 2013).

Western Blotting

A subset of primary cytotrophoblasts were used for western blot analyses. Total protein from 3×10^6 cells was isolated after 8hr or 72hr of culture using RIPA lysis buffer (EMD Millipore). Protein concentrations were measured using a BCA assay (Thermo Pierce). 15µg was loaded for SDS-PAGE and blotting was performed onto nitrocellulose using a Biorad Minicell (Biorad) for 60min at 100V/180mAh. Blots were probed with mouse anti-human FATP2 (1:500, ab175373, Abcam) and incubated overnight at 4°C. The blots were washed and probed with an anti-mouse HRP conjugated secondary antibody (1:1000, sc-2005, Santa Cruz Biotech) and developed for 5 minutes using a chemilumiscent substrate (SuperSignal, Thermo Pierce). Gels were imaged using a UVP gel doc and all images were quantified using Fiji gel analysis tool.

Statistical Methods

To model the relationship between fluorescence versus time in explant live

imaging uptake studies, the linear portion of the uptake curve was analyzed using linear regression. 2-way ANOVA with Sidak's multiple comparisons test was used for all *in vitro* uptake plate reader experiments. Paired Student t-test was used for western blot quantification. P-values less than 0.05 were considered significant.

Results

Using live-confocal microscopy, we quantified the rate of uptake of BODIPY- labeled fatty acids of various chain lengths into human term placental explants. In all experiments, uptake was first visible at the microvillous membrane and proceeded gradually across the placental tissue toward the fetal capillaries. Within 15 minutes of incubation, fatty acids of different chain lengths accumulated to differing degrees throughout the placental layers and in fetal capillaries (Figure 4.1). We have recently published video segments showing this process for BODIPY-C12 using time lapse microscopy (Kolahi et al., 2016). Because the BODIPY fluorophore is relatively insensitive to environmental conditions, quantification of fluorescence intensity is a relatively solid measure of tracer concentration (Hermanson, 2013). We quantified the temporal changes in fluorescence intensity in syncytiotrophoblast and capillary lumen in placental explants during continuous incubation with 2μM of each BODIPY- fatty acid. The initial 15 minutes of uptake, was used for linear regression modeling to compare the distribution and uptake rates of BODIPY-C5, BODIPY-C12, and BODIPY-C16.

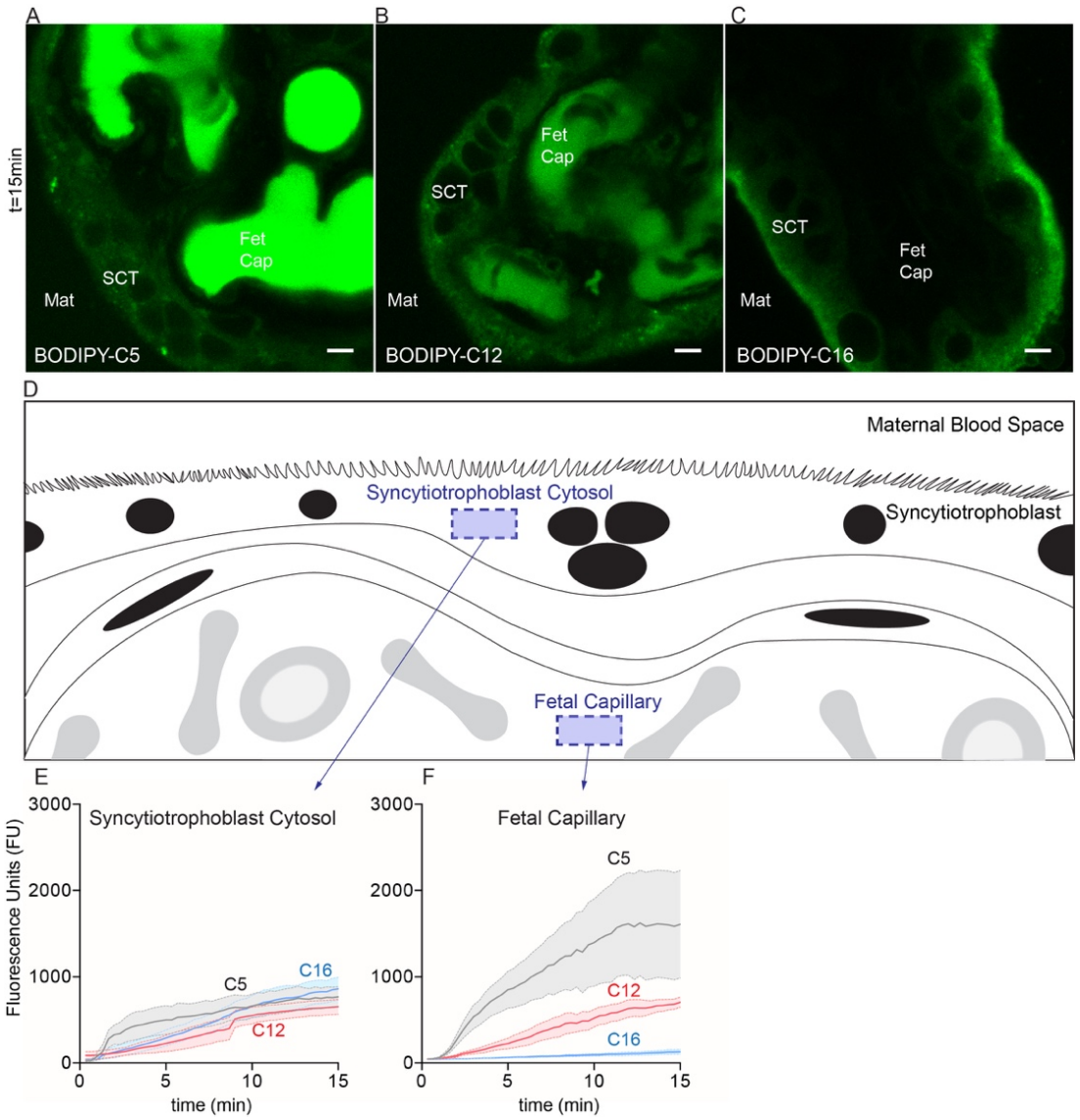

Figure 4.1. Kinetic distribution of various fatty acid analogues during uptake in living human term placental explants imaged via confocal microscopy.

Explants isolated immediately after cesarean section (< 2hrs) were placed into HBSS onto a stage top incubator (37°C/ambient air) of a confocal microscope. 2μM micromolar fluorescent fatty acids were added to explant medium after initialization the image acquisition. The tracer concentration in the medium was not sufficient to register a signal at these settings. Three fluorescent fatty acids were compared, BODIPY-C5 (medium chain fatty acid), BODIPY-C12 (long chain fatty acid), and BODIPY-C16 (very long chain fatty acid). Uptake distributions varied according to fatty acid chain length over 20 min of time. (A) BODIPY-C5 accumulated to the greatest degree within the fetal capillaries against an apparent concentration gradient; very little tracer was present in trophoblast or other placental cells at 20 minutes. (B) BODIPY-C12 appeared to distribute equally between all layers and compartments of placental explants by 20

minutes. (C) BODIPY-C16 largely incorporated into the syncytiotrophoblast cytosol; very little was present in capillaries at 20 minutes. (D) Schematic representation of regions quantified in explants to produce panels E and F. (E,F) Quantification of total fluorescence, of BODIPY-C5, BODIPY-C12, and BODIPY-C16 at two different locations in explants over time. Mat, Maternal blood space; SCT, Syncytiotrophoblast; Fet Cap, Fetal Capillary. Scale Bar: 5μm. Data are Mean±SEM, n=5 placentas.

The uptake rates into syncytiotrophoblast cytosol were different between the different fatty acids BODIPY-C5 42 ± 4.4 Fluorescence Units (FU) per minute, FU•min^{-1}, r^2=0.29 , BODIPY-C12 46 ± 2.9 FU•min^{-1}, r^2=0.54 and BODIPY-C16 61 ± 3.3 FU•min^{-1}, r^2=0.59 $p<0.001$ (Figure 4.1E). However, the final fluorescence values in the trophoblast cytosol was not different between fatty acids, $p>0.05$ (Figure 4.1E).

BODIPY-C_5, the shortest chain fatty acid used in this study, was rapidly transported into fetal capillaries and accumulated (Figure 4.1A). The uptake rates into fetal capillaries differed by fatty acid species. For BODIPY-C5 the uptake rate was 110 ± 13 FU•min^{-1}, r^2=0.26 compared to 50 ± 2.5 FU•min^{-1}, r^2=0.64 for BODIPY-C12 and 6.1 ± 0.46 FU•min^{-1}, r^2=0.44 for BODIPY-C16 $p<0.0001$ (Figure 4.1F). The mean fluorescence in the capillaries at 15 minutes was greater for BODIPY-C5 (1610 ± 623 FU) than BODIPY-C12 (705 ± 57.4 FU $p<0.05$) or BODIPY-C16 131 ± 28.0 FU $p<0.0001$). BODIPY-C12 and BODIPY-C16 mean fluorescence levels in capillaries at 15 minutes were not statistically different.

As the fatty acid chain length increased, accumulation into fetal capillaries declined. Several lines of evidence implicate transporter systems and active processes (e.g. esterification) that are chain-length dependent as the mechanisms that drive these differences. It was known that many cell types readily esterify long-chain fatty acids (e.g. BODIPY-C12) to LD, but less so for short-chain fatty acids (Huang et al., 2002).

To determine whether these processes are specific to long-chain fatty

acids, we repeated the live explant studies using a LD counterstain, LipidTOX, prior to the addition of fluorescent fatty acid to track pre-existing LD. We compared the short-chain (BODIPY-C_5) fatty acid with the long-chain fatty acid BODIPY-C12. Experiments using BODIPY-C_{12} had a very different result than with BODIPY-C_5. BODIPY-C_5 produced punctate structures in the syncytiotrophoblast (Figure 4.2A) but had more accumulation in the syncytium than the cytotrophoblast. However, the punctate structures were unlikely to represent LD because they did not co-localize with LD identified by LipidTOX (Figure 4.2B,C). In contrast, within minutes of addition of BODIPY-C12, numerous LD emerged (Figure 4.2D), and some of these LD incorporated into pre-existing LD predominantly in the cytotrophoblast (Figure 4.2E, F), signifying esterification of BODIPY-C12.

We quantified the number of particles, an estimate of LD accumulation, after 15 minutes of incubation with BODIPY-C12 or BODIPY-C5. The number of particles (irrespective of cell layer) accumulated by 15 minutes was higher with BODIPY-C_{12} ($2\times10^7 \pm 7\times10^6$ particles mm^{-3}) than BODIPY-C_5 ($4\times10^6 \pm 3\times10^6$ particles mm^{-3}; $p<0.05$, Figure 4.2G). There was no difference between the volumes of the particles incorporating BODIPY-C_{12} (0.21 ± 0.12 μm^3) vs BODIPY-C_5 (0.10 ± 0.046 μm^3) at 15 minutes (Figure 4.2H). There is greater co-localization (Pearson correlation) of BODIPY-C_{12} and LipidTOX ($r= 0.24 \pm 0.052$) than BODIPY-C_5 and LipidTOX ($r= -0.067 \pm 0.063$ $p<0.01$, Figure 4.2I).

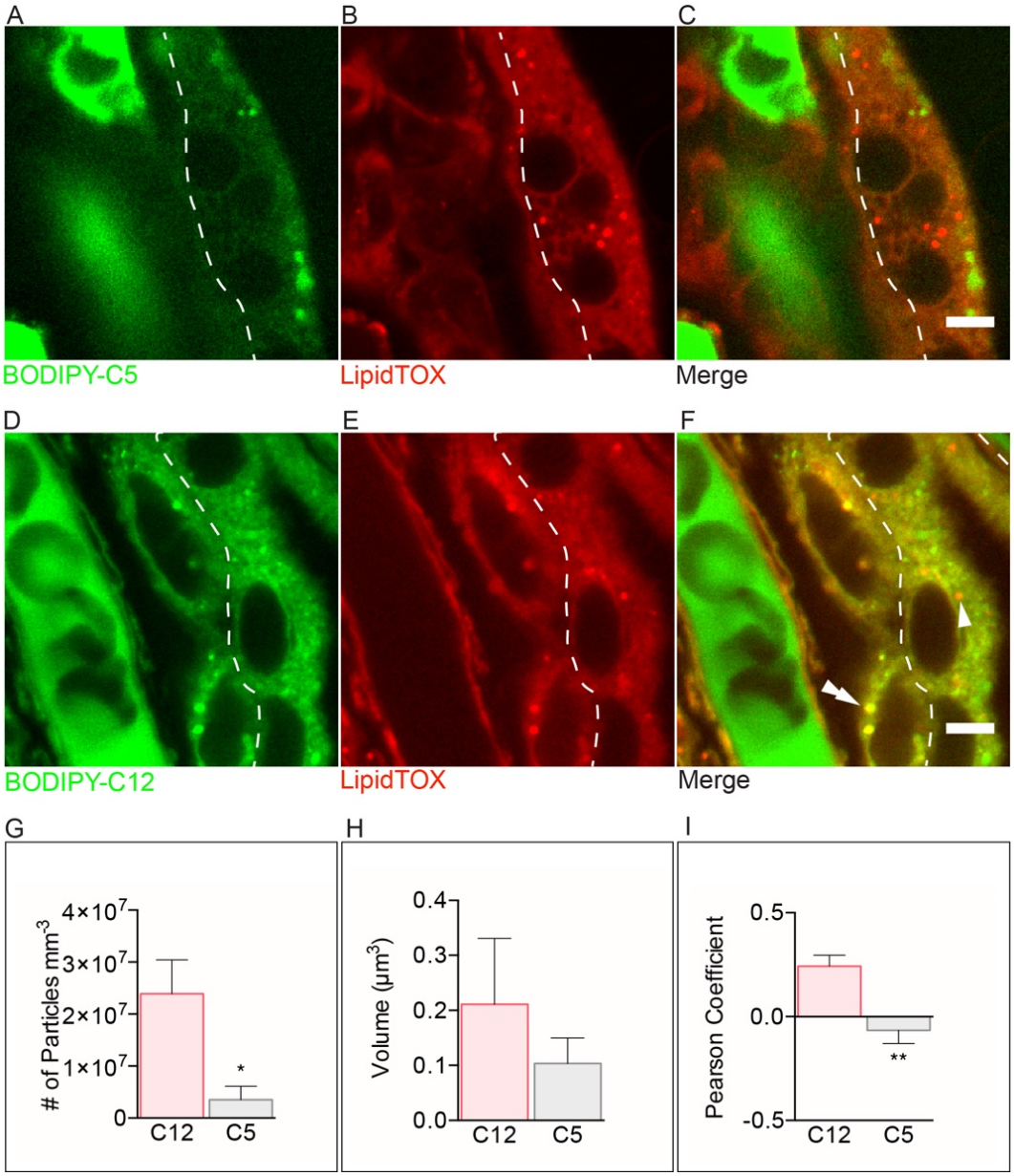

Figure 4.2. Comparison of short- and long-chain fatty acid uptake in human term placental explants after 15 min of incubation with BODIPY-C_5 or BODIPY- C_{12}.

The dashed line separates the syncytial and cytotrophoblast layers. (A-C) BODIPY-C_5 (green) (D-F) BODIPY-C_{12} (green) (A) The BODIPY-C5 fatty acid is found diffusely throughout all tissues and within immotile, unidentified punctate structures. (B) The green punctate structures shown in A are not stained with LipidTOX suggesting that they are not lipid droplets (LD). (C) Merge image shows that BODYPY-C_5 is not esterified nor incorporated into LD. (D-F) In contrast, BODIPY-C_{12} is esterified and incorporated into LD (double arrowhead) in the cytotrophoblast but not the syncytiotrophoblast (arrowhead). (G) There are significantly more punctate structures in explants incubated with BODIPY-C_{12} than with BODIPY-C_5. (H) Volumes of BODIPY-C_{12} and BODIPY-C_5 particles are

not different. (l) The long-chain fatty acid, BODIPY-C_{12} co-localizes with a greater frequency with LipidTOX stained droplets than does BODIPY-C_5. This suggests that BODIPY-C_{12} is being incorporated into LD to a greater extent than BODIPY-C_5. (A-F): Dashed line represents the syncytiotrophoblast-cytotrophoblast interface. Scale Bar: 5μm. (g-i): Data are mean ± SEM; n=7 BODIPY-C_{12}, n=5 BODIPY-C_5. Unpaired t-test, *= $p<0.05$, **=$p<0.01$ vs BODIPY-C_{12}.

These data indicate esterification systems contribute to placenta fatty acid uptake and are selective according to fatty acid chain length. FFA esterification to fatty Acyl-CoAs occurs concertedly with uptake, as members of the fatty acid transport proteins (FATP) contain an Acyl-CoA synthetase domain and transporters without this domain (e.g. Fatty acid Translocase (FAT/CD36)) are complexed with Acyl-CoA synthetases (Richards et al., 2006). To explore how these individual transport systems contribute to fatty acid uptake, we screened a number of inhibitors using isolated cytotrophoblast *in vitro*. We have previously shown that long-chain fatty acid esterification is marked in cytotrophoblast (**CTB**), which predominate at 8hrs in culture, but becomes suppressed by 72hrs in culture, when most cytotrophoblast have syncytialized (**SCT**). We thus compared uptake of BODIPY-C5, BODIPY-C12, BODIPY-C16 in CTB and SCT and tested if uptake would be sensitive to: competition by natural fatty acids present in fetal bovine serum, inhibition of FATP2 (CB-2), or ACSL (1,3,4, 5) inhibition (Triacsin C).

Total uptake of BODIPY-labeled fatty acids was quantified after 15 minutes of incubation using a 96-well plate reader (Sandoval et al., 2010). Consistent with explant experiments, little BODIPY-C5 accumulated within cells (Figure 4.3A). CTB uptake of BODIPY-C5 at 15 minutes was 29±8.9 Fluorescence Units (FU)·μg protein^{-1} , and was not significantly affected by any of the treatments utilized (serum: 15±8.2 FU·μg protein^{-1}, Triacsin C: 23±13 FU·μg protein^{-1}, CB-2: 59±18 FU·μg protein^{-1}, $p>0.05$ vs control) (Figure 4.3A). SCT uptake of BODIPY-C5 was also not significantly different as compared to CTB

(15±7.4 FU·μg protein^{-1} , p>0.05), and uptake was also not detectable by treatment (serum: 5.1±2.2 FU·μg protein^{-1}, Triacsin C: 23±7.8 FU·μg protein^{-1}, CB-2: 28±7.5 FU·μg protein^{-1}, p>0.05 vs control).

Total uptake of BODIPY-C12 and BODIPY-C16 was substantially greater than BODIPY-C5. The total uptake of BODIPY-C12 into CTB was 556±128 FU·μg protein^{-1}, and was inhibited by FBS (165±42.3 FU·μg protein^{-1}, p<0.0001), triacsin C (394±81.2 FU·μg protein^{-1}, p<0.05), and CB-2 (339±91.2 FU·μg protein^{-1} , p<0.01) (Figure 4.3B). The uptake of BODIPY-C12 into SCT was substantially less than CTB (131±10.6 FU·μg protein^{-1} p<0.0001 vs CTB), and was not inhibited by serum (57.5±3.62 FU·μg protein^{-1}, p=n.s.), triacsin C (142±39.5 FU·μg protein^{-1}, p=n.s.), or CB-2 (114±10.8 FU·μg protein^{-1}, p=n.s.) (Figure 4.3B).

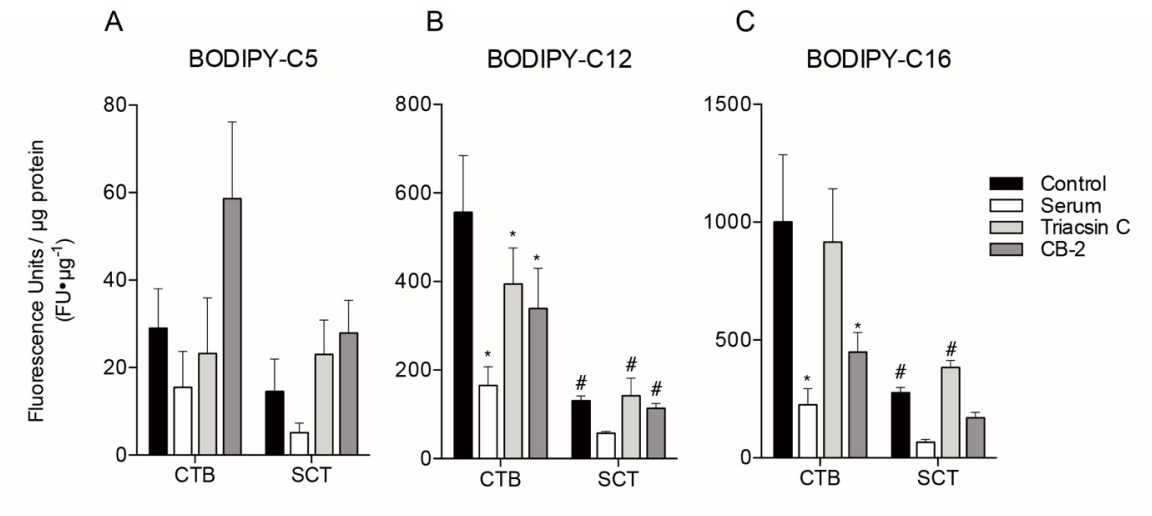

Figure 4.3. Quantification of total BODIPY-fatty acid uptake in primary isolated human term trophoblast cells with and without inhibitors.
Primary human trophoblast were isolated and plated onto 96 well plates. Cells were pre-treated with inhibitors 60 minutes before addition of 2μM BODIPY- fatty acid, and total uptake was measured after 20 minutes of incubation with BODIPY-fatty acid using plate reader fluorescence as a marker. Trophoblast tissues were assayed at two time points after initial plating, at 8hrs to measure cytotrophoblast uptake, or at 72hrs allow for differentiation to syncytiotrophoblast (SCT) before measuring uptake. (A) BODIPY-C5 uptake into cells was very low regardless of state of differentiation, and was insensitive to competition with fatty acids in fetal bovine serum (FBS), inhibition of long-chain Acyl-CoA synthetase by Triacsin C, or inhibition of FATP2 with CB-2. (B) BODIPY-C12 uptake in CTB was greater than BODIPY-C5 by an order of magnitude. BODIPY-C12 uptake was greater in CTB than SCT. CTB Uptake of BODIPY-C12 could be inhibited by FBS, Triacsin C, or CB-2. (C) BODIPY-C16 uptake was greater than BODIPY-C12. Similar to BODIPY-C12, uptake was greater for CTB than SCT. CTB uptake of BODIPY-C16 was sensitive to FBS and CB-2, but no affect was detectable with Triascin C, which is to be expected should BODIPY-C16 represent a very-long chain fatty acid. These data indicate uptake of long and very long chain fatty acids are transporter dependent. Data are Mean±SEM, n=5 placentas. *= $p<0.05$, **=$p<0.01$ vs corresponding cell type control. #=$p<0.05$ CTB vs SCT under same condition.

Of the fatty acid analogues tested, BODIPY-C16 uptake was the greatest. Uptake of BODIPY-C16 by CTB at 15 minutes was on average 1000±285 FU·μg protein^{-1}, and was less with FBS (225±68.8 FU·μg protein^{-1}, $p<0.0001$) and CB-2 (445±84.0 FU·μg protein^{-1} , $p<0.01$), but not triacsin C (915±227 FU·μg protein^{-1}, p=n.s.) (Figure 4.3C). Similar to BODIPY-C12, uptake of BODIPY-C16 by SCT was less than CTB, (277±23.4 FU·μg protein^{-1} $p<0.001$ vs CTB), and was not less with FBS (66.7±11.6 FU·μg protein^{-1}, p=n.s.), triacsin C (383±30.1 FU·μg protein^{-1}, p=n.s.), or CB-2 (170±23.6 FU·μg protein^{-1}, p=n.s.) (Figure 4.3C).

Differentiation of CTB to SCT is associated with suppression of long and very-long chain fatty acid uptake, but it is possible this effect is influenced by culture conditions. Thus, we tested if blocking differentiation could preclude the suppression in long-chain and very-long chain fatty acid uptake. Using a plate reader assay we measured total uptake of BODIPY-C12 in trophoblast cultured for 8, 24, and 72hrs with and without SB203580 p38 MAPK inhibitor to block differentiation. At 8 and 24 hrs the uptake of BODIPY-C12 was not different between treated and untreated CTB: (8hr: control 521±31.4 FU·μg protein^{-1} vs SB203580 495±42.8 FU·μg protein^{-1},p=n.s), (24hr: control 316±35.7 FU·μg protein^{-1} vs SB203580 357±43.5 FU·μg protein^{-1}, p=n.s) (Figure 4.4A). However, by 72hrs, when the majority of CTB have differentiated to SCT in the control group, uptake of BODIPY-C12 was greater in the SB203580 treated trophoblast (72hr: control 248±41.8 FU·μg protein^{-1} vs SB203580 351±52.1 FU·μg protein^{-1}, $p<0.001$) (Figure 4.4A). Similar to previous reports, we found that cytotrophoblast cultured for 72hr had predominantly fused and lost intercellular junctional

divisions as evidenced by desmoplakin staining (Figure 4.4B). SB203580 prevented cytotrophoblast fusion and desmoplakin remained intact (Figure 4.4C).

Since SLC27A2, the gene encoding FATP2, is the most highly expressed fatty acid transporter in human placenta, and this gene product appears to be localized to cytotrophoblast in human placenta (Kolahi et al., 2016), we surmised our *in vitro* observations of the greater CTB uptake of long and very-long chain fatty acids could be explained by higher levels of FATP2 protein levels. We tested this hypothesis by comparing CTB and SCT FATP2 levels via western blot. Indeed, we found that FATP2 protein levels were higher in CTB (2.3±0.25) than in SCT (1.5±0.083, $p<0.01$) (Figure 4.5). Thus, the lower uptake of long- and very-long chain fatty acids BODIPY-C12 and BODIPY-C16 in SCT could be due to a suppression in FATP2 protein expression that occurs concomitant with CTB syncytialization.

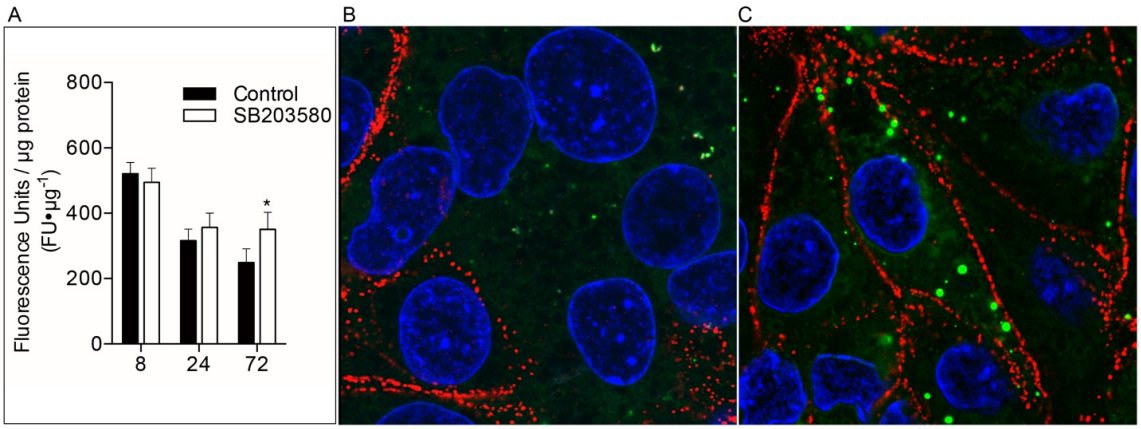

Figure 4.4. The suppression in long chain fatty acid uptake during differentiation of cytotrophoblasts to syncytiotrophoblast can be prevented with p38 MAPK inhibition.

(A) total uptake of BODIPY-C12 long chain fatty acid in isolated primary human term trophoblast was measured after 20 minutes of incubation using a plate reader. Uptake was measured at 8,24, and 72 hrs after initial plating with and without a differentiation blocker SB203580, an inhibitor of p38 MAPK. Treatment with 10μM SB203580 had no detectable effect on total uptake of BODIPY-C12 at 8 or 24hours time points in culture. Trophoblast at 8 and 24hrs represent cytotrophoblast (CTB) because the majority of cells have not syncytialized at these time points. However, by 72 hrs when CTB have largely fused to become syncytiotrophoblast (SCT), uptake of BODIPY-C12 is greater in cultures that were treated with the differentiation inhibitor SB203580. (B-C) Trophoblast were cultured for 72hr with and without SB203580, incubated with 2μM BODIPY-C12 (green) for 20 minutes, fixed and immunolabeled with desmoplakin (red) to visualize intercellular junctions and fatty acid uptake using confocal microscopy. Nuclei are labeled blue (Hoechst) (B) Desmoplakin shows large syncytial aggreggates in control 72hr cultures. (C) 72hr cultures treated with SB203580 show CTB have aggregated, but remain as discrete cells, as evidenced by clearly demarcated desmoplakin labeled intercellular junctions. These data indicate blocking differentiation of CTB to SCT is sufficient to preserve greater levels of BODIPY-C12 long chain fatty acid uptake. Data are Mean±SEM, n=8 placentas.

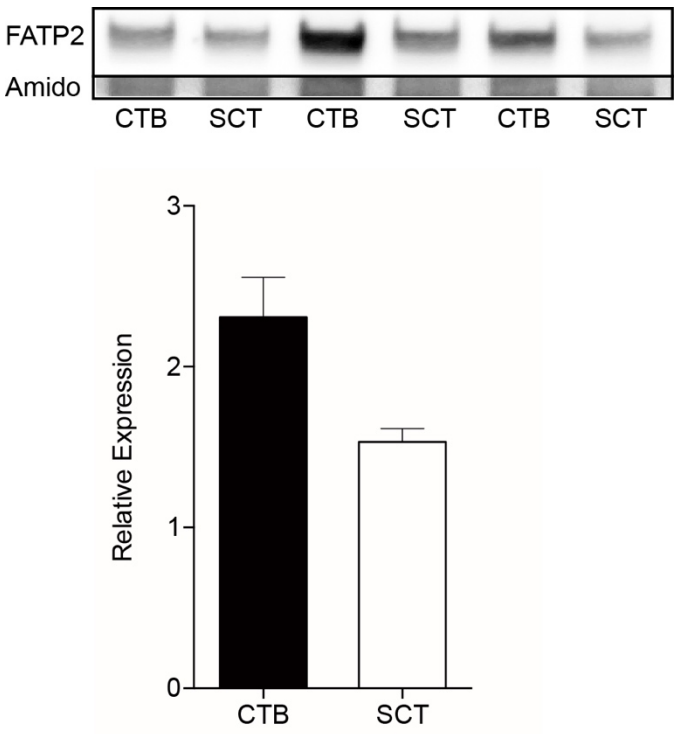

Figure 4.5. FATP2 western blots of cytotrophoblast and syncytiotrophoblast in vitro.
Primary human cytotrophoblast (CTB) were isolated and cultured for 8hrs before protein collection or 72hrs to allow for differentiation to syncytiotrophoblast (SCT) before protein collection. Lysates were analyzed by western blots and probed for Fatty acid transporter type 2 (FATP2). FATP2 protein levels appear to be greater in CTB than SCT. These data suggest the decrease in BODIPY-C12 and/or BODIPY-C16 fatty acid uptake after syncytialization may be due to the reduction in FATP2 expression. FATP2 levels were normalized to total protein visualized by amido-black. Data are Mean±SEM, n=6 placentas

Discussion

We have used real-time confocal microscopy to track the disposition of various fluorescently labeled fatty acid analogues in the human term placenta. The analogues represented medium- (BODIPY-C5), long- (BODIPY-C12) and very-long- (BODIPY-C16) fatty acids. As a working hypothesis, we tested whether the rate of fatty acid uptake into the trophoblast would be inversely proportional to chain length, consistent with a passive diffusion component to the transport process. However, we found large differences in the kinetics of uptake for the fatty acids based on chain length that were not compatible with diffusion alone. The rates of incorporation into the various layers of placenta were more different than would be predicted by their molecular weights and coefficients of free diffusion (MW: BODIPY-C5: 320 Da; BODIPY-C12: 418 Da; BODIPY-C16: 474 Da) (Thornburg et al., 1979; Adams et al., 1988). One possible explanation for our observations is that these molecules exhibit differential transport rates – by the action of transporters or other cellular processes. Since fatty acid transporters are required for uptake into cells we hypothesized the presence of transporters specific by fatty acid type or active cellular processes such as esterification could account for the differences in kinetics we have observed here.

The shorter chain fatty acid (BODIPY-C5) accumulated very little in any cell layer of the placenta but instead rapidly appeared and accumulated within the fetal capillaries. BODIPY-C5 must therefore be transported at a high rate against a concentration gradient. In contrast, BODIPY-C12 and BODIPY-C16, representing long- and very-long chain fatty acids, respectively, accumulated in

trophoblast cells. Within the thirty minute durations and over the concentrations tested, a significant proportion of BODIPY-C12 did accumulate in the capillaries, but very little of BODIPY-C16 was found in the capillaries by 30 minutes. BODIPY-C12 and BODIPY-C16 (data not shown) were esterified and incorporated into lipid droplets in cytotrophoblast. We have previously shown that BODIPY-C12 is stored as lipid droplets in cytotrophoblast (Kolahi et al., 2016). BODIPY-C5 incorporation into lipid droplets was not detectable in explants or cells in culture. Esterification of fatty acid is an important intermediate step for long and very-long chain fatty acids, but how esterification might be related to the mechanisms and kinetics of fatty acid transport remains untested.

To shed light on the relationship between transporter esterification and uptake of fatty acids according to chain-length we determined the efficacy of several inhibitors of fatty acid uptake *in vitro* to test various uptake mechanisms. We have previously described differences in fatty acid uptake and esterification between CTB and SCT (Kolahi et al., 2016). In those experiments we showed that CTB and SCT lipid droplet formation and BODIPY-C12 uptake were inhibited by phloretin, triacsin C, and CB-2. Phloretin is a non-specific inhibitor of protein mediated transport, triacsin C inhibits Long chain Acyl-CoA Synthetase (ACSL1,3,4 and 5) (Kaemmerer et al., 2011), and CB-2 inhibits FATP2 (Sandoval et al., 2010).

Similar to our results in explants, very little BODIPY- C5 accumulated with in cell cultures of CTB or SCT. Uptake of BODIPY- C5 appeared to be insensitive to competition with natural fatty acids in FBS. This may be because there is no

natural lipid in FBS that competes with the BODIPY-C5 transport system. As expected, we observed no inhibition of uptake with Triacsin C, or CB-2, because these systems are specific for long and very long chain fatty acids (Sandoval et al., 2010; Kaemmerer et al., 2011). BODIPY-C5 differs from the other two tracers we studied in that it is a medium chain fatty acid with an odd number of carbons. The uptake and metabolism of odd chain and medium chain fatty acids may be specialized to serve a crucial role in the placenta for the maintenance of mitochondrial Krebs cycle intermediates especially in the context of metabolic diseases (Roe et al., 2002; Gillingham et al., 2003). We found that the total uptake of BODIPY- C12 and BODIPY- C16 was greater than for BODIPY- C5, even by as much as an order of magnitude. In fact, over a 20 minute period BODIPY-C16 uptake was greater than for BODIPY-C12.

In both explants and isolated trophoblast fatty acid uptake kinetics differed according to cell type. Similar to our previous report (Kolahi et al., 2016), we found cytotrophoblast uptake of BODIPY-C12 was greater than SCT. Uptake of long- and very-long chain fatty acids into CTB were sensitive to competition from FBS fatty acids, ACSL inhibitor Triascin C (BODIPY-C12 only), and FATP2 inhibition with CB-2; SCT demonstrated less sensitivity to these inhibitors. Since the ACSL family affects long chain fatty acids, but does not behave as a plasma membrane transporter, and because Triacsin C inhibits BODIPY-C12 uptake, it appears that BODIPY-C12 uptake into CTB is supported by esterification. BODIPY-C16 should serve as a ligand for very-long chain Acyl-CoA Synthetases (ACSVL) of which FATP2 is a member (Stahl et al., 2001).

FATP2 is especially relevant in the human placenta because it is the most highly expressed fatty acid transporter in the human placenta (Weedon-Fekjaer et al., 2010), and FATP2 is selective for the uptake and esterification of very long chain polyunsaturated fatty acids like Docosahexaenoate (Melton et al., 2011). FATP2 is localized to the syncytiotrophoblast BPM and cytotrophoblast (Weedon-Fekjaer et al., 2010; Kolahi et al., 2016; Lager et al., 2016). Because BODIPY-C16 uptake may serve as an indicator of FATP2 activity, our data showing that CTB uptake of BODIPY-C16 is greater than SCT suggests that CTB plays a unique role in the uptake of fatty acids similar to DHA.

It is not immediately clear whether the lower uptake of BODIPY-C12 and BODIPY-C16 after CTB to SCT differentiation was associated with the reduction in the expression of FATP2 (Kolahi et al., 2016). We used a CTB differentiation inhibitor, SB203580, that directly blocks p38 MAPK activation, and CTB syncytialization *in vitro* (Daoud et al., 2005; Johnstone et al., 2005). With SB203580 treatment we observed a decrease in BODIPY-C12 uptake over the differentiation 72hr time course, but the decrease was not as large as found in normal differentiation. This effect was seen in spite of the fact that the syncytialization process appeared to be blocked by SB203580. The most important conclusion from these experiments is that blocking differentiation of CTB was sufficient to preserve the ability of CTB to maintain higher levels of BODIPY-C12 uptake than would be expected if differentiation had occurred.

One unexpected result of our study was the degree of fatty acid tracer accumulation in fetal capillary spaces and the rapid rate at which the tracer

intensity increased. Our experimental model differs from studies using the dually perfused placenta in that we allow tracer to accumulate in the capillaries in which there is no flow. A portion of this fluorescence in the capillary may represent the export of long-chain fatty acids incorporated into esterified lipids. The absolute concentration of LCPUFA in esterified lipids is much higher in umbilical than maternal blood (Berghaus et al., 1998). It is possible that the export of esterified BODIPY-fatty acids, presumably integrated within lipoproteins, is significant. The placenta may export lipoproteins as a mechanism of fatty acid transfer as well (Madsen et al., 2004).

We are not the first to report that some attributes of placental fatty acid transport are inadequately described by passive or facilitative mechanisms. La Fond et al. found that arachidonic acid uptake, most similar in chain length to BODIPY-C16 , is ATP and Na dependent in syncytiotrophoblast BPM (Lafond et al., 2000). A common mechanism for BODIPY-C16 uptake and arachidonic acid may explain our observation that BODIPY-C16 accumulated to the greatest degree in explants and isolated trophoblast. Arachidonic acid is known to accumulate to higher degrees than other long-chain fatty acids in the placenta (Haggarty et al., 1997). Alternatively, Thomas et al. observed cord blood enrichment of medium and long-chain fatty acids of partially oxidized long-chain fatty acids and suggested peroxisomal beta-oxidation may facilitate fatty acid transport (Thomas et al., 1985). These reports and others have proposed placental fatty acid transport appears to be regulated and is metabolically expensive.

Importantly, we find that fatty acid uptake and transport cannot be explained by diffusion alone. The fatty acids we tested were taken up into placental cells and fetal capillaries against a concentration gradient. The concentration of fatty acid probes was much greater in explant tissues than in the incubation medium. We found, along with others (Tobin et al., 2009; Krammer et al., 2011; Brass et al., 2013), that uptake of long and very long chain fats are transporter dependent. The mechanism of fatty acid uptake by FATP and transporters in complex with ACSL involves an esterification step that utilizes 2-ATP equivalents per fatty acid molecule (Stahl et al., 2001; Schwenk et al., 2010). Thus, describing the mechanism of fatty acid uptake process as passive or facilitated is not compatible with our observations.

In conclusion, fatty acid uptake in the human term placenta differs according to chain length. Differential and selective esterification may account for differences in uptake in trophoblast cells. Differentiation of CTB to SCT results in a down regulation in long- and very-long chain fatty acid analogue uptake, suggesting these cells play differing roles in lipid uptake and processing in the human term placenta. Our observations showing that tracer fatty acids enter the syncytium, the cytotrophoblast and the fetal capillary against a concentration gradient are compatible only with the conclusion that these molecules are actively transported.

Chapter V: Cytotrophoblast, Not Syncytiotrophoblast, Dominates Glycolysis And Oxidative Phosphorylation In Human Term Placenta[1].

[1]The experiments outlined in this chapter were carried out jointly with Dr. Amy Valent.

Abstract

The placenta is capable of mimicking the essential metabolic functions of an integrated multi-organ system with only a few cell types. Placental function is attributed to a specialized syncytial monolayer, the syncytiotrophoblast, which is derived from a progenitor epithelium, the cytotrophoblast. As gestation advances, the cytotrophoblast layer becomes more difficult to distinguish from the syncytiotrophoblast which becomes more extensive, thus leading to the prevailing view that the term cytotrophoblasts is inconsequential. However, we show that the metabolism of the human placenta during late gestation is driven by a persistent, highly active cytotrophoblast layer. Differentiation of cytotrophoblasts into syncytiotrophoblasts leads to metabolic suppression with fragmentation of the mitochondrial network. The oxygen consumption rate (OCR) and extracellular acidification rate (ECAR), a proxy of glycolytic lactate production, were greater in cytotrophoblast than in syncytiotrophoblast *in vitro* (CTB: 96±16 vs SCT: 46±14 pmol $O_2 \cdot min^{-1} \cdot 100ng\ DNA^{-1}$, $p<0.001$) and (CTB: 43±6.7 vs SCT 1.4±1.0 $\Delta mpH \cdot min^{-1} \cdot 100ng\ DNA^{-1}$, $p<0.0001$). Blocking differentiation or promoting self-renewal of the cytotrophoblast through Epidermal Growth Factor and p38 MAPK signaling prevents the suppression of metabolism. We conclude that the undifferentiated cytotrophoblast has tremendous fuel flexibility and contributes to placental metabolism during late human gestation, which until now has gone unnoticed.

Introduction

The human placenta is a temporary organ whose tissues are generated by the fetus. Its primary function is to ensure that the fetus receives all necessary nutrients found in maternal blood. For this enormous task, it has an extraordinarily high metabolic rate, consuming approximately 40% of the oxygen used by the entire conceptus while accounting for only 20% of the total mass (Oxygen consumption rate: 40 ml/min/kg) (Battaglia and Meschia, 1978; Sparks et al., 1983; Bonds et al., 1986; Lurie et al., 1999). The placental produces hormones, transports and biochemically transforms all essential nutrients required to support fetal development; these processes exact a high metabolic cost. The survival of the fetus depends upon a placenta that is able to extract the oxygen it needs, is highly efficient for transport and is also able to provide for metabolic and growth needs of the developing fetus. As one would presume, placental metabolic dysfunction is a hallmark of maternal-fetal disorders such as pre-eclampsia and gestational diabetes (Bloxam et al., 1987; Austdal et al., 2015; Muralimanoharan et al., 2016). The metabolic contributions made by each of the cell types in the placenta have been little studied (Bax and Bloxam, 1997).

The maternal facing surface of the materno-placental exchange barrier is composed of a monolayer of terminally differentiated trophoblast cells, the syncytialized trophoblast (SCT). During placental development the SCT is derived from progenitor cells in the underlying layer, the cytotrophoblast layer (CTB). The SCT has been presumed to account for the largest proportion of

placental metabolic activity because it is in direct contact with maternal blood, synthesizes and secretes large quantities of protein and steroid hormones, and is believed to be the primary transport tissue for all nutrients acquired by the fetus. However, in the previous chapters we have shown the degree of fatty acid uptake and esterification is greater in the CTB than in the SCT.

Our recent discovery that the CTB exclusively esterifies free-fatty acids, casts doubt on the prevailing theory that all nutrient processes are restricted to the SCT (Kolahi et al., 2016). Unlike the SCT, the CTB rapidly generates lipid droplets and other lipid species, like phospholipids, from free fatty acids. A host of genes that regulate lipid metabolism are more highly expressed in the CTB than in SCT (Kolahi et al., 2016). Esterification of free-fatty acids poses a high ATP cost and is prerequisite to fatty acid metabolism suggesting that the CTB may generate more ATP than previously thought. However, this possibility has not been previously investigated. Thus, we tested the hypothesis that CTB is more metabolically active than SCT and more capable of generating ATP. To thoroughly examine the metabolic properties of the two trophoblast cell types, we compared their capacity to generate ATP to utilize oxidative phosphorylation and glycolysis with different fuel substrates. We also tested the hypothesis that activity-sensitive mitochondrial dyes could distinguish the two trophoblast cell types using optical analysis.

Methods

Subject Details

Placentas were collected from women undergoing a scheduled cesarean delivery at the Oregon Health & Science University (OHSU) obstetric unit between 06/2015 to 05/2016. This study was approved by the Institutional Review Board (IRB #5684) and informed consent was obtained prior to delivery. Uncomplicated, singleton placental samples were included, excluding pregnancies complicated by the following characteristics: prepregnancy obesity (BMI ≥30 kg/m^2), multifetal gestation, fetal chromosomal or structural anomalies, preeclampsia or hypertensive spectrum, immunosuppressive, or chronic maternal morbidities. Maternal data was obtained from medical records included age, parity, race, gestational age at delivery, height, and weight (1st trimester). Neonatal data included birth weight, crown-heel length, and sex. Placenta weight and length and width dimensions were measured during tissue collection. Maternal characteristics are summarized in Table 5.1.

Table 5.1: Maternal Characteristics

	Mean±S.D. (n=28)	**95% Confidence Interval**
Age (yr)	31±5	[28, 34]
Body Mass Index (BMI: kg/m^2)	23±5	[20, 26]
Parity	2±2	[1 , 3]
Gestational Age (weeks)	39±1	[39, 40]

Birth Weight (g)	3300±550	[3000 , 3700]
Placenta Weight (g)	493±104	[429, 557]

Primary human villous cytotrophoblast isolation and culture

All placental samples were processed within 30 minutes of delivery. CTB cells were isolated using a trypsin-DNAse I digestion followed by Percoll enrichment as previously described (Guilbert et al., 2002). In brief, chorion and maternal decidua were removed, and 40-50g of villous placental tissue was finely minced and thoroughly washed with 1x phosphate-buffered saline (PBS). Villous fragments were subjected to three or four sequential 10-15 minute (37°C) digestions in 0.25% Trypsin (Gibco) and 200 U/mL DNAse I (Roche). CTB were purified by Percoll (GE Healthcare Bio-sciences AB) discontinuous density gradient centrifugation at 1200 rcf for 25 minutes (room temperature). Purity of trophoblast isolations was assessed by positive immunohistochemical staining of cyokeratin-7 (MAI-06315, Thermo Scientific), a marker of trophoblast cells. All isolations comprised of >90% pure, viable CTB.

CTB were plated at an optimal density of 3×10^5 cells/cm^2 and cultured in Iscoves Modified Dulbecco's Medium (IMDM, Gibco®) or Minimum Essential Media alpha GlutaMAX™ without nucleosides (MEMα, Gibco®) supplemented with 10% fetal bovine serum (FBS, Gibco®), 100 U/mL penicillin, and 100 µg/mL streptomycin and incubated at 37°C 5% CO_2. Growth medium was replaced every 24 hours. Prior studies have demonstrated CTB undergo fusion and differentiation into multinucleated, syncytialized giant cells by 72 hours in culture (Kliman et al., 1986). Therefore, cells were studied at 8 hours (CTB) to study

prior to differentiation and 72 hours (maximum) to study SCT.

Metabolic Flux Analyses

Primary human trophoblast cells (40,000/well) were plated into 96-well culture plates and oxygen consumption rate (OCR) and extracellular acidification rate (ECAR) was measured using the Seahorse XF^{e}96 flux analyzer (Seahorse Bioscience, North Billerica, MA). At the time of assay, growth medium was removed, replaced with the appropriate pre-warmed assay medium and trophoblast were subjected to a Mitochondria or Glycolytic stress test™ (Seahorse Bioscience). For fatty acid oxidation studies, assay medium was composed of warmed serum-free 1x Krebs Henseleit Buffer (KHB) supplemented with 0.5 mM glucose, 0.5 mM carnitine and 5 mM HEPES (pH 7.4). Fatty acid:Bovine Serum Albumin (BSA) (~6:1) conjugates were prepared according to the manufacturers recommendations and supplemented to KHB assay medium(Pike Winer and Wu, 2014). Immediately prior to assay measurements fatty acid supplements were added with the following final concentrations C16 [250μM], C18:1 [250μM] or vehicle (BSA [41μM]) +/- etomoxir (Eto 40μM), a carnitine palmitoyltransferase 1 inhibitor (CPT1) of fatty acid oxidation. Under these conditions the following injections and final concentrations were: (1) 2μM oligomycin (ATP synthase inhibitor; Sigma), (2) 5 μM carbonyl cyanide p-trifluoromethoxyphenyl-hydrazone (FCCP) (mitochondrial uncoupling agent; Sigma), and a (3) mixture of 2μM Rotenone (mitochondrial complex I inhibitor; Sigma) and 2μM Antimycin A (Mitochondrial complex III inhibitor; Sigma). OCR was recorded for three cycles following by each timed injection.

For glycolytic stress test measurements, XF Base Medium (Seahorse Biosciences) supplemented with 1mM pyruvate and 4mM L-glutamine was used and the following glycolytic stress test injections and final concentrations were: (1) 25mM Glucose, (2) 1μM oligomycin, (3) 100mM 2-Deoxyglucose (hexokinase inhibitor; Sigma).

For metabolic studies with Epidermal growth factor, CTB were cultured in MEMα medium in the presence or absence of 10ng/mL epidermal growth factor (EGF) +/- 1μM of MK 2206 (allosteric inhibitor of protein kinase Akt), +/- 10μM SB203580 (p38α and p38β inhibitor). After 8 (CTB) and 72 hours (SCT) of culture, growth medium was removed and replaced with an assay medium containing glucose (5mM), glutamine (4mM), pyruvate (1mM) and fatty-acids (C16 25μM) was utilized to measure full metabolic capacity. Four serial baseline OCR and ECAR measurements were averaged and analyzed. Metabolic flux was measured in triplicate for each condition and all experimental replicates were normalized to DNA content using Quant-iT™ PicoGreen® dsDNA kit (Molecular Probes; Eugene, OR).

Intracellular ATP quantification

Isolated CTB were plated on flat-bottom 96-well plates as previously described and cultured in complete growth medium for 8 and 72 hours. The growth media was removed and 40μL of the cell lysate was used to quantify intracellular ATP using an ATP luminescence assay (ATPlite™, PerkinElmer®). Luminescence was measured using a Biotek Synergy H1 plate reader (Biotek). ATP content was normalized to lysate protein concentration using a bicinchoninic

acid assay assay (Thermo Pierce).

Mitochondrial labeling, imaging, and quantification

Isolated CTB were plated on glass coverslips and cultured for 8 or 72 hours in complete growth medium. At each specified time point, 500nM of Mitotracker Orange (CM-H_2TMRosa; Molecular Probes) was added to each well and incubated for 2 hours. Twenty minutes before these two hours had elapsed, 4µg/ml Wheat Germ Agluttinin-CF640R (Biotium) was added to demarcate the plasma membrane. After 2 hours, cells were fixed with pre-warmed 3.7% paraformaldehyde (pH 7.4) in complete growth medium for 30 minutes and incubated at 37°C/5% CO_2. After fixation, the coverslips were submersed into -20°C Acetone for 10 minutes and subsequently washed up to 3 times in 1x PBS. The coverslips were counterstained with 2µg/ml Hoechst 33258 (Molecular Probes) to identify nuclei for 20 minutes and mounted in Slowfade Diamond (Molecular Probes, Inc) before confocal imaging. Imaging was performed using a Zeiss 880 LSM Confocal with Airyscan™ with a 63× High N.A. objective (N.A.=1.4; Zeiss). Each field of view was comprised of serial Z-“stack” of images measuring 67.5µm by 67.5µm (x-y) spaced 0.2µm apart with 2µM total thickness. All raw, 32-channel single-color images were processed using automatically determined Airyscan parameters in Zen software (Zeiss). Processed images were analyzed using Fiji software (Schindelin et al., 2012) using Otsu automatic thresholding to segment mitochondria. The mitochondrial volume ratio was calculated by normalizing the quantified mitochondrial volumes to cytoplasmic volumes quantified from plasma membrane images. A minimum of 3 fields of

view were used per biological replicate.

Placental explant collection, culture, and imaging.

Explants (<1mm^3) were isolated as previously described (Brass et al., 2013), with some modifications. Placental tissue was isolated from two different cotyledons that appeared healthy and placed in pre-warmed (37°C) MEMα culture media (Gibco) supplemented with serum and 25mM Hepes (pH 7.4). Three to four explants from different cotyledons were cultured per well on transwell permeable supports (Corning) in 12-well plastic culture plates(Corning) containing 2.0mL of growth medium and incubated at 37°C in 5% CO_2/95% air. Mitochondrial labeling proceeded immediately after collection (<30min) as described above for cells, and total incubation time until fixation was 2.5 hours. Explants were assayed within a known window when markers of explant health and fatty acid uptake are not compromised (Brass et al., 2013).

Immunofluorescence (whole mount explants, cells)

Fixed explants and cells were blocked and permeabilized using Block-Aid (Life Technologies)/0.1% Tween-20 (ThermoFisher) for 30 minutes before overnight incubation with primary antibody at 4°C. Samples were labeled with antibodies against HAI-1 (1:100; 9B10, eBioscience). Following primary antibody incubation, samples were washed 3 times with 0.01% Tween-20 in PBS and labeled with secondary antibodies rabbit anti-mouse Alexa Fluor 488 (1:500, A27023, Invitrogen) for 1 hour at room temperature. After washing 3 times, the samples were counterstained with 2μg/ml Hoechst 33258 for 20 minutes and immersed in Slowfade Diamond (Molecular Probes) immediately before confocal

imaging.

Quantification of mRNA expression

Total RNA from 3 × 10^6 cells was isolated after 8hr or 72hr of culture using Qiagen RNeasy isolation kit. RNA content was assessed by spectroscopy at 260nm/280nm and integrity via visualization of ribosomal RNA using gel-electrophoresis. Reverse transcription of 1µg of RNA to cDNA was performed using the High Capacity cDNA Reverse Transcription kit (Life Technologies). cDNA was stored at -20°C. Gene specific primers were designed for *VPS29* house-keeping gene using NCBI primer-BLAST (Ye et al., 2012). Sequences for primers for BHCG (*CGB*) were taken from Kolahi et al (Kolahi et al., 2016). (Primer sequences for *VPS29* were: F GACAGGATGTTGGTGTTGGT. R TAGCTGGCAAACTGTTGCAC. qPCR was performed as described previously (O'Tierney et al., 2012). Relative expression quantities were expressed as a ratio of the gene of interest to the reference gene (*VPS29*) in each sample; *VPS29* expression did not differ at 8 hours versus 72 hours.

Statistics

2-way ANOVA with Sidak's post-hoc testing was used to compare metabolic fluxes between conditions. An unpaired Student's t-test was used to compare mitochondrial volume ratios. All data were analyzed using GraphPad Prism 6 and are presented as mean ± SEM unless noted otherwise. P-values <0.05 were considered statistically significant.

Results

Isolated CTB had a greater oxygen consumption rate (OCR) at baseline and at maximal capacity in the presence of long-chain fatty acids compared to SCT; Palmitate(C16) [baseline: 85±11 vs 47±6 pmol $O_2 \cdot min^{-1} \cdot 100ng\ DNA^{-1}$, $p<0.01$; maximal: 153±27 vs 60±10 pmol $O_2 \cdot min^{-1} \cdot 100ng\ DNA^{-1}$, $p<0.001$ (Figure 5.1A)] and Oleate (C18:1) [baseline: 108±14 vs 66±11 pmol $O_2 \cdot min^{-1} \cdot 100ng\ DNA^{-1}$, $p<0.001$; maximal: 176±23 vs 68±11 pmol $O_2 \cdot min^{-1} \cdot 100ng\ DNA^{-1}$, $p<0.0001$ (Figure 5.1B)].

Treatment with Etomoxir, an inhibitor of Carnitine Palmitoyl-transferase 1a, reduced maximal OCR in both CTB [C16: 69±11 pmol $O_2 \cdot min^{-1} \cdot 100ng\ DNA^{-1}$, $p<0.0001$; C18:1: 78±9.2 pmol $O_2 \cdot min^{-1} \cdot 100ng\ DNA^{-1}$, $p<0.0001$ (Figure 5.1C,D)] and SCT [C16: 27±7.3 pmol $O_2 \cdot min^{-1} \cdot 100ng\ DNA^{-1}$, <0.0001; C18:1: 36±5.4 pmol $O_2 \cdot min^{-1} \cdot 100ng\ DNA^{-1}$, $p<0.0001$ (Figure 5.1C,D)]. To determine whether the greater levels of oxygen consumption were associated with differences in ATP production or utilization, we measured intracellular ATP content in each cell type. Greater ATP levels were observed in CTB compared to SCT [6.2±2.9 vs 2.4±0.55 nmol·ug $protein^{-1}$; $p<0.01$ (Figure 5.1E)]. It has been previously established that SCT is the primary cell for steroid production. SCT is transcriptionally active and the production of large quantities of chorionic gonadotropin is a distinguishing feature [5933±150%; $p<0.0001$ (Figure 5.1F)] compared to CTB, which produced very little.

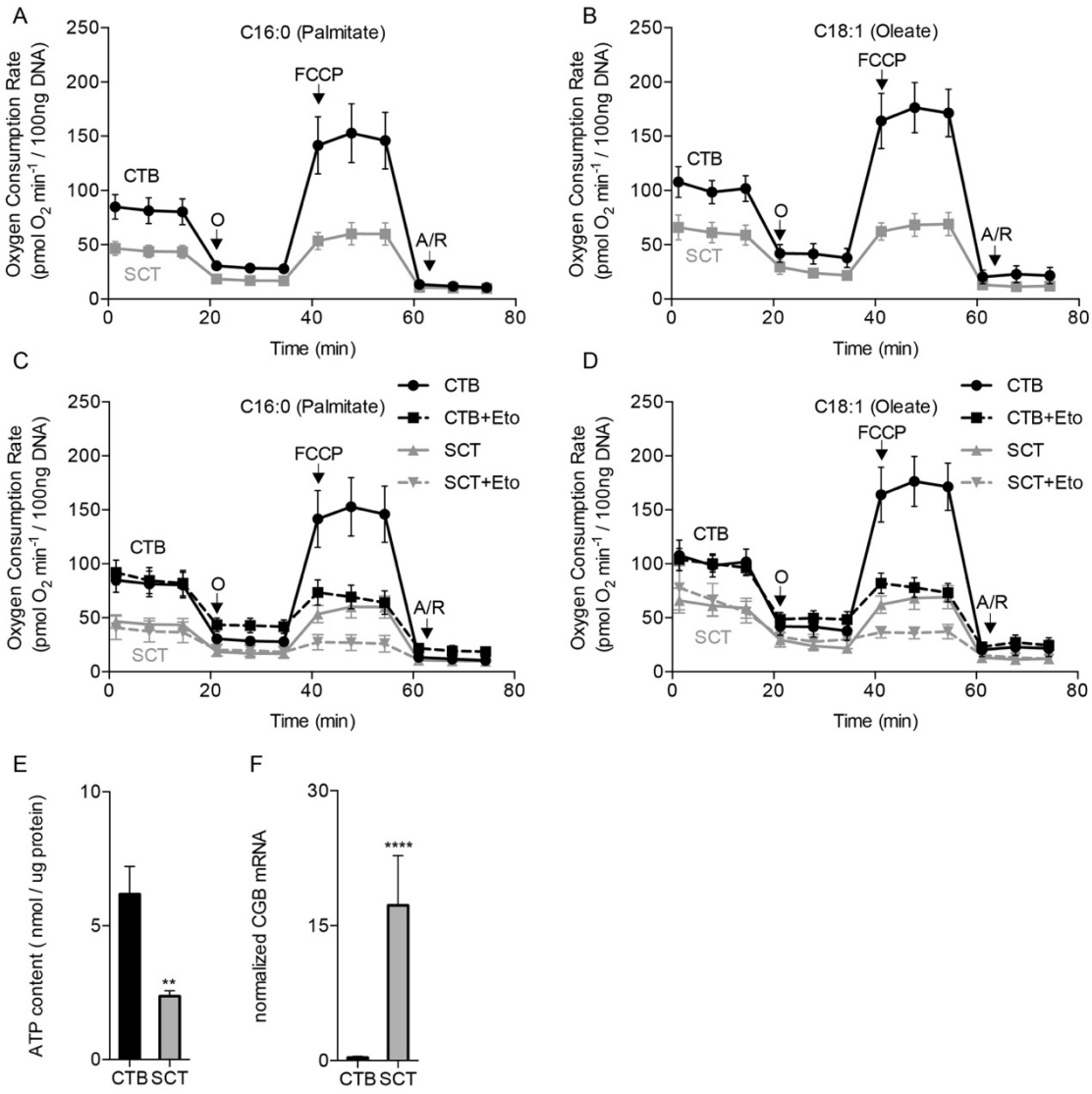

Figure 5.1. Human cytotrophoblast respiration rates are greater than syncytiotrophoblast.

Human cytotrophoblast cells (CTB) were isolated from term placentas and studied *in vitro* before and after differentiation into syncytiotrophoblast (SCT). (A-B) Respiration was measured in media containing 250μM of either saturated long-chain fatty acid palmitate (C16) or the monounsaturated oleate (C18). Oxygen consumption rate (OCR) was greater in CTB than in SCT at baseline and at all points of the mitochondrial stress protocol. (C-D) Etomoxir, an inhibitor of CPT1, reduced maximal OCR after FCCP injection in both CTB and SCT for both fatty acids but not at baseline. (E) Resting ATP levels in CTB are much greater than in SCT. (F) Evidence of the identity of each cell type is shown; SCT, but not CTB produces high levels of CGB. Oligomycin (O), Antimycin/Rotenone (A/R). Data are Mean±SEM, n=7 placentas.

Human trophoblasts have specialized free-fatty acid uptake systems to serve as the selective conduit for maternal long- and very-long chain polyunsaturated fatty acids. Since our assay media contained primarily fatty acids as a fuel source, we hypothesized the greater OCR in CTB could be a byproduct of their greater free-fatty acid uptake capacity and SCT may selectively metabolize other fuels. An important fuel for the placenta and fetus is glucose. Glucose is metabolized to yield lactate in fetal and placental tissues to minimize oxygen utilization. Thus, the SCT could possibly meet its metabolic needs exclusively through glycolysis. We tested this hypothesis by measuring glycolysis in CTB and SCT using the Seahorse XF Bioanalyzer. We found that differences between CTB and SCT in extracellular acidification rate (ECAR), a proxy for lactate production through glycolysis, were even more dramatic than OCR (Figure 5.2A). This effect was independent of glucose concentration (Figure 5.2A). Baseline ECAR in CTB and SCT were (53±5.8 and 18±3.4 ΔmpH$\cdot$min$^{-1}\cdot$100ng DNA^{-1}, $p<0.0001$) at 5mM glucose. The effect of glucose concentration on ECAR could only be detected in CTB at 25mM glucose (63±5.5 ΔmpH$\cdot$min$^{-1}\cdot$100ng DNA^{-1} $p=0.04$) (Figure 5.2B). Maximal ECAR, a measurement of glycolytic capacity, was similarly greater in CTB compared to SCT (245±10 vs 129±19 ΔmpH$\cdot$min$^{-1}\cdot$100ng DNA^{-1}, $p=0.001$). Glycolytic reserve, the difference between baseline glycolysis and maximal glycolysis, was not different between CTB and SCT (Figure 5.2D). The estimate of mitochondrial respiration to glycolytic respiration, the OCR to ECAR ratio, was substantially higher in SCT than in CTB (3.5±0.20 vs.1.3±0.075; $p<0.01$) (Figure 5.2E), suggesting that SCT usually

depends more on oxidative phosphorylation than does CTB even though CTB is more capable at oxidative phosphorylation under specific fuel conditions.

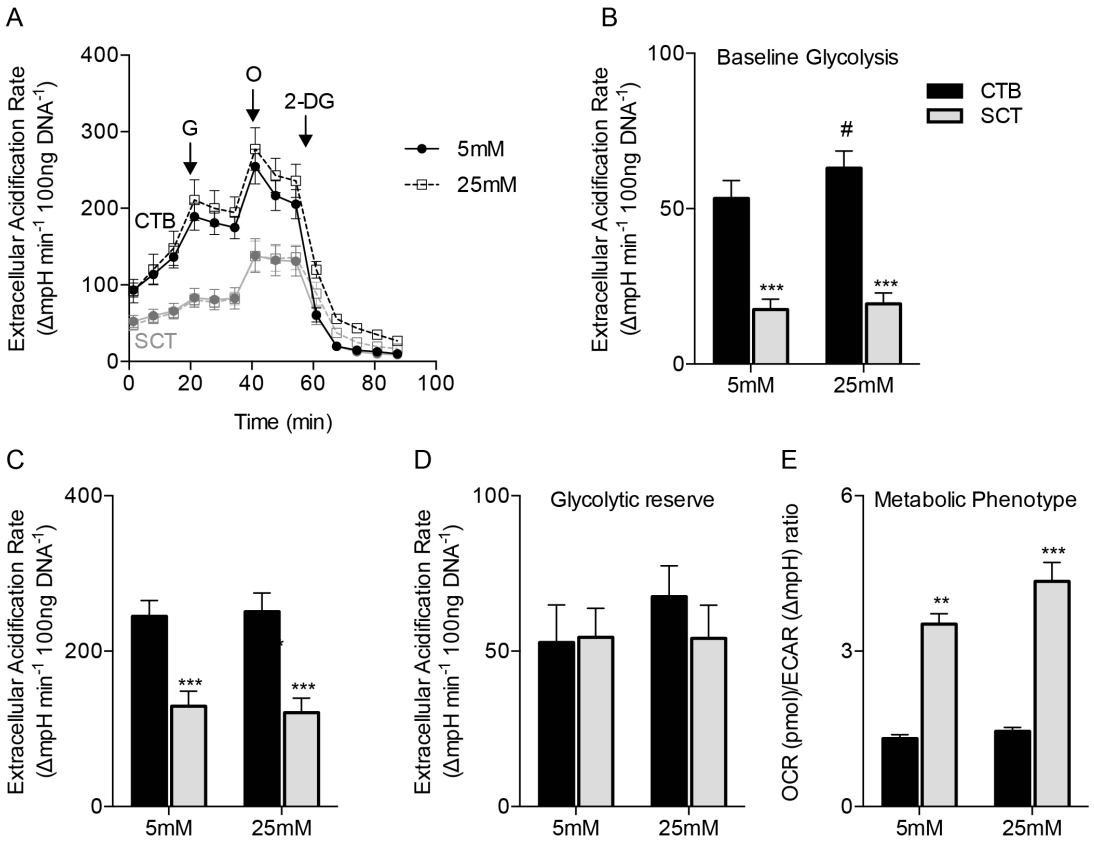

Figure 5.2. Cytotrophoblast are highly glycolytic.
The glycolytic metabolism of primary human trophoblast was measured *in vitro* using the Seahorse XF Bioanalyzer. (A) Cytotrophoblast (CTB) and syncytiotrophoblast (SCT) extracellular acidification rates (ECAR), a metric of lactate production via glycolysis, was measured during a glycolytic stress experiment with medium containing 5mM or 25mM glucose injected at G and pyruvate and glutamine. (B) ECAR was higher in CTB than in SCT at baseline and not affected by glucose concentration. (C) maximal glycolytic capacity after oligomycin (O) injection which inhibits ATP production was highest in CTB, but (D) glycolytic reserve, the difference between maximal capacity and baseline was not different between groups. These data suggest the presence of a substantially greater glycolytic flux in CTB than in SCT. (E) The ratio of oxygen consumption rate (OCR) to ECAR at both concentrations of glucose indicates that CTB is more glycolytic than SCT under these conditions. Data are Mean±SEM, n=6 placentas. # $p<0.05$ vs glucose concentrations.

CTB had the capacity for higher levels of glycolysis and mitochondrial respiration than did SCT. Previous investigations have described differences in mitochondrial morphology between CTB and SCT via TEM of tissue sections and isolated mitochondria (De los Rios Castillo et al., 2011). We postulated the differences in mitochondrial activity could underlie our observations of the differences in metabolic flux between CTB and SCT. We utilized Mitotracker, CM-H2TMRosa whose uptake and fluorescence are dependent upon mitochondrial membrane potential ($\Delta\psi$) and oxidative activity. CTB contain numerous elongated mitochondria in a tightly packed network (Figure 5.3A). In contrast, SCT demonstrate fewer mitochondria that are fragmented and distributed around cytoplasmic vesicles (Figure 5.3B). The mitochondrial area ratio in CTB was greater than in SCT (0.22±0.03 vs 0.11±0.01, p=0.025). We used the Mitotracker method to localize active mitochondria in human term placental explants and found that the most active mitochondria were predominantly in cytotrophoblast and to a lesser degree in endothelium (Figure 5.3C). These data indicate that differentiation of human placental CTB into SCT in culture leads to changes in the mitochondrial morphology and network topology.

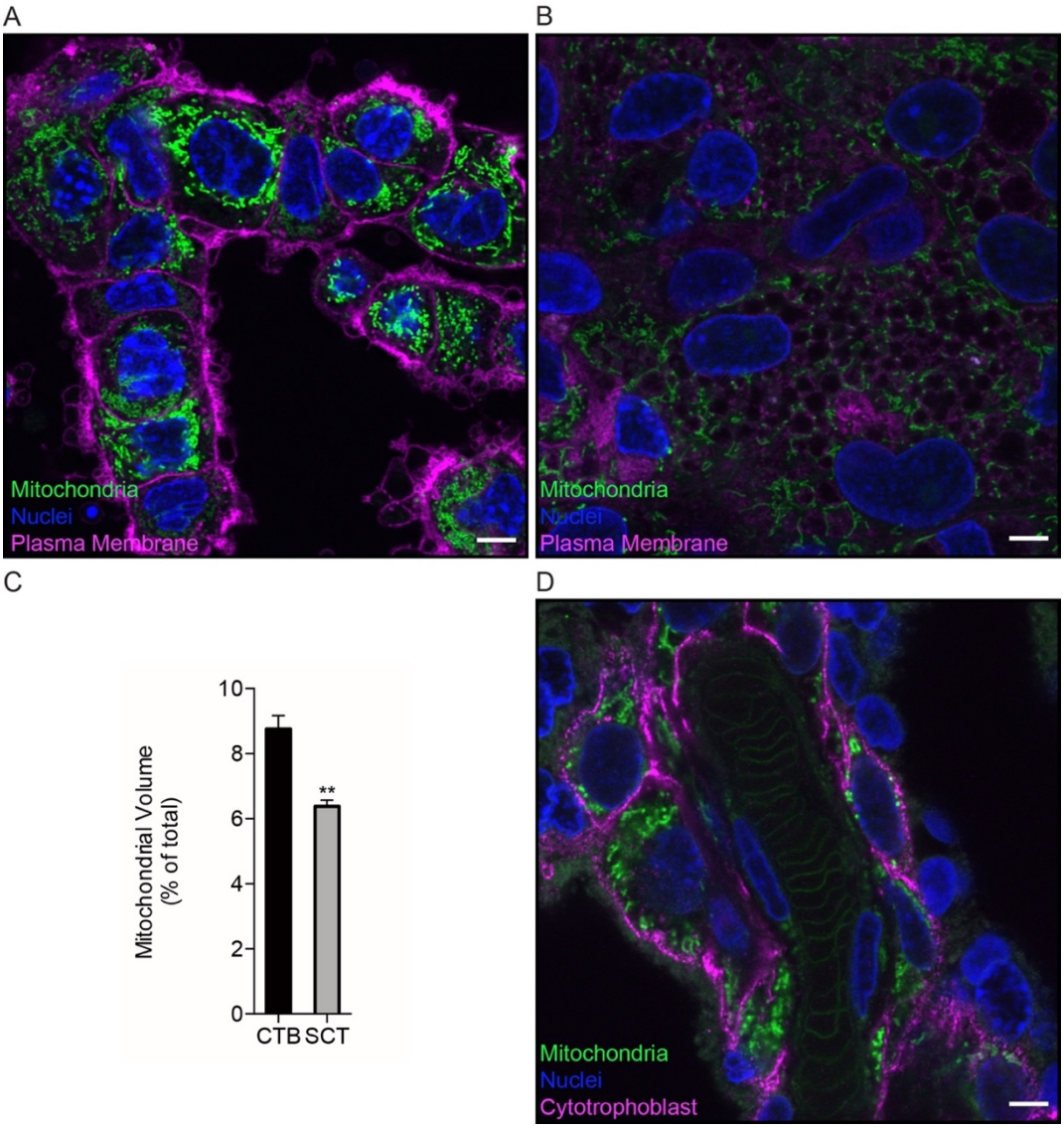

Figure 5.3. Differentiation of Cytotrophoblast to Syncytiotrophoblast leads to a fragmented mitochondrial network.

The mitochondrial activity indicator dye, Mitotracker (CM-H_2TMRos) was used to localize active mitochondria in cytotrophoblast (CTB) and syncytiotrophoblast (SCT) in living explants of human term placentas using super-resolution fluorescence microscopy. Wheat germ agglutinin (magenta) was used to label plasma membrane in (A) and (B) and nuclei are labeled with Hoechst dye (blue). HAI-1 was used to label cytotrophoblast (magenta) in (D).

(A) Mitochondria (green) in CTB are tightly packed in a perinuclear fashion. (B) The differentiation of CTB to SCT leads to a change in mitochondrial morphology and to their placement adjacent to scattered vesicles. (C) Mitochondrial volume is relatively larger in CTB than in SCT. (D) In fresh explants of human term placenta, the most active and most brightly stained mitochondria are located in the cytotrophoblast. Some active mitochondria are also visible in endothelium. Scale Bar: 5μm. Data are Mean±SEM. Representative images from n=3 placentas.

To explore the mechanism leading to metabolic changes in cytotrophoblast differentiating to syncytiotrophoblast we tested the effect of EGF, a known modulator of the differentiation process (Johnstone et al., 2005). Trophoblast cultures were exposed to EGF in C16 fatty acid supplemented complete growth medium. We measured baseline respiration (OCR) and glycolysis (ECAR) of CTB and SCT. EGF-exposed CTB and SCT had increased rates of glycolysis compared to non-EGF treated trophoblasts [(CTB: 97±12 vs 43±6.7 ΔmpH·min^{-1}·100ng DNA^{-1}, $p<0.0001$); (SCT: 29±5 vs 1.4±1.0 ΔmpH·min^{-1}·100ng DNA^{-1}, $p<0.01$), Figure 5.4A]. Surprisingly, oxidative respiration also increased in both CTB and SCT with constant exposure to EGF compared to the non-EGF treated state [(CTB: 164±22 vs 96±16 pmol O_2·min^{-1}·100ng DNA^{-1}, $p<0.001$); (SCT: 119±18 vs 46±14 pmol O_2·min^{-1}·100ng DNA^{-1}, $p<0.001$), Figure 5.4B]. EGF potently stimulated both baseline glycolysis and mitochondrial respiration in trophoblast.

While EGF modulates metabolism via several signaling pathways (Fisher and Lakshmanan, 1990), Akt, is a central metabolic hub that has been shown to regulate glycolytic rates in many systems (Elstrom et al., 2004). To test the role of Akt in trophoblast metabolism, MK2206, an Akt S473 phosphorylation inhibitor, was applied. The addition of MK2206 to EGF reduced ECAR in CTB and in SCT compared to EGF exposure alone [(CTB: 70±15 vs 97±12 ΔmpH·min^{-1}·100ng DNA^{-1}, $p<0.01$); (SCT: 4.3±3.3 vs 29±5 ΔmpH·min^{-1}·100ng DNA^{-1}, $p=0.01$), Figure 5.4A]. MK2206 also led to a significant decrease in OCR in SCT but a decreasing trend not in CTB did not reach significance [(SCT: 60±19 vs

119±18 pmol $O_2 \cdot min^{-1} \cdot 100ng\ DNA^{-1}$, $p<0.001$); (CTB: 136±24 vs 164±22 pmol $O_2 \cdot min^{-1} \cdot 100ng\ DNA^{-1}$, $p=0.06$), Figure 5.4B). We could detect no effect on metabolism with MK2206 in trophoblast in the absence of EGF, suggesting Akt must be activated for MK2206 to exert an effect.

Considering the possibility that EGF could exert a direct metabolic effect on SCT to stimulate metabolism or support the preservation of CTB by leading to alterations of CTB differentiation, we studied mitochondrial activity using Mitotracker in EGF treated cultures. In the absence of EGF, trophoblast fusion and differentiation to form a syncytial sheet was virtually complete, and mitochondrial networks became fragmented as described previously (Figure 5.4C). However, EGF treated cultures displayed a striking and distinct arrangement composed of two cell layers (Figure 5.4D). A layer of fused cells with no visible intercellular divisions and very few detectable active mitochondria was visible (Figure 5.4E), but interspersed throughout this layer there were clusters of individual, unfused, cells with highly active mitochondria (Figure 5.4E). These cell clusters contained visible intercellular divisions, implying that these cells are undifferentiated CTB. Thus, it appears that while EGF stimulation leads to greater SCT formation, but also maintains CTB in the unfused condition.

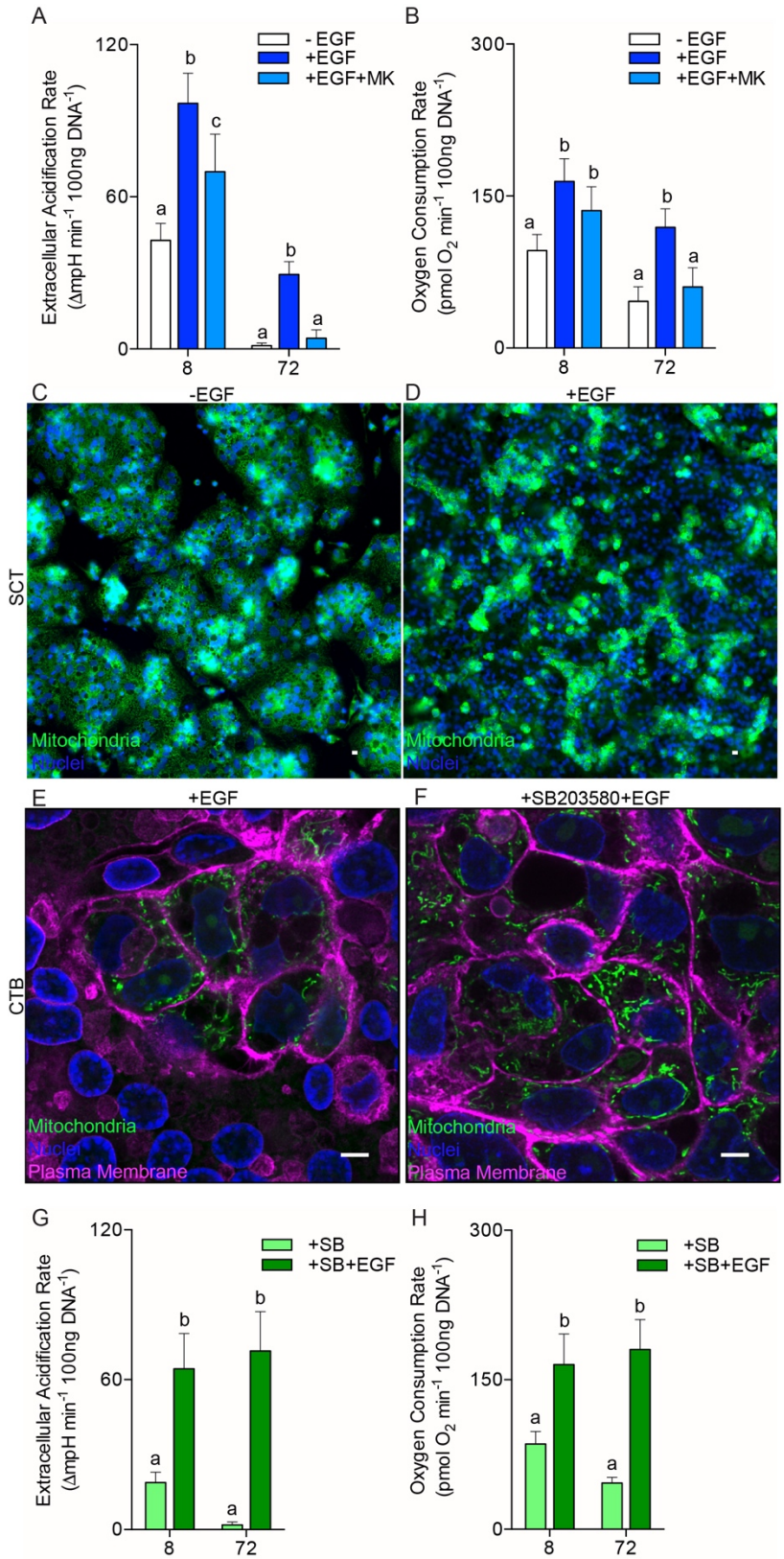

Figure 5.4. Epidermal Growth Factor and Akt contribute to metabolism and differentiation of Cytotrophoblast.

Differentiated (SCT) primary human trophoblasts were studied at 72hrs in serum free medium supplemented with fatty acids (25μM C16). (A) Extracellular acidification rate (ECAR) and oxygen consumption rate (OCR) (B) were powerfully stimulated using epidermal growth factor, EGF (10ng/ml). MK2206, an inhibitor of Akt activation suppressed the actions of EGF. (C) In the absence of EGF under control conditions, SCT has fragmented mitochondrial networks as described in Fig 5.3. (D) In the presence of EGF, trophoblast cultures contained sheets of SCT, with many aggregates of unfused cells that appeared undifferentiated. (E) A higher resolution confocal micrograph shows that the undifferentiated cells within the syncytial layer have prominent intercellular membranes (wheat germ agglutinin, magenta). Active mitochondria marked with Mitotracker, CM-H2TMRosa, green, are specifically observed in the CTB clusters. (F-H) The natural course of metabolic suppression during differentiation can be circumvented by employing an inhibitor of the p38 MAPK pathway (10μM SB203580, SB), a differentiation inhibitor, along with EGF stimulation. (F) Confocal micrograph of CTB treated with EGF and SB203580 for 72hrs and stained with mitotracker. Cell fusion does not occur in these conditions, and all cells have active mitochondria. CTB fusion was blocked with this combined treatment and active mitochondria can be observed in all cells. (G) OCR and (H) ECAR, are elevated with no apparent decrease between 8 and 72hrs when treated with both EGF and SB203580. Scale Bar: 5μm Data are Mean±SEM, n=6 placentas.

To test whether EGF affects trophoblastic differentiation and fusion by altering the differentiation process, we blocked the differentiation of CTB while exposed to EGF. We added the p38 MAPK inhibitor, SB203580, to block differentiation. As expected, blocking the differentiation program in CTB by combining SB203580 with EGF blocked CTB fusion (Figure 5.4F) and resulted in the highest levels of ECAR (64±14 ΔmpH·min^{-1}·100ng DNA^{-1}, $p<0.05$) relative to all treatments and OCR (165±31 pmol O_2·min^{-1}·100ng DNA^{-1}, $p<0.01$) with the exception of EGF only (Figure 5.4G,H). Interestingly in EGF and SB203580 exposed cultures, metabolism was maintained over time [(SCT ECAR: 71±16 ΔmpH·min^{-1}·100ng DNA^{-1}, $p<0.01$) and (SCT OCR: 180±30 pmol O_2·min^{-1}·100ng DNA^{-1}, $p<0.01$), Figure 5.4G,H].

An interesting finding was that independent of EGF, CTB in SB203580 medium alone did not maintain the high levels of glycolysis or oxidative respiration that usually characterizes CTB *in vitro* (SCT ECAR: 1.9±1.2 vs 1.4±1.0 ΔmpH·min^{-1}·100ng DNA^{-}, SB203580 vs control; $p=0.99$); (SCT OCR: 45±6.9 vs 32±3.8 pmol O_2·min^{-1}·100ng DNA^{-1} SB203580 vs control; $p=0.86$), Figure 5.4G,H. These results suggest EGF is necessary for maintenance of the CTB metabolic phenotype.

Discussion

We have provided several lines of evidence that CTB is the leading metabolic cell in the human placenta at term which contradicts the prevailing view that the SCT holds that position (Bax and Bloxam, 1997; Jansson et al., 2006b; Benirschke et al., 2012). We measured mitochondrial respiration and glycolysis in primary human trophoblast as undifferentiated progenitor cells (CTB) and after differentiation to SCT. We consistently found greater levels of both glycolysis and mitochondrial respiration in CTB compared to SCT. We also found that CTB have higher ATP levels. Of the total ATP generated by each cell type, a bigger proportion would likely be generated by oxidative phosphorylation in SCT than CTB. The most fascinating finding was that CTB is more metabolically flexible. CTB could better maintain respiratory rates under varying nutrient levels in the growth medium during our stress tests. Nevertheless, we found CTB are heavily glycolytic under resting conditions compared to the SCT, the latter which is supported almost entirely by oxidative respiration.

The placenta utilizes aerobic glycolysis as its primary metabolic fuel to conserve oxygen supplies for fetal tissues and produce lactate which is crucial fuel source for fetal growth (Battaglia and Meschia, 1978; Settle et al., 2006). Approximately 25% of the CO_2 produced by the fetus comes from the oxidation of lactate derived from maternal glucose (Burd et al., 1975); the placenta is the primary production site for lactate in the fetus (Burd et al., 1975; McGowan et al., 1995). It is possible then that placental glucose consumption through glycolysis

and lactate production is principally driven by the CTB. Measurements of glucose derived ECAR are indirect measurements of cellular export of lactate produced from glucose. A key player in the export of lactate is the monocarboxylate transporter 1 (MCT1), which is expressed very highly in the CTB of human placentas (Nagai et al., 2010). It is not known if the CTB participate in placental nutrient transport, but their high metabolic activity and continuity adjacent to the basal SCT plasma membrane suggest that the CTB layer could be important in nutrient transport (Mori et al., 2007; Kolahi et al., 2016).

Lactate production by CTB could be associated with anabolic metabolism. Aerobic glycolysis and lactate production support *de novo* lipogenesis (Costello and Franklin, 2005), including synthesis of cholesterol, which is a key metabolic activity in proliferating cells. CTB, but not SCT, are proliferative and CTB have much greater rates of *de novo* lipogenesis (Coleman and Haynes, 1987). Given the enormous importance of placental nutrient transport and metabolism in supporting normal development, and the surprisingly few studies investigating the role of the CTB in transport, the field is ripe for an all-out effort to understand the intricacies of the CTB biology.

Previous reports support the idea that cytotrophoblast is a highly metabolically active placental cell (Bax and Bloxam, 1997) and this suggestion is not exclusive to the term placenta (James et al., 2005). To our knowledge this study is the first to directly compare the metabolic flux rates CTB as they differentiate and become SCT. Other studies on isolated mitochondria from

placenta support our findings that CTB mitochondrial respiration is greater than SCT (Bustamante et al., 2014).

Our findings could be especially relevant to the numerous studies that have found alterations in placental metabolism in pre-eclampsia (Bloxam et al., 1987; Austdal et al., 2015) and in obesity (Muralimanoharan et al., 2016). Indeed, abnormal CTB differentiation and EGF signaling have been proposed as important in the pathophysiology of pre-eclampsia (Fisher, 2004; Armant et al., 2015).

Both mouse and human studies have suggested that fetoplacental growth can be regulated by the EGF axis (Fondacci et al., 1994; Faxén et al., 1998; Dackor et al., 2009). Our study focused on understanding normal metabolic rates of CTB compared to SCT, but future studies will test if pathological conditions like pre-eclampsia or fetal growth restriction lead to changes in CTB metabolism, and if this may be due to EGF signaling.

EGF signaling potently stimulated the metabolic rate of CTB and rescued the suppression in metabolism during the normal course of CTB differentiation to SCT. EGF has been described as a stimulator of CTB fusion and differentiation because cultures treated with EGF contain more SCT, but biochemical markers of differentiation do not fit with this notion (Johnstone et al., 2005). One paper was not consistent with this point of view, but this was likely because the concentrations of EGF were 100x lower than used in the others (Morrish et al., 1987). We propose that the controversy over whether or not EGF is a stimulator of CTB fusion could be explained if EGF were a stimulant of CTB proliferation *in*

vitro as we and others have observed (Johnstone et al., 2005). We are intrigued that pockets of undifferentiated cytotrophoblast remain along with syncytialized trophoblast in culture following EGF treatment.

Some of the direct metabolic effects of EGF could be attributed to Akt kinase signaling in CTB and Akt activity may contribute to the proliferation and/or differentiation of CTB (Yang et al., 2003). We tested the hypothesis that blocking differentiation of CTB with a p38 MAPK inhibitor could circumvent the metabolic suppression observed in the transformation of CTB to SCT. The p38 MAPK pathway regulates trophoblast development, proliferation, and differentiation (Adams et al., 2000; Mudgett et al., 2000) and activity of this pathway is altered in placentas of growth restricted fetuses (Laviola et al., 2005). While inhibition of the p38 MAPK in trophoblast did little to circumvent the normal suppression in metabolism observed when CTB differentiate to SCT, co-stimulation with EGF greatly stimulated and maintained the high levels of metabolism. These effects were greater than EGF alone as EGF does not preclude SCT formation. These observations are consistent with other works demonstrating the p38 MAPK pathway regulates the ability of trophoblast to respond to growth factors, including EGF (Johnstone et al., 2005) and serum (Daoud et al., 2005).

Mechanistically, we propose that fragmentation of the mitochondrial network is associated with changes in metabolism during differentiation of CTB to SCT. CTB mitochondria are larger, less dense, and contain abundant cristae (De los Rios Castillo et al., 2011), and SCT mitochondria remodel for steroidogenesis to become fragmented, smaller, more dense and lose identifiable cristae

(Wasilewski et al., 2012; Poidatz et al., 2015). While our super-resolution methods cannot distinguish mitochondrial cristae, we did find the mitochondrial network decreased in density after differentiation to SCT.

We measured the respiration and glycolysis of the two main trophoblast cell types in human placenta, CTB and SCT, but have not yet compared these to the other cells in placenta, e.g. stroma and endothelium. Yet our studies using a fluorescent mitochondrial activity reporter indicate that compared to CTB these other placental cells have either lower mitochondrial membrane potentials or mitochondrial oxidative activity or both. These explant studies lend further support to our observations that the CTB have higher metabolic rates compared to the *in vitro* differentiated SCT. Future studies should aim to directly quantify the metabolic rates of placental stroma and endothelium in addition to CTB and SCT.

In conclusion, we present multiple lines of evidence that the metabolic features of the placenta are driven not as much by the SCT as by the underlying CTB. Until now, the relevance of the CTB to human placental metabolism has not been appreciated. We suggest that future studies of placental biology should include comparisons of both CTB and SCT. These two cell types are highly specialized to serve unique and crucial roles during development that are only now being discovered.

Chapter VI: Summary and Conclusions

Regulation of placental metabolism and transport by cytotrophoblast

Scientists of the last century concluded that the cytotrophoblast played a minor role in nutrient transport and placental metabolism. As gestation advances, the cytotrophoblast layer thins and becomes less visible by light microscopy. Even with the high magnification of transmission electron microscopy the CTB layer can be difficult to discern (Benirschke et al., 2012). It has long been thought that by term, the cytotrophoblast had dispersed as an obvious adaptation to enhance maternal-fetal exchange by minimizing the distance over which substances would have to diffuse to reach the fetal capillaries (Benirschke et al., 2012).

However, immunofluorescence microscopy allows a new approach to the study of cell layers in the placenta. We were surprised to find a very thin, but continuous layer of cytotrophoblast underlying almost all of the syncytiotrophoblast in the term placenta. Other labs have reported similar findings, and have argued for a reappraisal of the cytotrophoblast layer continuity in the third trimester placenta (Mori et al., 2007; Jones et al., 2008).

The degree to which the cytotrophoblast is a continuous layer is important in interpreting the data reported in this thesis. If the cytotrophoblast layer is only rarely present beneath the syncytial layer in the near term placenta, as assumed by most scientists currently, the syncytiotrophoblast would then be the primary diffusional barrier for nutrients that cross the placenta by diffusion. However, data from the current experiments suggest a draw-back to the syncytiotrophoblast-only assumption. The capacity for sequestering glucose and

fatty acids in the syncytial layer is relatively low, which implies a limitation in its capacity for biochemical transformations of nutrients including fatty acid chain elongation and shortening, or conversion of maternal glucose to lactate. The fetus requires nutrients in adequate amounts, but each macronutrient class must be represented in an appropriate proportion to other macronutrients. For example, some fetal structures require a much higher concentration of LCPUFA than are provided by the mother. A robust active transport system in the placenta selectively accumulates the needed LCPUFA. Contrary to current belief among placentologists, our observations imply that the syncytiotrophoblast has limited capacity for extensive metabolism and processing of fatty acids..

Our data characterizing the low metabolic rate of the syncytiotrophoblast suggest that its modification of nutrients such as fatty acids during transit would be too low to account for fetal demands for processed molecular species. This low metabolic activity may be advantageous to overall placental function because the syncytiotrophoblast must transport large quantities of nutrients to deeper placental layers which can process those nutrients in various ways in preparation for local fuel consumption and transport to the fetus.

One cannot help but be impressed with the amazing metabolic activity of the placenta in late gestation. It consumes a significant share of the oxygen (~40%) and nutrients(e.g. ~50% glucose) that are given to the pregnant uterus each minute. Given the low metabolic rate of the syncytiotrohpoblast, this placental consumption of oxygen and glucose during transport is likely due to other cells types in the placenta. There are only two remaining cell types that

could account for the magnitude of oxygen consumption in the placenta, those cells composing the endothelial layer and the cytotrophoblast layer.

We propose that the cytotrophoblast layer drives the metabolic features of the placenta. Our data directly and indirectly indicate the cytotrophoblast has a rapid metabolic rate with a high oxygen consumption rate by oxidative phosphorylation. Glucose consumption via aerobic glycolysis is also an important feature of cytotrophoblastic metabolism. When we localized active mitochondria in term human placenta, we found the most active mitochondria in the cytotrophoblast. Lastly, we consistently observe the cytotrophoblast as a thin, but continuous (>90%) monolayer, which is in line with more recent re-evaluations of the cytotrophoblast integrity at term. This observation supports the idea that most nutrients must cross the cytotrophoblast and could be metabolized by the cytotrophoblast.

To our knowledge no one has measured oxygen consumption rates of microvascular endothelium in term placenta. However, endothelial cells in general do not have oxygen consumption rates that compare to placental cytotrophoblast. In support of this, data is available from studies of Human umbilical vein endothelial cells (HUVEC) (Panopoulos et al., 2012; Patella et al., 2015). HUVEC have been measured by similar techniques to ours, and have oxygen consumption rates that are 30% of what we measured in cytotrophoblast (Panopoulos et al., 2012; Patella et al., 2015).

If the cytotrophoblast dominates placental metabolism as our data suggest, then cytotrophoblast metabolism could be important in the

pathophysiology of abnormal pregnancies. Indeed, dysfunctional cytotrophoblast has been observed in pre-eclampsia and placental insufficiency and many have proposed alterations in these cells specifically lead to the pathology observed in these pregnancies (Crocker et al., 2004; Fisher, 2004; Longtine and Nelson, 2011). These will be discussed further in the following sections.

The original descriptions cytotrophoblast becoming thinner with advancing gestation, could represent an adaptation to promote nutrient transfer. A thinner cytotrophoblast would also represent an adaptation to support exchange and if each cytotrophoblast cell subtended a larger villi area in late compared to early gestation, each cytotrophoblast would have more regulatory control over transport flux.

Metabolic conversions in Cytotrophoblast

Otto Warburg's seminal observation that malignant cells undergo an unusual rate of aerobic glycolysis relative to mitochondrial respiration, is now recognized as a regular feature of proliferating cells (Vander Heiden et al., 2009). It is mysterious that a proliferating cell would employ such an inefficient strategy to produce ATP, but ATP is rarely limiting for proliferating cells (Vander Heiden et al., 2009). This is especially true for cells *in vivo* where homeostatic mechanisms are robustly regulated to ensure nutrient supplies are continuously replenished. Aerobic glycolysis may be advantageous for other reasons than to serve as a means for generating ATP. Several alternative theories have been proposed to explain aerobic glycolysis in proliferating cells.

One hypothesis is that proliferating cells require ample carbon and reducing equivalents (NADPH) to synthesize the molecular constituents of lipid membranes and nucleic acids. The rapid rate of aerobic glycolysis in cytotrophoblast cells could support the high capacity for lipid esterification and *de novo* fatty acid synthesis evident in these cells (Coleman and Haynes, 1987). NADH, a product of glycolysis, can be converted to NADPH during the successive actions of Malate Dehydrogenase and Malic Enzyme (Wise and Ball, 1964; Ballard and Hanson, 1967; Jiang et al., 2013). NADH is used by Malate dehydrogenase to reduce oxaloacetate to malate, and malate is subsequently converted to pyruvate and NADPH by the action of Malic Enzyme (Wise and Ball, 1964; Ballard and Hanson, 1967). Cytosolic NADPH levels are largely regulated by Malic Enzyme and the pentose phosphate pathway (Wise and Ball, 1964; Ballard and Hanson, 1967; Jiang et al., 2013). NADPH is necessary as a reducing agent during two steps in fatty acid synthesis, as a cofactor for 3-keto-acyl-ACP reductase and for Enoyl-ACP reductase (Nelson et al., 2008). Additionally, the glycerol-phosphate produced during glycolysis is required for as the backbone for glycerolipid formation. Since LCPUFA are most abundant and enriched in placental glycerophospholipids, glycolysis may be linked to placental LCPUFA incorporation.

Whether or not lactate production supports lipid anabolic metabolism, the production of lactate appears to be a priority for proliferating cells. Proliferating cells utilize an isoform of pyruvate kinase that favors pyruvate conversion to lactate over further oxidation to produce ATP (Mazurek et al 2005). This could

also occur in cytotrophoblast, and lactate produced could be exported to the fetal circulation for utilization by distant tissues.

Interestingly, these metabolic conversions could be regulated by external influences like oxygen tension and growth factors, which may have direct or indirect effects, through influencing cytotrophoblast differentiation for example. The rate of glycolysis and lactate production is for example, directly influenced by oxygen tension. Placental lobules with a greater blood flow rate would receive more oxygen, and cytotrophoblast in these locations would convert less glucose to lactate than areas with low oxygen tension (Schneider et al., 1989; Carter, 2000; Schneider, 2000). Because lactate is known to be a major fuel for cardiac and renal tissue in the fetus, it is likely that even under well oxygenated conditions lactate production is adequate to meet the needs of these fetal organs. Lipid metabolism could be directly affected by oxygen tension, too, as low oxygen promotes fatty acid uptake and esterification (Biron-Shental et al., 2007). Lastly, growth factors like EGF, stimulate oxygen consumption and lactate production as this thesis has shown. If such growth factors are synthesized locally there could be considerable variation by placental location (Schneider et al., 1989; Carter, 2000; Schneider, 2000).

In addition, our data indicate that metabolism in the placenta can be controlled indirectly by modulating cytotrophoblast differentiation. We found metabolic rate and fatty acid uptake was suppressed after differentiation of cytotrophoblast to syncytiotrophoblast. The ratio of cytotrophoblast to syncytiotrophoblast in a placenta must therefore affect the overall metabolic rate

and how nutrients are transported. The relative abundance of cytotrophoblast and syncytiotrophoblast changes over gestation (Simpson et al., 1992; Mayhew, 2014), and may reflect adaptations to meet varying fetal demands in pregnancy. The pathological condition known as advanced villous maturation, may be associated with increased rates of cytotrophoblast differentiation that could alter normal metabolic regulation. Others have proposed that dysfunctional cytotrophoblast differentiation may underlie the pathology of pre-eclampsia and placental insufficiency in intrauterine growth restriction (Crocker et al., 2004; Fisher, 2004; Longtine and Nelson, 2011).

Differentiation of cytotrophoblast appears to be regulated by several mechanisms. The p38 mitogen-activated protein kinases, a class of mitogen activated protein kinases (MAPK), that are responsive to stress stimuli such as cytokines, ultraviolet radiation, and heat and osmotic shock, regulate cytotrophoblast differentiation and proliferation (Han et al., 1994; Daoud et al., 2005; Johnstone et al., 2005). Inhibition of the p38 MAPK in cytotrophoblast blocks differentiation and syncytialization (Daoud et al., 2005; Johnstone et al., 2005). Since syncytialization of cytotrophoblast leads to cell-cycle exit, cytotrophoblast with reduced p38 MAPK retain their proliferative capacity (Daoud et al., 2005; Johnstone et al., 2005). The suppressive effect of p38 MAPK can be further potentiated by EGF stimulation. Alterations in the activation of EGF and p38 MAPK pathways could underlie how the compositions of cytotrophoblast and syncytiotrohpoblast are varied in placentas. In intrauterine growth restriction and pre-eclampsia reductions in p38 MAPK and EGF signaling parallel the reductions

in cytotrophoblast numbers and differentiation (Fondacci et al., 1994; Laviola et al., 2005; Webster et al., 2006; Armant et al., 2015).

The studies in this thesis have not tested the degree to which cytotrophoblast is involved in transplacental transport of key nutrients such as glucose, amino acids, and fatty acids. To understand how greater cytotrophoblastic surface area and volume would affect transport, a study would have to be carried out on syncytiotrophoblast alone and in combination with cytotrophoblast to make direct comparisons of transport capacity attributable to each tissue layer.

Complexities in trophoblast metabolism

As shown in table 6.1, some aspects of trophoblast biology are complex and are not easily explained. For example, It is unclear how EGF can stimulate syncytial formation and yet preserve unfused CTB. Additionally, OCR to ECAR ratios differ between CTB and SCT and this suggest these cells produce ATP through different means. While we present new exciting observations - future studies are warranted as EGF and placental metabolism are only superficially understood.

Table 6.1: Trophoblast Metabolic Profile

	OCR (pmol $O_2 \cdot min^{-1} \cdot 100ng\ DNA^{-1}$)	OCR + EGF (pmol $O_2 \cdot min^{-1} \cdot 100ng\ DNA^{-1}$)	ECAR ($\Delta mpH \cdot min^{-1} \cdot 100ng\ DNA^{-1}$)	ECAR + EGF ($\Delta mpH \cdot min^{-1} \cdot 100ng\ DNA^{-1}$)	ATP (nmol·ug $protein^{-1}$)	OCR:ECAR ratio
CTB	96±16	164±22	43±6.7	97±12	6.2±2.9	3.5±0.20
SCT	46±14	119±18	1.4±1.0	29±5	2.4±0.55	1.3±0.075

Overall, the contribution of cytotrophoblast to metabolic and nutrient transport processes in the placenta has been greatly neglected. The relative contributions of the syncytiotrophoblast and cytotrophoblast to placental function have been little studied heretofore. This thesis provides evidence that the two trophoblast layers must be considered together in future studies of placental biology.

Fatty acid uptake

Fatty acid transport in the placenta is the result of a system that has evolved to ensure that the fetus acquires the specific fatty acids in adequate amounts throughout development. The fatty acids acquired to the greatest degree by the fetus are the LCPUFA. LCPUFA uptake is highly selective in trophoblast (Coleman and Haynes, 1987; Haggarty et al., 1997; Tobin et al., 2009). There is considerable debate about whether transport is determined by passive, facilitative, or active transport. Arguments in favor of passive and facilitative processes point to the concentration gradient for free fatty acids, including LCPUFA, as being higher in maternal than fetal plasma.

However, fatty acids are virtually insoluble in aqueous solutions, and their concentrations are determined instead by binding proteins including the intracellular fatty acid binding proteins, and extracellular albumin (Schwenk et al., 2010). Fatty acids can also circulate as esterified lipids, in complex with lipoproteins, but only non-esterified fatty acids are available for transport (Duttaroy, 2009; Schwenk et al., 2010). Non-esterified fatty acids must be released from albumin as free fatty acids to bind to transporters (Schwenk et al., 2010). Albumin contains up to 7 binding sites for fatty acids, and the normal physiologic ratio of albumin to non-esterified fatty acids, including pregnancy, is about 1 to 1 or greater (Haggarty et al., 1997; Haggarty, 2010; Schwenk et al., 2010). Virtually all fatty acids are bound to albumin and the serum free fatty acid concentration is very low *in vivo* (~2nM) (Schwenk et al., 2010). Using concentration gradients of total fatty acids as evidence of active transport systems may be flawed logic since the concentrations of fatty acids in maternal and fetal plasma are determined more by the concentration and saturation of plasma albumin and the presence of particle-derived triglycerides.

Nevertheless, FATP are selective proteins and utilize ATP for fatty acid import, and for this reason do not qualify as facilitative transporters. The selective nature of placental uptake is apparent when the composition of placental and umbilical blood fatty acids is analyzed by weight proportion after maternal administration of stable-isotope labeled fatty acids; the LCPUFA increase in proportion to total fatty acids by 5-10 fold (Haggarty et al., 1997; Alvino et al., 2008). However, one overlooked detail is that while this process is highly

selective for LCPUFA, the proportion of saturated long chain fatty acids in placenta also increases 3-5 fold in placenta; this suggests a process that is not entirely exclusive to LCPUFA (Haggarty et al., 1997; Alvino et al., 2008).

There are several lines of evidence suggesting fatty acid transport is an active transport process. First, fatty acid transporters involved in the uptake process utilize 2-ATP equivalents to activate fatty acids for esterification to Acyl-CoA. This process can drive fatty acids into cells in an active fashion (Schwenk et al., 2010; Anderson and Stahl, 2013; Melton et al., 2013). Some scientists believe this process, termed vectorial acylation, does not represent active transport because first of all, transport across the MVM is driven by the concentration gradient and does require ATP, and secondly the binding of fatty acids to FATP in intracellular compartments removes their colligative properties (Ibrahimi et al., 1996; Abumrad et al., 1998).

Second, early experiments using the placental perfusion model were interpreted to support passive diffusion as a mechanism for lipid transport across the placenta. In these studies long chain fatty acids were not detectable in the fetal compartment until ~30 minutes after the initiation of perfusion (Dancis et al., 1973; Haggarty et al., 1997). These time scales agree with our observations of esterification being involved in placental uptake and our proposal that this step is an intermediate in transport. Others perfusion studies have noted that a significantly greater concentration of fatty acids appears on the fetal side than what was perfused on the maternal side, again implying movement against a concentration gradient (Perazzolo et al., 2015). Lastly, Arachidonic acid uptake

into syncytiotrophoblast BPM vesicles, is augmented by ATP and Na^+ gradients (Lafond et al., 2000). The concentrations of endogenous arachidonic acid are much higher in the placenta than in the maternal plasma (Klingler et al., 2003).

It is crucial that studies moving forward identify the importance of esterification during placental fatty acid transport. The vast majority of long chain fatty acids in the placenta are found in esterified lipids (Klingler et al., 2003; Larqué et al., 2003). LCPUFA seem to be preferentially incorporated into placental phospholipids, which is the most abundant lipid class, and saturated long-chain fatty acids into triglycerides (Klingler et al., 2003; Larqué et al., 2003). It is not yet known if these fatty acids are eventually transported to the fetal circulation, and nor is it known what forms are exported. Earlier studies have suggested fatty acid efflux may occur through multiple mechanisms, and differs by fatty acid species and placental cell type (Coleman and Haynes, 1987; Madsen et al., 2004; Lewis et al., 2011). It is likely that the mechanisms of LCPUFA esterification and efflux differ from other types of lipids because this fatty acid is transported preferentially compared to the other fatty acids, and because of its immense importance to human development.

While this work represents an advance in our understanding of normal human placental biology at term, many unanswered questions remain and desperately need attention. We will discuss a select few of these issues in greater detail in the following chapter.

Chapter VII: Future Directions

A list of topics in need of further investigation in the human placenta

This thesis raises many questions, and I argue the following list of topics are in most urgent need of further study.

1. The role of FATP2 function in fatty acid transport, including its role in LCPUFA transport.
2. Placental peroxisomal localization, biology, functions and the relationship of peroxisomes to the cytotrophoblast and FATP2.
3. An assessment of the characterization of the composition of the basal plasma membrane to define the predominant cell types that form this membrane layer.
4. Cytrotrophoblast epigenetic plasticity.

The background and relevance of these topics will be discussed in further detail in the following sections.

The role of Fatty acid transporter type 2 in human development

The human placenta enriches the long chain polyunsaturated fatty acids LCPUFA, docosahexaenoate (DHA) and arachidonate (AA), that are obtained from maternal blood. DHA and AA fatty acids are preferentially channeled into placental phospholipids; the ratio of these fatty acids in placental tissue is roughly 10-fold that of in maternal blood (Klingler et al., 2003; Alvino et al., 2008). From this pool of fatty acids, a subset is preferentially transported to the fetal compartment which serves to supply the enormous required quantities of AA and

DHA for the developing nervous and cardiovascular systems (Crawford et al., 1976). Because of its immense importance to normal human development, the placental transport systems are under intense investigation but so far, the mechanisms remain unknown.

Our discovery that placental fatty acid esterification and metabolism is determined by cytotrophoblast and not syncytiotrophoblast, suggests that the selective LCPUFA acquisition by placenta is due to functions of the cytotrophoblast. We speculate the mechanism of LCPUFA uptake in placenta is specifically attributable to FATP2 in this cell.

Our data indicate a relationship between between long and very long chain fatty acid analogue uptake and FATP2 in cytotrophoblast. Since FATP2 is the fatty acid transporter that is expressed most highly in the human placenta, this transporter may be responsible for the majority of long and very long chain fatty acid uptake in this organ. For unknown reasons, this transporter is absent from the mouse placenta and fetoplacental fatty acid uptake does not depend on FATP2 in this organism (Mishima et al., 2011). Mice are born with considerably smaller brains and less fat stores as a function of body weight (Ulijaszek, 2002), and a selective LCPUFA uptake system may not be necessary. The differences between small rodents and humans is the reason that such animals cannot be used to understand the intricacies of human placental transport.

FATP2 may mediate the transport of multiple species of long and very long chain fatty acid species, but it is especially interesting that this transporter is selective for DHA and AA (Melton et al., 2011). FATP2 selectively acquires DHA

and AA to channel these fatty acids via esterification into phospholipids (Melton et al., 2011; 2013). It is well known that DHA and AA in placenta are predominantly found incorporated into the phospholipid faction in placenta tissue *in vivo* (Klingler et al., 2003; Larqué et al., 2003). Our evidence that cytotrophoblast cells rapidly esterify long and very long chain fatty acid, coupled with the high expression of FATP2 in cytotrophoblast, implies that this cell type is responsible for placental AA and DHA uptake and that this occurs via FATP2.

FATP2 is localized to endoplasmic reticulum and peroxisomal membranes in hepatocytes (Falcon et al., 2010). The organs that express FATP2 most highly are the liver, kidney, and placenta (Melton et al., 2011). It may not be a coincidence that this tissue distribution reflects sites of high peroxisomal activity (Islinger et al., 2010). FATP2 may facilitate fatty acid uptake and subsequent oxidation by metabolism. Thomas et al. hypothesized peroxisomal beta-oxidation may enhance fatty acid flux by the placenta, suggesting again that placental metabolism and fatty acid transport are linked(Thomas et al., 1985). Peroxisomes and the pathways regulating them, including peroxisomal proliferator-activated receptor (PPAR), may be key during human development (Barak et al., 1999). Surprisingly, no data describing the localization of placental peroxisomes has been so far published. The function of this organelle in the placenta is unknown. Thus, the need to understand peroxisomal biology in the placenta is required for a complete understanding of lipid metabolism in the human placenta.

A reappraisal of the syncytiotrophoblast basal plasma membrane: is this actually cytotrophoblast?

In the syncytiotrophoblast the plasma membrane facing the maternal blood, the microvillous membrane (MVM), and the plasma membrane adhering to the basement membrane, the basal plasma membrane (BPM), can be purified and studied as microvesciles *in vitro* (Smith et al., 1977; Kelley et al., 1983; Glazier et al., 1998). Studies of isolated MVM and BPM vesicles have consistently led to the suggestion that the BPM is the rate limiting membrane in the transport of glucose, amino acids, and fatty acids. The transport of fatty acids and amino acids across the BPM appears to be ATP and Na gradient dependent, implying a metabolic association with BPM fluxes. In addition, the BPM glucose, amino acid, and fatty acid transporter expression appear to be more dynamically regulated, when fetal growth is altered. This has led others to suggest that regulation of transport across the BPM is the most critical step in influencing fetal growth rates.

The BPM was originally characterized as syncytiotrophoblastic in nature because it was assumed that the cytotrophoblast layer gradually disappears as gestation proceeds and is nearly non-existent at term. The assumed loss of cytotrophoblast implied that BPM could only belong to the syncytiotrophoblast. It was thus assumed that membranes attached to basement membrane were derived from syncytiotrophoblast. However, as discussed previously, new evidence indicates that the cytotrophoblast layer at term is a mostly intact thin membrane that underlies most of the syncytiotrophoblast. With this new insight

we speculate that isolated BPM is highly contaminated with membrane from cytotrophoblast, because cytotrophoblast cells lie against the basement membrane more often than does syncytrophoblast. Thus, the notion that the BPM is relatively pure syncytiotrophoblastic must be reconsidered.

We suggest that the isolated BPM as currently defined also represents the cytotrophoblast basolateral membrane. Multiple studies have noted that the so called syncytiotrophoblast BPM bears a striking resemblance to the term cytotrophoblast layer, which is also a thin membrane in this same location. It is possible the thin cytotrophoblast projections underneath the syncytiotrophoblast have been for so long incorrectly identified as being syncytiotrophoblastic. Our observations offer food for thought on the topic.

The original descriptions of characterizing purified BPM vesicles noted this membrane shares many features with polarized, basalolateral membranes of epithelia. If the syncytiotrophoblast indeed contains a polarized BPM an explanation would be needed to explain how cell polarity would be established and maintained in the syncytium, since cell polarity is not retained after cytotrophoblast cell fusion (Sivasubramaniyam et al., 2013).

A distinguishing feature of the cytotrophoblast is the presence of adherens junctions which are not present in syncytiotrophoblast. The adherens junctions in cytotrophoblast could represent a major clue in understanding the mechanisms of unidirectional transport. Adherens junctions, mediated by epithelial-cadherin, are the only known mechanism by which polarity is established in cells (Baum and Georgiou, 2011) though others may be present in the placenta. The

adherens junctions form a barrier between the basolateral and apical plasma membranes that enables two distinct membrane compositions to be maintained. A second function of the adherens junction is to maintain cell shape to support the generation of a polarized cytoskeletal network.

The cytotrophoblast, but not the syncytiotrophoblast is characterized by an intact apicobasal cell polarity. It is possible the apicobasal polarity established in the cytotrophoblast is maintained in the syncytiotropholbast, however the loss in the integrity of the adherens junctions that occurs during syncytialization permits the once polarized membranes to mix. This results in a loss of cell polarity. Surprisingly, many intracellular transport processes that are presumed to function in syncytiotrophoblast would necessitate an endomembrane trafficking systems that depends upon apicobasal and cytoskeletal polarity, arguing for its presence. For example, a crucial feature of the human placenta that is essential for postnatal survival is the transport of immune IgG to acquire passive immunity from the mother. Cell polarity would be required in the syncytiotrophoblast to transport vesicles containing IgG in a unidirectional manner, but the existence of such a system is wholly unknown. As a next step we need to understand whether it is the cytotrophoblast or syncytiotrophoblast plasma membrane that forms the basal plasma membrane layer in the human term placenta.

Integration of maternofetal signals into cytotrophoblast epigenetic code

The syncytiotrophoblast is constantly shed into maternal blood. It has

long been known that the cytotrophoblast is on alert to repair areas of syncytiotrophoblast loss. One consequence of this process is that information that may be programmed in the syncytiotrophoblast would be eventually lost with shedding. However, programming “memory” could be potentially maintained through the whole of pregnancy in the cytotrophoblast. Coincidentally, the cytotrophoblast appears to be more epigenetically plastic than the syncytiotrophoblast (Fogarty et al., 2015). This implies that the cytotrophoblast is also more receptive to external influences that lead to epigenetic programming.

If the cytotrophoblast can integrate and maintain epigenetic signals from the environment, and if it is a central driver of placental functions including metabolism and nutrient transport, the cytotrophoblast may hold the key for understanding how the placenta adapts to maintain fetal growth in the face of constant environmental change. In other words, properties of the cytotrophoblast may permit placental plasticity, an intensively studied phenomenon, but occurs through unknown mechanisms.

Understanding how the placenta can be plastic is crucial to devising interventions that might exploit these mechanisms in pregnancies where fetal growth is dysregulated. If the cytotrophoblast is central to placental epigenetic programming and plasticity, this concept would revolutionize our understanding of the mechanisms underlying the developmental origins hypothesis. It is unknown how fetal maturation and growth trajectories are defined, and the cytotrophoblast may be a logical regulator given the findings of this thesis. Studies investigating how the cytotrophoblast may integrate epigenetic signals

from the environment and contribute to placental plasticity are paramount. These studies reveal new placental biological mechanisms that could someday guide clinical studies to improve pregnancy outcomes and the lifelong health of offspring.

References

Abumrad N, Harmon C, Ibrahimi A. Membrane transport of long-chain fatty acids: evidence for a facilitated process. J. Lipid Res. 1998 Dec;39(12):2309–18.

Adams AK, Reid DL, Thornburg KL, Faber JJ. In vivo placental permeability to hydrophilic solutes as a function of fetal weight in the guinea pig. Placenta. 1988 Jul;9(4):409–16.

Adams RH, Porras A, Alonso G, Jones M, Vintersten K, Panelli S, et al. Essential role of p38alpha MAP kinase in placental but not embryonic cardiovascular development. Mol Cell. 2000 Jul;6(1):109–16.

Afzal I, Cunningham P, Naftalin RJ. Interactions of ATP, oestradiol, genistein and the anti-oestrogens, faslodex (ICI 182780) and tamoxifen, with the human erythrocyte glucose transporter, GLUT1. Biochem. J. Portland Press Limited; 2002 Aug 1;365(Pt 3):707–19. PMCID: PMC1222738

Alvino G, Cozzi V, Radaelli T, Ortega H, Herrera E, Cetin I. Maternal and fetal fatty acid profile in normal and intrauterine growth restriction pregnancies with and without preeclampsia. Pediatr. Res. 2008 Dec;64(6):615–20.

Anderson CM, Stahl A. SLC27 fatty acid transport proteins. Mol. Aspects Med. 2013 Apr;34(2-3):516–28. PMCID: PMC3602789

Araújo JR, Correia-Branco A, Ramalho C, Keating E, Martel F. Gestational diabetes mellitus decreases placental uptake of long-chain polyunsaturated fatty acids: involvement of long-chain acyl-CoA synthetase. The Journal of Nutritional Biochemistry. 2013 Oct;24(10):1741–50.

Armant DR, Fritz R, Kilburn BA, Kim YM, Nien JK, Maihle NJ, et al. Reduced expression of the epidermal growth factor signaling system in preeclampsia. Placenta. 2015 Mar;36(3):270–8.

Austdal M, Thomsen LC, Tangeras LH, Skei B, Mathew S, Bjorge L, et al. Metabolic profiles of placenta in preeclampsia using HR-MAS MRS metabolomics. Placenta. 2015 Dec;36(12):1455–62.

Avagliano L, Garò C, Marconi AM. Placental amino acids transport in intrauterine growth restriction. Journal of Pregnancy. Hindawi Publishing Corporation; 2012;2012(1):972562–6. PMCID: PMC3401547

Baier LJ, Sacchettini JC, Knowler WC, Eads J, Paolisso G, Tataranni PA, et al. An amino acid substitution in the human intestinal fatty acid binding protein is associated with increased fatty acid binding, increased fat oxidation, and

insulin resistance. J. Clin. Invest. 1995 Mar;95(3):1281–7. PMCID: PMC441467

Baker J, Workman M, Bedrick E, Frey MA, Hurtado M, Pearson O. Brains versus brawn: an empirical test of Barker's brain sparing model. American Journal of Human Biology. Wiley Subscription Services, Inc., A Wiley Company; 2010 Mar;22(2):206–15.

Ballard FJ, Hanson RW. The citrate cleavage pathway and lipogenesis in rat adipose tissue: replenishment of oxaloacetate. J. Lipid Res. 1967 Mar;8(2):73–9.

Barak Y, Nelson MC, Ong ES, Jones YZ, Ruiz-Lozano P, Chien KR, et al. PPAR gamma is required for placental, cardiac, and adipose tissue development. Mol Cell. 1999 Oct;4(4):585–95.

Barbour LA, McCurdy CE, Hernandez TL, Kirwan JP, Catalano PM, Friedman JE. Cellular mechanisms for insulin resistance in normal pregnancy and gestational diabetes. Diabetes Care. American Diabetes Association; 2007 Jul;30 Suppl 2(Supplement 2):S112–9.

Barker DJ. The fetal and infant origins of adult disease. BMJ. 1990 Nov 17;301(6761):1111. PMCID: PMC1664286

Barker DJ, Osmond C. Infant mortality, childhood nutrition, and ischaemic heart disease in England and Wales. Lancet. 1986 May 10;1(8489):1077–81.

Barker DJ, Winter PD, Osmond C, Margetts B, Simmonds SJ. Weight in infancy and death from ischaemic heart disease. Lancet. 1989 Sep 9;2(8663):577–80.

Barker DJP, Osmond C, Thornburg KL, Kajantie E, Eriksson JG. The lifespan of men and the shape of their placental surface at birth. Placenta. Elsevier; 2011 Oct;32(10):783–7. PMCID: PMC4280009

Barker DJP, Thornburg KL. Placental programming of chronic diseases, cancer and lifespan: a review. Placenta. Elsevier; 2013a Oct;34(10):841–5.

Barker DJP, Thornburg KL. The obstetric origins of health for a lifetime. Clin Obstet Gynecol. 2013b Sep;56(3):511–9.

Bartelds B, Knoester H, Beaufort-Krol GC, Smid GB, Takens J, Zijlstra WG, et al. Myocardial lactate metabolism in fetal and newborn lambs. Circulation. 1999 Apr 13;99(14):1892–7.

Battaglia FC, Meschia G. Principal substrates of fetal metabolism. Physiol Rev. 1978 Apr;58(2):499–527.

Baum B, Georgiou M. Dynamics of adherens junctions in epithelial

establishment, maintenance, and remodeling. J Cell Biol. Rockefeller Univ Press; 2011 Mar 21;192(6):907–17. PMCID: PMC3063136

Baumann MU, Deborde S, Illsley NP. Placental glucose transfer and fetal growth. Endocrine. Humana Press; 2002 Oct;19(1):13–22.

Bax BE, Bloxam DL. Energy metabolism and glycolysis in human placental trophoblast cells during differentiation. Biochim Biophys Acta. 1997 Apr 11;1319(2-3):283–92.

Bell AW, Hay WW, Ehrhardt RA. Placental transport of nutrients and its implications for fetal growth. J. Reprod. Fertil. Suppl. 1999;54:401–10.

Benirschke K, Burton GJ, Baergen RN. Pathology of the Human Placenta. Springer; 2012.

Berghaus TM, Demmelmair H, Koletzko B. Fatty acid composition of lipid classes in maternal and cord plasma at birth. European Journal of Pediatrics. 1998 Aug 27;157(9):763–8.

Bianco-Miotto T, Blundell C, Buckberry S, Chamley L, Chong S, Cottrell E, et al. IFPA meeting 2015 workshop report I: Placental mitochondrial function, transport systems and epigenetics. Placenta. Elsevier; 2015 Nov 28;0(0).

Bildirici I, Roh C-R, Schaiff WT, Lewkowski BM, Nelson DM, Sadovsky Y. The lipid droplet-associated protein adipophilin is expressed in human trophoblasts and is regulated by peroxisomal proliferator-activated receptor-gamma/retinoid X receptor. Journal of Clinical Endocrinology & Metabolism. 2003 Dec;88(12):6056–62.

Biron-Shental T, Schaiff WT, Ratajczak CK, Bildirici I, Nelson DM, Sadovsky Y. Hypoxia regulates the expression of fatty acid-binding proteins in primary term human trophoblasts. Am. J. Obstet. Gynecol. 2007 Nov;197(5):516.e1–6. PMCID: PMC2151846

Bloxam DL, Bullen BE, Walters BN, Lao TT. Placental glycolysis and energy metabolism in preeclampsia. Am. J. Obstet. Gynecol. 1987 Jul;157(1):97–101.

Bonds DR, Crosby LO, Cheek TG, Hägerdal M, Gutsche BB, Gabbe SG. Estimation of human fetal-placental unit metabolic rate by application of the Bohr principle. J. Dev. Physiol. 1986 Feb;8(1):49–54.

Bouchoux J, Beilstein F, Pauquai T, Guerrera IC, Chateau D, Ly N, et al. The proteome of cytosolic lipid droplets isolated from differentiated Caco-2/TC7 enterocytes reveals cell-specific characteristics. Biol. Cell. 2011 Nov;103(11):499–517. PMCID: PMC3181828

Brass E, Hanson E, O'Tierney-Ginn PF. Placental oleic acid uptake is lower in

male offspring of obese women. Placenta. 2013 Jun;34(6):503–9. PMCID: PMC3641530

Bu SY, Mashek DG. Hepatic long-chain acyl-CoA synthetase 5 mediates fatty acid channeling between anabolic and catabolic pathways. J. Lipid Res. American Society for Biochemistry and Molecular Biology; 2010 Nov;51(11):3270–80. PMCID: PMC2952567

Budowski P, Leighfield MJ, Crawford MA. Nutritional encephalomalacia in the chick: an exposure of the vulnerable period for cerebellar development and the possible need for both omega 6- and omega 3-fatty acids. Br. J. Nutr. 1987 Nov;58(3):511–20.

Burd LI, Jones MD, Simmons MA, Makowski EL, Meschia G, Battaglia FC. Placental production and foetal utilisation of lactate and pyruvate. Nature. 1975 Apr 24;254(5502):710–1.

Bustamante J, Ramírez-Vélez R, Czerniczyniec A, Cicerchia D, Aguilar de Plata AC, Lores-Arnaiz S. Oxygen metabolism in human placenta mitochondria. J. Bioenerg. Biomembr. Springer US; 2014 Dec;46(6):459–69.

Campbell FM, Bush PG, Veerkamp JH, Dutta-Roy AK. Detection and cellular localization of plasma membrane-associated and cytoplasmic fatty acid-binding proteins in human placenta. Placenta. 1998 Jul;19(5-6):409–15.

Campbell FM, Gordon MJ, Dutta-Roy AK. Preferential uptake of long chain polyunsaturated fatty acids by isolated human placental membranes. Mol Cell Biochem. 1996;155(1):77–83.

Carlson SE, Werkman SH, Rhodes PG, Tolley EA. Visual-acuity development in healthy preterm infants: effect of marine-oil supplementation. Am. J. Clin. Nutr. 1993 Jul;58(1):35–42.

Carter AM. Placental Oxygen Consumption. Part I: In Vivo Studies—A Review. Placenta. 2000 Mar;21:S31–7.

Catalano PM, Thomas A, Huston-Presley L, Amini SB. Increased fetal adiposity: a very sensitive marker of abnormal in utero development. Am. J. Obstet. Gynecol. 2003 Dec;189(6):1698–704.

Cetin I, Alvino G, Cardellicchio M. Long chain fatty acids and dietary fats in fetal nutrition. J. Physiol. (Lond.). Blackwell Publishing Ltd; 2009 Jul 15;587(Pt 14):3441–51. PMCID: PMC2742273

Cetin I, Marconi AM, Corbetta C, Lanfranchi A, Baggiani AM, Battaglia FC, et al. Fetal amino acids in normal pregnancies and in pregnancies complicated by intrauterine growth retardation. Early Hum. Dev. 1992 Jun;29(1-3):183–6.

Chambaz J, Ravel D, Manier MC, Pepin D, Mulliez N, Bereziat G. Essential fatty acids interconversion in the human fetal liver. Biol. Neonate. 1985;47(3):136–40.

Clandinin MT, Chappell JE, Leong S, Heim T, Swyer PR, Chance GW. Intrauterine fatty acid accretion rates in human brain: implications for fatty acid requirements. Early Hum. Dev. 1980 Jun;4(2):121–9.

Cnattingius S, Bergström R, Lipworth L, Kramer MS. Prepregnancy weight and the risk of adverse pregnancy outcomes. N. Engl. J. Med. 1998 Jan 15;338(3):147–52.

Coburn CT, Knapp FF, Febbraio M, Beets AL, Silverstein RL, Abumrad NA. Defective uptake and utilization of long chain fatty acids in muscle and adipose tissues of CD36 knockout mice. J Biol Chem. 2000 Oct 20;275(42):32523–9.

Coleman RA, Haynes EB. Synthesis and release of fatty acids by human trophoblast cells in culture. J. Lipid Res. 1987 Nov;28(11):1335–41.

Coleman RA, Lee DP. Enzymes of triacylglycerol synthesis and their regulation. Progress in Lipid Research. 2004 Mar;43(2):134–76.

Costello LC, Franklin RB. “Why do tumour cells glycolyse?”: from glycolysis through citrate to lipogenesis. Mol Cell Biochem. NIH Public Access; 2005 Dec;280(1-2):1–8. PMCID: PMC4461431

Costes SV, Daelemans D, Cho EH, Dobbin Z, Pavlakis G, Lockett S. Automatic and quantitative measurement of protein-protein colocalization in live cells. Biophysj. 2004 Jun;86(6):3993–4003. PMCID: PMC1304300

Crawford MA, Costeloe K, Ghebremeskel K, Phylactos A, Skirvin L, Stacey F. Are deficits of arachidonic and docosahexaenoic acids responsible for the neural and vascular complications of preterm babies? Am. J. Clin. Nutr. 1997 Oct;66(4 Suppl):1032S–1041S.

Crawford MA, Hassam AG, Williams G. Essential fatty acids and fetal brain growth. Lancet. 1976 Feb 28;1(7957):452–3.

Crocker IP, Tansinda DM, Baker PN. Altered cell kinetics in cultured placental villous explants in pregnancies complicated by pre-eclampsia and intrauterine growth restriction. J. Pathol. John Wiley & Sons, Ltd; 2004 Sep;204(1):11–8.

Cummings JH, Pomare EW, Branch WJ, Naylor CP, Macfarlane GT. Short chain fatty acids in human large intestine, portal, hepatic and venous blood. Gut. 1987 Oct;28(10):1221–7. PMCID: PMC1433442

Dackor J, Caron KM, Threadgill DW. Placental and embryonic growth restriction

in mice with reduced function epidermal growth factor receptor alleles. Genetics. Genetics; 2009 Sep;183(1):207–18. PMCID: PMC2746145

Dancis J, Jansen V, Kayden HJ, Schneider H, Levitz M. Transfer across perfused human placenta. II. Free fatty acids. Pediatr. Res. 1973 Apr;7(4):192–7.

Daoud G, Amyot M, Rassart E, Masse A, Simoneau L, Lafond J. ERK1/2 and p38 regulate trophoblasts differentiation in human term placenta. J. Physiol. (Lond.). Blackwell Science Ltd; 2005 Jul 15;566(Pt 2):409–23. PMCID: PMC1464762

Day PE, Cleal JK, Lofthouse EM, Hanson MA, Lewis RM. What factors determine placental glucose transfer kinetics? Placenta. 2013a Oct;34(10):953–8. PMCID: PMC3776928

Day PEL, Cleal JK, Lofthouse EM, Goss V, Koster G, Postle A, et al. Partitioning of glutamine synthesised by the isolated perfused human placenta between the maternal and fetal circulations. Placenta. Elsevier; 2013b Dec;34(12):1223–31. PMCID: PMC3851744

De los Rios Castillo D, Zarco-Zavala M, Olvera-Sanchez S, Pardo JP, Juarez O, Martinez F, et al. Atypical cristae morphology of human syncytiotrophoblast mitochondria: role for complex V. J Biol Chem. 2011 Jul 8;286(27):23911–9.

Desforges M, Greenwood SL, Glazier JD, Westwood M, Sibley CP. The contribution of SNAT1 to system A amino acid transporter activity in human placental trophoblast. Biochemical and Biophysical Research Communications. 2010 Jul 16;398(1):130–4. PMCID: PMC2941036

Desoye G, Shafrir E. Placental metabolism and its regulation in health and diabetes. Mol. Aspects Med. 1994;15(6):505–682.

Douglas GC, King BF. Differentiation of human trophoblast cells in vitro as revealed by immunocytochemical staining of desmoplakin and nuclei. J Cell Sci. 1990 May;96 (Pt 1):131–41.

Dutta-Roy AK. Transport mechanisms for long-chain polyunsaturated fatty acids in the human placenta. Am. J. Clin. Nutr. 2000 Jan;71(1 Suppl):315S–22S.

Duttaroy A. Transport of fatty acids across the human placenta: A review. Progress in Lipid Research. 2009 Jan;48(1):52–61.

Elstrom RL, Bauer DE, Buzzai M, Karnauskas R, Harris MH, Plas DR, et al. Akt stimulates aerobic glycolysis in cancer cells. Cancer Res. American Association for Cancer Research; 2004 Jun 1;64(11):3892–9.

Ericsson A, Hamark B, Powell TL, Jansson T. Glucose transporter isoform 4 is

expressed in the syncytiotrophoblast of first trimester human placenta. Hum Reprod. Oxford University Press; 2005 Feb;20(2):521–30.

Faber JJ, Thornburg KL. Placental physiology: structure and function of fetomaternal exchange. 1983.

Falcon A, Doege H, Fluitt A, Tsang B, Watson N, Kay MA, et al. FATP2 is a hepatic fatty acid transporter and peroxisomal very long-chain acyl-CoA synthetase. Am. J. Physiol. Endocrinol. Metab. 2010 Sep;299(3):E384–93. PMCID: PMC2944282

Farquharson J, Cockburn F, Patrick WA, Jamieson EC, Logan RW. Infant cerebral cortex phospholipid fatty-acid composition and diet. Lancet. 1992 Oct 3;340(8823):810–3.

Faxén M, Nasiell J, Blanck A, Nisell H, Lunell NO. Altered mRNA expression pattern of placental epidermal growth factor receptor (EGFR) in pregnancies complicated by preeclampsia and/or intrauterine growth retardation. Am J Perinatol. 1998 Jan;15(1):9–13.

Fisher DA, Lakshmanan J. Metabolism and effects of epidermal growth factor and related growth factors in mammals. Endocrine Reviews. 1990 Aug;11(3):418–42.

Fisher DJ, Heymann MA, Rudolph AM. Myocardial oxygen and carbohydrate consumption in fetal lambs in utero and in adult sheep. Am J Physiol. 1980 Mar;238(3):H399–405.

Fisher SJ. The placental problem: linking abnormal cytotrophoblast differentiation to the maternal symptoms of preeclampsia. Reprod. Biol. Endocrinol. 2004 Jul 5;2:53.

Fogarty NME, Burton GJ, Ferguson-Smith AC. Different epigenetic states define syncytiotrophoblast and cytotrophoblast nuclei in the trophoblast of the human placenta. Placenta. Elsevier; 2015 Aug;36(8):796–802.

Fondacci C, Alsat E, Gabriel R, Blot P, Nessmann C, Evain-Brion D. Alterations of human placental epidermal growth factor receptor in intrauterine growth retardation. J. Clin. Invest. American Society for Clinical Investigation; 1994 Mar;93(3):1149–55. PMCID: PMC294064

Frendo J-L, Cronier L, Bertin G, Guibourdenche J, Vidaud M, Evain-Brion D, et al. Involvement of connexin 43 in human trophoblast cell fusion and differentiation. J Cell Sci. The Company of Biologists Ltd; 2003 Aug 15;116(Pt 16):3413–21.

Friedman Z, Danon A, Lamberth EL, Mann WJ. Cord blood fatty acid composition in infants and in their mothers during the third trimester. J. Pediatr. 1978

Mar;92(3):461–6.

Gaccioli F, Aye ILMH, Roos S, Lager S, Ramirez VI, Kanai Y, et al. Expression and functional characterisation of System L amino acid transporters in the human term placenta. Reprod. Biol. Endocrinol. BioMed Central; 2015;13(1):57. PMCID: PMC4462079

Gaither K, Quraishi AN, Illsley NP. Diabetes alters the expression and activity of the human placental GLUT1 glucose transporter. Journal of Clinical Endocrinology & Metabolism. Endocrine Society; 1999 Feb;84(2):695–701.

Gauster M, Hiden U, Blaschitz A, Frank S, Lang U, Alvino G, et al. Dysregulation of placental endothelial lipase and lipoprotein lipase in intrauterine growth-restricted pregnancies. Journal of Clinical Endocrinology & Metabolism. Endocrine Society; 2007 Jun;92(6):2256–63.

Gil-Sanchez A, Larque E, Demmelmair H, Acien MI, Faber FL, Parrilla JJ, et al. Maternal-fetal in vivo transfer of [13C]docosahexaenoic and other fatty acids across the human placenta 12 h after maternal oral intake. Am. J. Clin. Nutr. American Society for Nutrition; 2010 Jul;92(1):115–22.

Gil-Sánchez A, Koletzko B, Larqué E. Current understanding of placental fatty acid transport. Curr Opin Clin Nutr Metab Care. 2012 May;15(3):265–72.

Gilbert SF. An Introduction to Early Developmental Processes. Sinauer Associates; 2000.

Gillingham MB, Connor WE, Matern D, Rinaldo P, Burlingame T, Meeuws K, et al. Optimal dietary therapy of long-chain 3-hydroxyacyl-CoA dehydrogenase deficiency. Mol. Genet. Metab. NIH Public Access; 2003 Jun;79(2):114–23. PMCID: PMC2813192

Glatz JFC, Luiken JJFP, Bonen A. Membrane fatty acid transporters as regulators of lipid metabolism: implications for metabolic disease. Physiol Rev. American Physiological Society; 2010 Jan;90(1):367–417.

Glazier J, Ayuk P, Grey AM, Sides K. Syncytiotrophoblast basal plasma membrane isolation. Placenta. 1998 Jul;19(5-6):443–4.

Greenwood SL, Clarson LH, Sides MK, Sibley CP. Membrane potential difference and intracellular cation concentrations in human placental trophoblast cells in culture. J. Physiol. (Lond.). 1996 May 1;492(3):629–40.

Guilbert LJ, Winkler-Lowen B, Sherburne R, Rote NS, Li H, Morrish DW. Preparation and Functional Characterization of Villous Cytotrophoblasts Free of Syncytial Fragments. Placenta. 2002 Feb;23(2-3):175–83.

Guo W, Huang N, Cai J, Xie W, Hamilton JA. Fatty acid transport and

metabolism in HepG2 cells. Am. J. Physiol. Gastrointest. Liver Physiol. 2006 Mar;290(3):G528–34.

Haggarty P. Placental regulation of fatty acid delivery and its effect on fetal growth--a review. Placenta. Elsevier; 2002 Apr;23 Suppl A:S28–38.

Haggarty P. Fatty acid supply to the human fetus. Annu. Rev. Nutr. Annual Reviews; 2010 Aug 21;30(1):237–55.

Haggarty P, Allstaff S, Hoad G, Ashton J, Abramovich DR. Placental nutrient transfer capacity and fetal growth. Placenta. 2002 Jan;23(1):86–92.

Haggarty P, Page K, Abramovich DR, Ashton J, Brown D. Long-chain polyunsaturated fatty acid transport across the perfused human placenta. Placenta. 1997 Nov;18(8):635–42.

Han J, Lee JD, Bibbs L, Ulevitch RJ. A MAP kinase targeted by endotoxin and hyperosmolarity in mammalian cells. Science. 1994 Aug 5;265(5173):808–11.

Hashidate-Yoshida T, Harayama T, Hishikawa D, Morimoto R, Hamano F, Tokuoka SM, et al. Fatty acid remodeling by LPCAT3 enriches arachidonate in phospholipid membranes and regulates triglyceride transport. Elife. 2015;4. PMCID: PMC4436788

Hay WW. Regulation of placental metabolism by glucose supply. Reprod. Fertil. Dev. 1995;7(3):365–75.

Hay WW, Sparks JW, Wilkening RB, Battaglia FC, Meschia G. Fetal glucose uptake and utilization as functions of maternal glucose concentration. Am J Physiol. 1984 Mar;246(3 Pt 1):E237–42.

Hay WWJ. Placental-fetal glucose exchange and fetal glucose metabolism. Trans Am Clin Climatol Assoc. 2006;117:321–39–discussion339–40. PMCID: PMC1500912

Heerwagen MJR, Miller MR, Barbour LA, Friedman JE. Maternal obesity and fetal metabolic programming: a fertile epigenetic soil. AJP: Regulatory, Integrative and Comparative Physiology. 2010 Sep;299(3):R711–22. PMCID: PMC2944425

Henkin AH, Ortegon AM, Cho S, Shen W-J, Falcon A, Kraemer FB, et al. Evidence for protein-mediated fatty acid efflux by adipocytes. Acta Physiol (Oxf). Blackwell Publishing Ltd; 2012 Apr;204(4):562–70. PMCID: PMC3271185

Hermanson GT. Bioconjugate Techniques. Academic Press; 2013.

Hernández-Albaladejo I, Ruíz-Palacios M, Gázquez A, Blanco JE, Parrilla JJ,

Larqué E. A method for lipid droplet isolation from human placenta for further analyses in clinical trials. Acta Obstet Gynecol Scand. 2014 Nov;93(11):1198–202.

Horvath A, Koletzko B, Szajewska H. Effect of supplementation of women in high-risk pregnancies with long-chain polyunsaturated fatty acids on pregnancy outcomes and growth measures at birth: a meta-analysis of randomized controlled trials. Br. J. Nutr. 2007 Aug;98(2):253–9.

Hsu KT, Storch J. Fatty acid transfer from liver and intestinal fatty acid-binding proteins to membranes occurs by different mechanisms. J Biol Chem. 1996 Jun 7;271(23):13317–23.

Huang H, Starodub O, McIntosh A, Kier AB, Schroeder F. Liver fatty acid-binding protein targets fatty acids to the nucleus. Real time confocal and multiphoton fluorescence imaging in living cells. J Biol Chem. 2002 Aug 9;277(32):29139–51.

Ibrahimi A, Sfeir Z, Magharaie H, Amri EZ, Grimaldi P, Abumrad NA. Expression of the CD36 homolog (FAT) in fibroblast cells: effects on fatty acid transport. Proc Natl Acad Sci USA. 1996 Apr 2;93(7):2646–51. PMCID: PMC39684

Illsley NP. Glucose transporters in the human placenta. Placenta. Elsevier; 2000 Jan;21(1):14–22.

Illsley NP, Caniggia I, Zamudio S. Placental metabolic reprogramming: do changes in the mix of energy-generating substrates modulate fetal growth? Int. J. Dev. Biol. 2010;54(2-3):409–19.

Innis SM. Essential fatty acid transfer and fetal development. Placenta. 2005 Apr;26 Suppl A:S70–5.

Innis SM. Dietary (n-3) fatty acids and brain development. J. Nutr. 2007;137:855–859PB–.

Islinger M, Cardoso MJR, Schrader M. Be different--the diversity of peroxisomes in the animal kingdom. Biochim Biophys Acta. 2010 Aug;1803(8):881–97.

James JL, Stone PR, Chamley LW. Cytotrophoblast differentiation in the first trimester of pregnancy: evidence for separate progenitors of extravillous trophoblasts and syncytiotrophoblast. Reproduction. 2005 Jul;130(1):95–103.

Jansson N, Pettersson J, Haafiz A, Ericsson A, Palmberg I, Tranberg M, et al. Down-regulation of placental transport of amino acids precedes the development of intrauterine growth restriction in rats fed a low protein diet. J. Physiol. (Lond.). 2006a Nov 1;576(Pt 3):935–46. PMCID: PMC1892642

Jansson T. Amino acid transporters in the human placenta. Pediatr. Res. Nature

Publishing Group; 2001 Feb;49(2):141–7.

Jansson T, Cetin I, Powell TL, Desoye G, Radaelli T, Ericsson A, et al. Placental transport and metabolism in fetal overgrowth -- a workshop report. Placenta. 2006b. p. S109–13.

Jansson T, Wennergren M, Illsley NP. Glucose transporter protein expression in human placenta throughout gestation and in intrauterine growth retardation. Journal of Clinical Endocrinology & Metabolism. 1993 Dec;77(6):1554–62.

Jansson T, Ylvén K, Wennergren M, Powell TL. Glucose transport and system A activity in syncytiotrophoblast microvillous and basal plasma membranes in intrauterine growth restriction. Placenta. Elsevier; 2002 May;23(5):392–9.

Jiang P, Du W, Mancuso A, Wellen KE, Yang X. Reciprocal regulation of p53 and malic enzymes modulates metabolism and senescence. Nature. Nature Research; 2013 Jan 31;493(7434):689–93. PMCID: PMC3561500

Johansen M, Redman CW, Wilkins T, Sargent IL. Trophoblast deportation in human pregnancy--its relevance for pre-eclampsia. Placenta. Elsevier; 1999 Sep;20(7):531–9.

Johnstone ED, Sibley CP, Lowen B, Guilbert LJ. Epidermal growth factor stimulation of trophoblast differentiation requires MAPK11/14 (p38 MAP kinase) activation. Biology of Reproduction. Society for the Study of Reproduction; 2005 Dec;73(6):1282–8.

Jones CJP, Harris LK, Whittingham J, Aplin JD, Mayhew TM. A re-appraisal of the morphophenotype and basal lamina coverage of cytotrophoblasts in human term placenta. Placenta. 2008 Feb;29(2):215–9.

Kaemmerer E, Peuscher A, Reinartz A, Liedtke C, Weiskirchen R, Kopitz J, et al. Human intestinal acyl-CoA synthetase 5 is sensitive to the inhibitor triacsin C. World J. Gastroenterol. 2011 Nov 28;17(44):4883–9. PMCID: PMC3235631

Karmen A, Whyte M, Goodman DS. Fatty Acid Esterification and Chylomicron Formation during Fat Absorption. J. Lipid Res. 1963 Jul;4:312–21.

Kassan A, Herms A, Fernández-Vidal A, Bosch M, Schieber NL, Reddy BJN, et al. Acyl-CoA synthetase 3 promotes lipid droplet biogenesis in ER microdomains. J Cell Biol. Rockefeller Univ Press; 2013 Dec 23;203(6):985–1001. PMCID: PMC3871434

Kay HH, Zhu S, Tsoi S. Hypoxia and lactate production in trophoblast cells. Placenta. Elsevier; 2007 Aug;28(8-9):854–60.

Kelley LK, Smith CH, King BF. Isolation and partial characterization of the basal cell membrane of human placental trophoblast. Biochim Biophys Acta. 1983

Sep 21;734(1):91–8.

Kim JH, Lewin TM, Coleman RA. Expression and characterization of recombinant rat Acyl-CoA synthetases 1, 4, and 5. Selective inhibition by triacsin C and thiazolidinediones. Journal of Biological Chemistry. American Society for Biochemistry and Molecular Biology; 2001 Jul 6;276(27):24667–73.

Kliman HJ, Nestler JE, Sermasi E, Sanger JM, Strauss JF. Purification, characterization, and in vitro differentiation of cytotrophoblasts from human term placentae. Endocrinology. The Endocrine Society; 1986 Apr;118(4):1567–82.

Klingler M, Demmelmair H, Larque E, Koletzko B. Analysis of FA contents in individual lipid fractions from human placental tissue. Lipids. 2003 May;38(5):561–6.

Kolahi K, Louey S, Varlamov O, Thornburg K. Real-Time Tracking of BODIPY-C12 Long-Chain Fatty Acid in Human Term Placenta Reveals Unique Lipid Dynamics in Cytotrophoblast Cells. PLoS ONE. 2016;11(4):e0153522. PMCID: PMC4849650

Krammer J, Digel M, Ehehalt F, Stremmel W, Füllekrug J, Ehehalt R. Overexpression of CD36 and acyl-CoA synthetases FATP2, FATP4 and ACSL1 increases fatty acid uptake in human hepatoma cells. Int J Med Sci. Ivyspring International Publisher; 2011;8(7):599–614. PMCID: PMC3198256

Kudo Y, Boyd CA. Characterization of amino acid transport systems in human placental basal membrane vesicles. Biochim Biophys Acta. 1990 Jan 29;1021(2):169–74.

Kulkarni AV, Mehendale SS, Yadav HR, Joshi SR. Reduced placental docosahexaenoic acid levels associated with increased levels of sFlt-1 in preeclampsia. Prostaglandins Leukot. Essent. Fatty Acids. 2011 Jan;84(1-2):51–5.

Kuruvilla AG, D'Souza SW, Glazier JD, Mahendran D, Maresh MJ, Sibley CP. Altered activity of the system A amino acid transporter in microvillous membrane vesicles from placentas of macrosomic babies born to diabetic women. J. Clin. Invest. American Society for Clinical Investigation; 1994 Aug;94(2):689–95. PMCID: PMC296147

Lafond J, Moukdar F, Rioux A, Ech-Chadli H, Brissette L, Robidoux J, et al. Implication of ATP and sodium in arachidonic acid incorporation by placental syncytiotrophoblast brush border and basal plasma membranes in the human. Placenta. 2000 Sep;21(7):661–9.

Lager S, Powell TL. Regulation of Nutrient Transport across the Placenta. Journal of Pregnancy. Hindawi Publishing Corporation; 2012 Dec

10;2012(7153):1–14. PMCID: PMC3523549

Lager S, Ramirez VI, Gaccioli F, Jang B, Jansson T, Powell TL. Protein expression of fatty acid transporter 2 is polarized to the trophoblast basal plasma membrane and increased in placentas from overweight/obese women. Placenta. Elsevier; 2016 Apr;40:60–6. PMCID: PMC4809740

Langbein M, Strick R, Strissel PL, Vogt N, Parsch H, Beckmann MW, et al. Impaired cytotrophoblast cell-cell fusion is associated with reduced Syncytin and increased apoptosis in patients with placental dysfunction. Mol. Reprod. Dev. Wiley Subscription Services, Inc., A Wiley Company; 2008 Jan;75(1):175–83.

Lapillonne A, Jensen CL. Reevaluation of the DHA requirement for the premature infant. Prostaglandins Leukot. Essent. Fatty Acids. 2009 Aug;81(2-3):143–50.

Larqué E, Demmelmair H, Berger B, Hasbargen U, Koletzko B. In vivo investigation of the placental transfer of (13)C-labeled fatty acids in humans. J. Lipid Res. 2003 Jan;44(1):49–55.

Laviola L, Perrini S, Belsanti G, Natalicchio A, Montrone C, Leonardini A, et al. Intrauterine growth restriction in humans is associated with abnormalities in placental insulin-like growth factor signaling. Endocrinology. Endocrine Society; 2005 Mar;146(3):1498–505.

Lemons JA, Adcock EW, Jones MD, Naughton MA, Meschia G, Battaglia FC. Umbilical uptake of amino acids in the unstressed fetal lamb. J. Clin. Invest. American Society for Clinical Investigation; 1976 Dec;58(6):1428–34. PMCID: PMC333314

Levy E, Beaulieu JF, Delvin E, Seidman E, Yotov W, Basque JR, et al. Human crypt intestinal epithelial cells are capable of lipid production, apolipoprotein synthesis, and lipoprotein assembly. J. Lipid Res. 2000 Jan;41(1):12–22.

Lewis RM, Brooks S, Crocker IP, Glazier J, Hanson MA, Johnstone ED, et al. Review: Modelling placental amino acid transfer--from transporters to placental function. Placenta. Elsevier; 2013 Mar;34 Suppl:S46–51.

Lewis RM, Hanson MA, Burdge GC. Umbilical venous-arterial plasma composition differences suggest differential incorporation of fatty acids in NEFA and cholesteryl ester pools. Br. J. Nutr. Cambridge University Press; 2011 Aug;106(4):463–7.

Lindegaard MLS, Olivecrona G, Christoffersen C, Kratky D, Hannibal J, Petersen BL, et al. Endothelial and lipoprotein lipases in human and mouse placenta. J. Lipid Res. American Society for Biochemistry and Molecular Biology; 2005 Nov;46(11):2339–46.

Listenberger LL, Han X, Lewis SE, Cases S, Farese RV, Ory DS, et al. Triglyceride accumulation protects against fatty acid-induced lipotoxicity. Proc Natl Acad Sci USA. 2003 Mar 18;100(6):3077–82. PMCID: PMC152249

Longtine MS, Nelson DM. Placental dysfunction and fetal programming: the importance of placental size, shape, histopathology, and molecular composition. Semin. Reprod. Med. © Thieme Medical Publishers; 2011 May;29(3):187–96. PMCID: PMC3682832

Lurie S, Feinstein M, Mamet Y. Human fetal-placental weight ratio in normal singleton near-term pregnancies. Gynecol. Obstet. Invest. 1999;48(3):155–7.

Madsen EM, Lindegaard MLS, Andersen CB, Damm P, Nielsen LB. Human placenta secretes apolipoprotein B-100-containing lipoproteins. J Biol Chem. 2004 Dec 31;279(53):55271–6.

Magnusson AL, Waterman IJ, Wennergren M, Jansson T, Powell TL. Triglyceride hydrolase activities and expression of fatty acid binding proteins in the human placenta in pregnancies complicated by intrauterine growth restriction and diabetes. Journal of Clinical Endocrinology & Metabolism. 2004 Sep;89(9):4607–14.

Mahendran D, Byrne S, Donnai P, D'Souza SW, Glazier JD, Jones CJ, et al. Na+ transport, H+ concentration gradient dissipation, and system A amino acid transporter activity in purified microvillous plasma membrane isolated from first-trimester human placenta: comparison with the term microvillous membrane. Am. J. Obstet. Gynecol. 1994 Dec;171(6):1534–40.

Martinez M. Tissue levels of polyunsaturated fatty acids during early human development. J. Pediatr. 1992 Apr;120(4 Pt 2):S129–38.

Mashek DG, Li LO, Coleman RA. Long-chain acyl-CoA synthetases and fatty acid channeling. Future Lipidol. Future Medicine Ltd London, UK; 2007 Aug;2(4):465–76. PMCID: PMC2846691

Mayhew TM. Turnover of human villous trophoblast in normal pregnancy: what do we know and what do we need to know? Placenta. Elsevier; 2014 Apr;35(4):229–40.

McGowan JE, Aldoretta PW, Hay WW. Contribution of fructose and lactate produced in placenta to calculation of fetal glucose oxidation rate. Am J Physiol. 1995 Nov;269(5 Pt 1):E834–9.

Melton EM, Cerny RL, DiRusso CC, Black PN. Overexpression of human fatty acid transport protein 2/very long chain acyl-CoA synthetase 1 (FATP2/Acsvl1) reveals distinct patterns of trafficking of exogenous fatty acids. Biochemical and Biophysical Research Communications. 2013 Nov 1;440(4):743–8.

Melton EM, Cerny RL, Watkins PA, DiRusso CC, Black PN. Human fatty acid transport protein 2a/very long chain acyl-CoA synthetase 1 (FATP2a/Acsvl1) has a preference in mediating the channeling of exogenous n-3 fatty acids into phosphatidylinositol. J Biol Chem. American Society for Biochemistry and Molecular Biology; 2011 Sep 2;286(35):30670–9. PMCID: PMC3162428

Miller BF. Human muscle protein synthesis after physical activity and feeding. Exerc Sport Sci Rev. 2007 Apr;35(2):50–5.

Mishima T, Miner JH, Morizane M, Stahl A, Sadovsky Y. The expression and function of fatty acid transport protein-2 and -4 in the murine placenta. Wang H, editor. PLoS ONE. 2011;6(10):e25865. PMCID: PMC3197585

Montoudis A, Delvin E, Ménard D, Beaulieu J-F, Jean D, Tremblay E, et al. Intestinal-fatty acid binding protein and lipid transport in human intestinal epithelial cells. Biochemical and Biophysical Research Communications. 2006 Jan 6;339(1):248–54.

Mori M, Ishikawa G, Luo S-S, Mishima T, Goto T, Robinson JM, et al. The cytotrophoblast layer of human chorionic villi becomes thinner but maintains its structural integrity during gestation. Biology of Reproduction. Society for the Study of Reproduction; 2007 Jan;76(1):164–72.

Morrish DW, Bhardwaj D, Dabbagh LK, Marusyk H, Siy O. Epidermal growth factor induces differentiation and secretion of human chorionic gonadotropin and placental lactogen in normal human placenta. Journal of Clinical Endocrinology & Metabolism. The Endocrine Society; 1987 Dec;65(6):1282–90.

Morrish DW, Dakour J, Li H, Xiao J, Miller R, Sherburne R, et al. In vitro cultured human term cytotrophoblast: A model for normal primary epithelial cells demonstrating a spontaneous differentiation programme that requires EGF for extensive development of syncytium. Placenta. 1997 Sep;18(7):577–85.

Mudgett JS, Ding J, Guh-Siesel L, Chartrain NA, Yang L, Gopal S, et al. Essential role for p38alpha mitogen-activated protein kinase in placental angiogenesis. Proc Natl Acad Sci USA. National Acad Sciences; 2000 Sep 12;97(19):10454–9. PMCID: PMC27045

Muralimanoharan S, Maloyan A, Myatt L. Mitochondrial function and glucose metabolism in the placenta with gestational diabetes mellitus: role of miR-143. Clinical Science. Portland Press Limited; 2016 Jun 1;130(11):931–41.

Murphy EJ. L-FABP and I-FABP expression increase NBD-stearate uptake and cytoplasmic diffusion in L cells. Am J Physiol. 1998 Aug;275(2 Pt 1):G244–9.

Nagai A, Takebe K, Nio-Kobayashi J, Takahashi-Iwanaga H, Iwanaga T. Cellular expression of the monocarboxylate transporter (MCT) family in the placenta of

mice. Placenta. 2010 Feb;31(2):126–33.

Nagan N, Zoeller RA. Plasmalogens: biosynthesis and functions. Progress in Lipid Research. 2001 May;40(3):199–229.

Nelson DL, Lehninger AL, Cox MM. Lehninger principles of biochemistry. 2008.

O'Tierney PF, Lewis RM, McWeeney SK, Hanson MA, Inskip HM, Morgan TK, et al. Immune response gene profiles in the term placenta depend upon maternal muscle mass. Reprod Sci. SAGE Publications; 2012 Oct;19(10):1041–56. PMCID: PMC4052206

O'Tierney-Ginn P, Presley L, Minium J, Hauguel deMouzon S, Catalano PM. Sex-specific effects of maternal anthropometrics on body composition at birth. Am. J. Obstet. Gynecol. Elsevier; 2014 Sep;211(3):292.e1–9. PMCID: PMC4149857

Ockner RK, Manning JA. Fatty acid-binding protein in small intestine. Identification, isolation, and evidence for its role in cellular fatty acid transport. J. Clin. Invest. 1974 Aug;54(2):326–38. PMCID: PMC301560

Okamoto Y, Sakata M, Ogura K, Yamamoto T, Yamaguchi M, Tasaka K, et al. Expression and regulation of 4F2hc and hLAT1 in human trophoblasts. Am J Physiol, Cell Physiol. 2002 Jan;282(1):C196–204.

Ornoy A, Ratzon N, Greenbaum C, Wolf A, Dulitzky M. School-age children born to diabetic mothers and to mothers with gestational diabetes exhibit a high rate of inattention and fine and gross motor impairment. J. Pediatr. Endocrinol. Metab. 2001;14 Suppl 1:681–9.

Ortega-Senovilla H, Alvino G, Taricco E, Cetin I, Herrera E. Gestational diabetes mellitus upsets the proportion of fatty acids in umbilical arterial but not venous plasma. Diabetes Care. American Diabetes Association; 2009 Jan;32(1):120–2. PMCID: PMC2606843

Pagan A, Prieto-Sanchez MT, Blanco-Carnero JE, Gil-Sanchez A, Parrilla JJ, Demmelmair H, et al. Materno-fetal transfer of docosahexaenoic acid is impaired by gestational diabetes mellitus. AJP: Endocrinology and Metabolism. 2013 Oct 1;305(7):E826–33.

Panopoulos AD, Yanes O, Ruiz S, Kida YS, Diep D, Tautenhahn R, et al. The metabolome of induced pluripotent stem cells reveals metabolic changes occurring in somatic cell reprogramming. Cell Res. Nature Publishing Group; 2012 Jan;22(1):168–77. PMCID: PMC3252494

Patella F, Schug ZT, Persi E, Neilson LJ, Erami Z, Avanzato D, et al. Proteomics-based metabolic modeling reveals that fatty acid oxidation (FAO) controls endothelial cell (EC) permeability. Mol. Cell Proteomics. American Society for

Biochemistry and Molecular Biology; 2015 Mar;14(3):621–34. PMCID: PMC4349982

Perazzolo S, Hirschmugl B, Wadsack C, Desoye G, Lewis RM, Sengers BG. Computational modelling of fatty acid transport in the human placenta. Conf Proc IEEE Eng Med Biol Soc. IEEE; 2015 Aug;2015:8054–7.

Pfaffl MW. A new mathematical model for relative quantification in real-time RT-PCR. Nucleic Acids Res. Totowa, NJ: Oxford University Press; 2001 May 1;29(9):e45–87. PMCID: PMC55695

Pike Winer LS, Wu M. Rapid analysis of glycolytic and oxidative substrate flux of cancer cells in a microplate. Sobol RW, editor. PLoS ONE. Public Library of Science; 2014;9(10):e109916. PMCID: PMC4215881

Poidatz D, Santos Dos E, Gronier H, Vialard F, Maury B, De Mazancourt P, et al. Trophoblast syncytialisation necessitates mitochondrial function through estrogen-related receptor-gamma activation. Mol. Hum. Reprod. 2015 Feb;21(2):206–16.

Powell TL, Jansson T, Illsley NP, Wennergren M, Korotkova M, Strandvik B. Composition and permeability of syncytiotrophoblast plasma membranes in pregnancies complicated by intrauterine growth restriction. Biochim Biophys Acta. 1999 Aug 20;1420(1-2):86–94.

Radaelli T, Lepercq J, Varastehpour A, Basu S, Catalano PM, Hauguel-De Mouzon S. Differential regulation of genes for fetoplacental lipid pathways in pregnancy with gestational and type 1 diabetes mellitus. Am. J. Obstet. Gynecol. 2009 Aug;201(2):209.e1–209.e10. PMCID: PMC3613858

Rambold AS, Cohen S, Lippincott-Schwartz J. Fatty acid trafficking in starved cells: regulation by lipid droplet lipolysis, autophagy, and mitochondrial fusion dynamics. Dev Cell. 2015 Mar 23;32(6):678–92. PMCID: PMC4375018

Redgrave TG. Association of Golgi membranes with lipid droplets (pre-chylomicrons) from within intestinal epithelial cells during absorption of fat. Aust J Exp Biol Med Sci. 1971 Apr;49(2):209–24.

Richards MR, Harp JD, Ory DS, Schaffer JE. Fatty acid transport protein 1 and long-chain acyl coenzyme A synthetase 1 interact in adipocytes. J. Lipid Res. American Society for Biochemistry and Molecular Biology; 2006 Mar;47(3):665–72.

Rizzo T, Metzger BE, Burns WJ, Burns K. Correlations between antepartum maternal metabolism and child intelligence. N. Engl. J. Med. 1991 Sep 26;325(13):911–6.

Roe CR, Sweetman L, Roe DS, David F, Brunengraber H. Treatment of

cardiomyopathy and rhabdomyolysis in long-chain fat oxidation disorders using an anaplerotic odd-chain triglyceride. J. Clin. Invest. American Society for Clinical Investigation; 2002 Jul;110(2):259–69. PMCID: PMC151060

Roels F, Verdonck V, Pauwels M, De Catte L, Lissens W, Liebaers I, et al. Light microscopic visualization of peroxisomes and plasmalogens in first trimester chorionic villi. Prenat. Diagn. 1987 Sep;7(7):525–30.

Roos S, Jansson N, Palmberg I, Säljö K, Powell TL, Jansson T. Mammalian target of rapamycin in the human placenta regulates leucine transport and is down-regulated in restricted fetal growth. J. Physiol. (Lond.). 2007 Jul 1;582(Pt 1):449–59. PMCID: PMC2075295

Roseboom TJ, van der Meulen JH, Ravelli AC, Osmond C, Barker DJ, Bleker OP. Effects of prenatal exposure to the Dutch famine on adult disease in later life: an overview. Molecular and Cellular Endocrinology. 2001 Dec 20;185(1-2):93–8.

Rossant J, Cross JC. Placental development: lessons from mouse mutants. Nat. Rev. Genet. 2001 Jul;2(7):538–48.

Rybakowski C, Mohar B, Wohlers S, Leichtweiss HP, Schröder H. The transport of vitamin C in the isolated human near-term placenta. Eur. J. Obstet. Gynecol. Reprod. Biol. 1995 Sep;62(1):107–14.

Sandoval A, Chokshi A, Jesch ED, Black PN, DiRusso CC. Identification and characterization of small compound inhibitors of human FATP2. Biochem. Pharmacol. 2010 Apr 1;79(7):990–9. PMCID: PMC2814954

Schaefer-Graf UM, Graf K, Kulbacka I, Kjos SL, Dudenhausen J, Vetter K, et al. Maternal lipids as strong determinants of fetal environment and growth in pregnancies with gestational diabetes mellitus. Diabetes Care. 2008 Sep;31(9):1858–63. PMCID: PMC2518359

Schaiff WT, Bildirici I, Cheong M, Chern PL, Nelson DM, Sadovsky Y. Peroxisome proliferator-activated receptor-gamma and retinoid X receptor signaling regulate fatty acid uptake by primary human placental trophoblasts. Journal of Clinical Endocrinology & Metabolism. 2005 Jul;90(7):4267–75.

Schindelin J, Arganda-Carreras I, Frise E, Kaynig V, Longair M, Pietzsch T, et al. Fiji: an open-source platform for biological-image analysis. Nat. Methods. 2012 Jul 1;9(7):676–82. PMCID: PMC3855844

Schneider H. Placental oxygen consumption. Part II: in vitro studies--a review. Placenta. 2000 Mar;21 Suppl A:S38–44.

Schneider H, Malek A, Duft R, Bersinger N. Evaluation of an In Vitro Dual Perfusion System for the Study of Placental Proteins: Energy Metabolism.

Placenta as a Model and a Source. Boston, MA: Springer US; 1989. p. 39–50.

Schwenk RW, Holloway GP, Luiken JJFP, Bonen A, Glatz JFC. Fatty acid transport across the cell membrane: regulation by fatty acid transporters. Prostaglandins Leukot. Essent. Fatty Acids. Elsevier; 2010 Apr;82(4-6):149–54.

Scifres CM, Chen B, Nelson DM, Sadovsky Y. Fatty acid binding protein 4 regulates intracellular lipid accumulation in human trophoblasts. J. Clin. Endocrinol. Metab. 2011 Jul;96(7):E1083–91. PMCID: PMC3135200

Sciullo E, Cardellini G, Baroni MG, Torresi P, Buongiorno A, Pozzilli P, et al. Glucose transporter (Glut1, Glut3) mRNA in human placenta of diabetic and non-diabetic pregnancies. Early Pregnancy. 1997 Sep;3(3):172–82.

Settle P, Sibley CP, Doughty IM, Johnston T, Glazier JD, Powell TL, et al. Placental lactate transporter activity and expression in intrauterine growth restriction. J. Soc. Gynecol. Investig. SAGE Publications; 2006 Jul;13(5):357–63.

Sibley CP, Brownbill P, Dilworth M, Glazier JD. Review: Adaptation in placental nutrient supply to meet fetal growth demand: implications for programming. Placenta. 2010 Mar;31 Suppl:S70–4.

Simán CM, Sibley CP, Jones CJ, Turner MA, Greenwood SL. The functional regeneration of syncytiotrophoblast in cultured explants of term placenta. Am. J. Physiol. Regul. Integr. Comp. Physiol. 2001 Apr;280(4):R1116–22.

Simpson RA, Mayhew TM, Barnes PR. From 13 weeks to term, the trophoblast of human placenta grows by the continuous recruitment of new proliferative units: a study of nuclear number using the disector. Placenta. 1992 Sep;13(5):501–12.

Sivasubramaniyam T, Garcia J, Tagliaferro A, Melland-Smith M, Chauvin S, Post M, et al. Where polarity meets fusion: role of Par6 in trophoblast differentiation during placental development and preeclampsia. Endocrinology. Endocrine Society Chevy Chase, MD; 2013 Mar;154(3):1296–309.

Smith CH, Nelson DM, King BF, Donohue TM, Ruzycki S, Kelley LK. Characterization of a microvillous membrane preparation from human placental syncytiotrophoblast: a morphologic, biochemical, and physiologic, study. Am. J. Obstet. Gynecol. 1977 May 15;128(2):190–6.

Sooranna SR, Oteng-Ntim E, Meah R, Ryder TA, Bajoria R. Characterization of human placental explants: morphological, biochemical and physiological studies using first and third trimester placenta. Hum Reprod. 1999 Feb 1;14(2):536–41.

Sparks JW, Girard JR, Battaglia FC. An estimate of the caloric requirements of the human fetus. Biol. Neonate. 1980;38(3-4):113–9.

Sparks JW, Hay WW, Bonds D, Meschia G, Battaglia FC. Simultaneous measurements of lactate turnover rate and umbilical lactate uptake in the fetal lamb. J. Clin. Invest. American Society for Clinical Investigation; 1982 Jul;70(1):179–92. PMCID: PMC370240

Sparks JW, Hay WWJ, Meschia G, Battaglia FC. Partition of maternal nutrients to the placenta and fetus in the sheep. Eur. J. Obstet. Gynecol. Reprod. Biol. 1983 Feb;14(5):331–40.

Stahl A, Gimeno RE, Tartaglia LA, Lodish HF. Fatty acid transport proteins: a current view of a growing family. Trends Endocrinol. Metab. 2001 Aug;12(6):266–73.

Stahl A, Hirsch DJ, Gimeno RE, Punreddy S, Ge P, Watson N, et al. Identification of the major intestinal fatty acid transport protein. Mol Cell. 1999 Sep;4(3):299–308.

Strain JJ, Davidson PW, Bonham MP, Duffy EM, Stokes-Riner A, Thurston SW, et al. Associations of maternal long-chain polyunsaturated fatty acids, methyl mercury, and infant development in the Seychelles Child Development Nutrition Study. Neurotoxicology. 2008 Sep;29(5):776–82. PMCID: PMC2574624

Szabo AJ, Grimaldi RD, De Lellis R. Triglyceride synthesis by the human placenta. II. The effect of cyanide and fluoride on the incorporation of labeled palmitate into placental triglycerides. Am. J. Obstet. Gynecol. 1973 Jan 15;115(2):263–6.

Szajewska H, Horvath A, Koletzko B. Effect of n-3 long-chain polyunsaturated fatty acid supplementation of women with low-risk pregnancies on pregnancy outcomes and growth measures at birth: a meta-analysis of randomized controlled trials. Am. J. Clin. Nutr. 2006 Jun;83(6):1337–44.

Szitanyi P, Koletzko B, Mydlilova A, Demmelmair H. Metabolism of 13C-labeled linoleic acid in newborn infants during the first week of life. Pediatr. Res. 1999 May;45(5 Pt 1):669–73.

Tan N-S, Shaw NS, Vinckenbosch N, Liu P, Yasmin R, Desvergne B, et al. Selective cooperation between fatty acid binding proteins and peroxisome proliferator-activated receptors in regulating transcription. Mol Cell Biol. 2002 Jul;22(14):5114–27. PMCID: PMC139777

Tannetta DS, Dragovic RA, Gardiner C, Redman CW, Sargent IL. Characterisation of syncytiotrophoblast vesicles in normal pregnancy and pre-eclampsia: expression of Flt-1 and endoglin. Wang Y-L, editor. PLoS ONE.

Public Library of Science; 2013;8(2):e56754. PMCID: PMC3577732

Thame M, Osmond C, Trotman H. Fetal growth and birth size is associated with maternal anthropometry and body composition. Matern Child Nutr. 2015 Oct;11(4):574–82.

Thomas B, Ghebremeskel K, Lowy C, Min Y, Crawford MA. Plasma AA and DHA levels are not compromised in newly diagnosed gestational diabetic women. Eur J Clin Nutr. 2004 Nov;58(11):1492–7.

Thomas CR, Evans JL, Buttriss C, Lowy C. Lipid chain length alterations during placental transfer in the guinea pig. J. Dev. Physiol. 1985 Oct;7(5):305–11.

Thornburg KL, Binder ND, Faber JJ. Diffusion permeability and ultrafiltration-reflection-coefficients of Narand Cl- in the near-term placenta of the sheep. J. Dev. Physiol. 1979 Feb;1(1):47–60.

Thornburg KL, Faber JJ. The steady state concentration gradients of an electron-dense marker (ferritin in the three-layered hemochorial placenta of the rabbit. J. Clin. Invest. American Society for Clinical Investigation; 1976 Oct;58(4):912–25. PMCID: PMC333254

Thornburg KL, Marshall N. The placenta is the center of the chronic disease universe. Am. J. Obstet. Gynecol. Elsevier; 2015 Oct;213(4 Suppl):S14–20. PMCID: PMC4593619

Tobin KAR, Johnsen GM, Staff AC, Duttaroy AK. Long-chain polyunsaturated fatty acid transport across human placental choriocarcinoma (BeWo) cells. Placenta. Elsevier; 2009 Jan;30(1):41–7.

Ulijaszek SJ. Comparative energetics of primate fetal growth. American Journal of Human Biology. Wiley Subscription Services, Inc., A Wiley Company; 2002 Sep 1;14(5):603–8.

Van Horn CG, Caviglia JM, Li LO, Wang S, Granger DA, Coleman RA. Characterization of recombinant long-chain rat acyl-CoA synthetase isoforms 3 and 6: identification of a novel variant of isoform 6. Biochemistry. 2005 Feb 8;44(5):1635–42.

Vander Heiden MG, Cantley LC, Thompson CB. Understanding the Warburg effect: the metabolic requirements of cell proliferation. Science. American Association for the Advancement of Science; 2009 May 22;324(5930):1029–33. PMCID: PMC2849637

Varlamov O, Chu MP, McGee WK, Cameron JL, O'Rourke RW, Meyer KA, et al. Ovarian cycle-specific regulation of adipose tissue lipid storage by testosterone in female nonhuman primates. Endocrinology. 2013 Nov;154(11):4126–35. PMCID: PMC3800767

Veerkamp JH, Paulussen RJA, Peeters RA, Maatman RGHJ, Moerkerk HTB, Kuppevelt THMSM. Detection, tissue distribution and (sub)cellular localization of fatty acid-binding protein types. Mol Cell Biochem. 1990;98(1-2).

Verrey F. System L: heteromeric exchangers of large, neutral amino acids involved in directional transport. Pflugers Arch. 2003 Feb;445(5):529–33.

W Hay W, Meznarich HK. Effect of Maternal Glucose Concentration on Uteroplacental Glucose Consumption and Transfer in Pregnant Sheep. Experimental Biology and Medicine. 1989 Jan 1;190(1):63–9.

Wang H, Wei E, Quiroga AD, Sun X, Touret N, Lehner R. Altered lipid droplet dynamics in hepatocytes lacking triacylglycerol hydrolase expression. Mol Biol Cell. American Society for Cell Biology; 2010 Jun 15;21(12):1991–2000. PMCID: PMC2883943

Wasilewski M, Semenzato M, Rafelski SM, Robbins J, Bakardjiev AI, Scorrano L. Optic atrophy 1-dependent mitochondrial remodeling controls steroidogenesis in trophoblasts. Curr Biol. Elsevier; 2012 Jul 10;22(13):1228–34. PMCID: PMC3396839

Waterman IJ, Emmison N, Dutta-Roy AK. Characterisation of triacylglycerol hydrolase activities in human placenta. Biochim Biophys Acta. 1998 Nov 2;1394(2-3):169–76.

Webster RP, Brockman D, Myatt L. Nitration of p38 MAPK in the placenta: association of nitration with reduced catalytic activity of p38 MAPK in pre-eclampsia. Mol. Hum. Reprod. Oxford University Press; 2006 Nov;12(11):677–85.

Weedon-Fekjaer MS, Dalen KT, Solaas K, Staff AC, Duttaroy AK, Nebb HI. Activation of LXR increases acyl-CoA synthetase activity through direct regulation of ACSL3 in human placental trophoblast cells. J. Lipid Res. American Society for Biochemistry and Molecular Biology; 2010 Jul;51(7):1886–96. PMCID: PMC2882745

Weisinger HS, Armitage JA, Sinclair AJ, Vingrys AJ, Burns PL, Weisinger RS. Perinatal omega-3 fatty acid deficiency affects blood pressure later in life. Nat. Med. 2001 Mar;7(3):258–9.

Wendel AA, Lewin TM, Coleman RA. Glycerol-3-phosphate acyltransferases: rate limiting enzymes of triacylglycerol biosynthesis. Biochim Biophys Acta. 2009 Jun;1791(6):501–6. PMCID: PMC2737689

Widdowson EM. Chemical composition of newly born mammals. Nature. 1950 Oct 14;166(4224):626–8.

Wijendran V, Bendel RB, Couch SC, Philipson EH, Cheruku S, Lammi-Keefe CJ.

Fetal erythrocyte phospholipid polyunsaturated fatty acids are altered in pregnancy complicated with gestational diabetes mellitus. Lipids. 2000 Aug;35(8):927–31.

Wijendran V, Bendel RB, Couch SC, Philipson EH, Thomsen K, Zhang X, et al. Maternal plasma phospholipid polyunsaturated fatty acids in pregnancy with and without gestational diabetes mellitus: relations with maternal factors. Am. J. Clin. Nutr. 1999 Jul;70(1):53–61.

Winn VD, Haimov-Kochman R, Paquet AC, Yang YJ, Madhusudhan MS, Gormley M, et al. Gene Expression Profiling of the Human Maternal-Fetal Interface Reveals Dramatic Changes between Midgestation and Term. Endocrinology. 2007 Mar;148(3):1059–79.

Wise EM, Ball EG. Malic Enzyme and Lipogenesis. Proc Natl Acad Sci USA. National Academy of Sciences; 1964 Nov;52(5):1255–63. PMCID: PMC300433

Wu X, Xie C, Zhang Y, Fan Z, Yin Y, Blachier F. Glutamate-glutamine cycle and exchange in the placenta-fetus unit during late pregnancy. Amino Acids. 2015 Jan;47(1):45–53.

Yang Z-Z, Tschopp O, Hemmings-Mieszczak M, Feng J, Brodbeck D, Perentes E, et al. Protein kinase B alpha/Akt1 regulates placental development and fetal growth. Journal of Biological Chemistry. American Society for Biochemistry and Molecular Biology; 2003 Aug 22;278(34):32124–31.

Ye J, Coulouris G, Zaretskaya I, Cutcutache I, Rozen S, Madden TL. Primer-BLAST: a tool to design target-specific primers for polymerase chain reaction. BMC Bioinformatics. BioMed Central Ltd; 2012;13(1):134. PMCID: PMC3412702

Yoshida Y. GLYCOGEN FORMATION IN THE CYTOTROPHOBLAST OF HUMAN PLACENTA IN EARLY PREGNANCY, AS REVEALED BY ELECTRON MICROSCOPY. Experimental Cell Research. 1964 Apr;34:293–304.

Zhu J, Lee B, Buhman KK, Cheng J-X. A dynamic, cytoplasmic triacylglycerol pool in enterocytes revealed by ex vivo and in vivo coherent anti-Stokes Raman scattering imaging. J. Lipid Res. 2009 Jun;50(6):1080–9. PMCID: PMC2681390

Biographical Sketch

OMB No. 0925-0001 and 0925-0002 (Rev. 10/15 Approved Through 10/31/2018)

BIOGRAPHICAL SKETCH

NAME: Kevin Sohail Kolahi

eRA COMMONS USER NAME (credential, e.g., agency login): kolahik

POSITION TITLE: MD/PhD Student, 3rd year PhD

EDUCATION/TRAINING *(Begin with baccalaureate or other initial professional education, such as nursing, include postdoctoral training and residency training if applicable. Add/delete rows as necessary.)*

INSTITUTION AND LOCATION	DEGREE *(if applicable)*	Completion Date MM/YYYY	FIELD OF S
University of California, Berkeley	BA	05/2007	Molecular and Biology
University of California, Berkeley / San Francisco	MS	05/2009	Bioengineering
Oregon Health and Science University	MD/PhD	06/2018	Biomedical Engineering/M
Oregon Health and Science University	certificate	06/2016	Human Investig

A. Personal Statement

My primary area of interest is fetoplacental development. I am fascinated by the highly coordinated processes that must occur to ensure fetal survival and a successful transition to *ex utero* life. More recently, I have come to appreciate the broad capacity and plasticity of these processes, and the diverse mechanisms employed, in particular by the placenta, to ensure this success.

While my interest in physics and science was originally piqued in elementary school, I began formal biochemical research as an undergraduate student at UC Berkeley. While studying signal transduction, I serendipitously learned about the concept of mechanotransduction and was immediately intrigued as to how mechanical forces could be translated into a biochemical language. For my Masters thesis (UC Berkley, Dept Bioengineering), I investigated the actin-binding protein, filamin, and expanded my studies from single cell cytoskeletal mechanics to ask how tissues behaved mechanically during development in *Drosophila* oocytes. I quickly became enamored with the dynamic nature of developmental biology and the physical processes that influence it, yet it also became clear that the interplay between these fields was understudied. At this same time, as a graduate school instructor (UCSF, Dept Anatomy) I learned about the negative effects of poor nutrition on embryos fertilized and cultured *in vitro*. I integrated what I had learned in all aspects of my training to ask if mechanotransduction was medically relevant to *in vitro* fertilized and cultured mouse embryos. This is when I was first introduced to fetoplacental development, and culminated into my most recent research project.

The idea of developmental origins of adult disease, has gained

momentum in the past 20 years. That many chronic adult diseases (cardiovascular disease, type 2 diabetes, certain cancers) have their origins in utero marries my interests in fetoplacental development, and clinical medicine. I was excited to learn that responses and sometimes subtle adaptations made by the fetus and placenta in response to stressors can have lifelong consequences for health not only because it extends our understanding the limits of the biological system, but also because it demonstrates how these systems are balanced during normal development. The Thornburg laboratory has a long track record of fetal and placental physiology and has expertise in techniques ranging from whole animal preparations to *ex vivo* and *in vitro* preparations, right down to the molecular level. Together with a reputation for being collaborative and stimulating for new ideas, in particular for junior scientists, the environment of the Thornburg laboratory is ideal for my research training. The interdisciplinary investigations pursued in the Thornburg lab will provide me with a more thorough understanding of placental function. This will enable me to propose new scientific insights that may be used to devise approaches to improve the outcomes of babies born with placental dysfunction.

B. Positions and Honors

Professional & Research Experience

ACTIVITY/OCCUPATION	BEGINNING DATE	ENDING DATE	FIELD	INSTITUTION/COMPANY	SUPERVISOR/ EMPLOYER
Research Associate	06/2010	06/2011	Reproductive Science	University of California, San Francisco	Paolo F. Rinaudo M.D./ Ph.D.
Volunteer	10/2009	04/2010	Bioengineering/ Oncology	Lawrence Berkeley National Laboratory	Mina J. Bissell Ph.D.
Graduate Student	05/2007	10/2009	Bioengineering	University of California, Berkeley	Mohammad R.K. Mofrad Ph.D.
Undergraduate	05/2003	05/2007	Bioengineering	University of California, Berkeley	Mohammad R.K. Mofrad Ph.D.

Academic and Professional Honors

2004	Deans Honor List (University of California, Berkeley [UCB])
2007	Deans Honor List (UCB)
2007	High Honors (UCB)
2007	Outstanding Graduate Student Instructor (UCB)
2011	Golden Humanism Honor Award, Medical School (Oregon Health & Science University [OHSU])
2014	Charles Patrick Memorial Scholarship, Department of Biomedical Engineering (OHSU)
2014	N. L. Tartar Trust Fellowship Award, (Project support, OHSU)
2014	NIH-Ruth L. Kirchstein National Research Service Award Individual Fellowship (F30; MD/PhD)
2015	NIH New Investigator Travel Award (International Federation of Placenta Associations)
2016	Leadership in Student Service / Excellence in Journalism Awards (OHSU)

Memberships in Professional Societies
2011-present American Physician Scientists Association

C. Contribution to Science

Placental Fatty Acid Transport and Metabolism

I employed state of the art microscopy to track subcellular trafficking of fluorescently labeled fatty acids in the human placenta. I pioneered these methods to investigate placental fatty acid metabolism and transport in real time in living tissue and cells. The human placenta has a selective system to acquire long chain fatty acids but the mechanism is unknown. These studies led to the discovery that the cells that were driving placental long chain fatty acid uptake and metabolism were a cell type that was presumed to play little role, if any, in placental nutrient processes. In subsequent experiments we found that these cells, a progenitor cell type called the cytotrophoblast, were the metabolic power houses of the placenta and displayed an unparalleled level of mitochondrial and glycolytic function. A relatively high level of metabolic genes are expressed in cytotrophoblast. These works culminated into my PhD thesis where I concluded the cytotrophoblast drives fatty acid uptake and metabolic activity in the human term placenta.

- **Kolahi K,** Louey S, Varlamov O, Thornburg K. (2016). Real-Time Tracking of BODIPY-C12 Long-Chain Fatty Acid in Human Term Placenta Reveals Unique Lipid Dynamics in Cytotrophoblast Cells. PLoS One, 11(4):e0153522. PMCID: PMC4849650

Mechanotransduction in Acting-binding proteins.

I investigated how cells can translate forces into biochemical signals. One interesting phenomenon of the actin-cytoskeleton is that it will stiffen to resist forces imparted on the cell. Since this phenomenon implicated regulation through actin-binding proteins, I looked for an explanation in how actin-binding proteins conformations changed during mechanical loading. To investigate this phenomenon, I focused on the actin-binding protein family, the Filamins. I employed molecular dynamics to simulate forces applied to the rod domain of Filamins' atomic structures. After my first publication, I mentored an undergraduate student and we probed more Filamin atomic structures. We found that during mechanical loading, conformational changes take place in the rod domain that expose filamin binding sites for kinases and integrins. We contributed equally to a second publication on a more comprehensive structural analysis of Filamin-A during loading. These observations provide one possible explanation for how the actin cytoskeletal network can be stiffened during mechanical loading and for how forces induce conformational changes in protein structure that can initiate intracellular biochemical cascades.

- **Kolahi KS**, Mofrad MRK. (2008). Molecular mechanics of filamin's rod domain. Biophysj, 94(3), 1075–83. PMCID: PMC2186249
- Chen HS, **Kolahi KS**, Mofrad MRK. (2009). Phosphorylation facilitates the integrin binding of filamin under force. Biophysj, 97(12), 3095–104. PMCID: PMC2793350

Biophysics of Epithelial Morphogenesis.

During my morphometric analysis of fruit fly oogenesis using custom Matlab image processing software, I found that the biophysical explanations for the epithelial cuboidal to columnar or cuboidal to squamous transitions were physically inconsistent. It was clear the epithelial sheet covering the Drosophila oocyte was undergoing intense actin-myosin contraction during early stages of development, and this observation was used to explain how the cuboidal epithelial cells were growing in height to become columnar, but also for how a separate population of cuboidal cells were flattening during the concerted cuboidal to squamous transition. However, when I measured the epithelial cells I found they every cell was expanding, despite the intense actin-myosin contractility. This would imply that the net force in both cell populations is expansive and outward, again despite the inward forces generated by contractility. I hypothesized that this outward force was due to the tensile forces imparted by the 10,000-fold growth in volume experienced during these 18 hours of development. It is possible the cell contractility is necessary to resist excessive stretching during this time period. Some cells resisted more than others. Those that resisted poorly were stretched into a squamous cell; the columnar cells must therefore be due to a cell volume increase rather than directly due to contraction. Furthermore, I tested these mechanisms by generating mutants to show that disrupting contraction resulted in flattening of cells that were destined to be columnar. Surprisingly, our results supported a previous observation that after disrupting a columnar cell and forcing it to flatten and become squamous, the columnar cell begins to express squamous cell specific markers, indicating that cell shape and identity are intertwined.

- **Kolahi KS**, White PF, Shreter DM, Classen A-K, Bilder D, Mofrad MRK. (2009). Quantitative analysis of epithelial morphogenesis in Drosophila oogenesis: New insights based on morphometric analysis and mechanical modeling. Developmental Biology, 331(2), 129–39. PMCID: PMC3145632
- **Kolahi KS**, Mofrad MRK. (2010). Mechanotransduction: a major regulator of homeostasis and development. Wiley Interdiscip Rev Syst Biol Med, 2(6), 625–39. PMID: 20890961.

Pre-implantation Embryos Sense Mechanical Cues.

Embryonic stem cells are exquisitely sensitive to microenvironmental cues during differentiation. Embryos cultured and manipulated for assisted reproduction are permanently influenced by their short term *in vitro* exposure. Since the *in vitro* culture environment is over 1 million times stiffer than the uterine environment in which the embryos normally grow, I wondered if the increased mechanical stresses could negatively effect early embryo development. I found that the developing embryo would less likely growth-arrest on softer environments that more closely recapitulated the uterus. I invented a soft embryo culture chamber that mimicked the stiffness and biochemical cues of the uterus to improve early embryo development.

- **Kolahi KS**, Donjacour A, Liu X, Lin W, Simbulan RK, Bloise E, et al. (2012). Effect of substrate stiffness on early mouse embryo development. PLoS ONE, 7(7), e41717. PMCID: PMC3409240

- Bloise E, Lin W, Liu X, Simbulan R, **Kolahi KS**, Petraglia F, et al. (2012). Impaired placental nutrient transport in mice generated by in vitro fertilization. Endocrinology, 153(7), 3457–67. PMCID: PMC3380310

Complete List of Published Work in MyBibliography:
http://www.ncbi.nlm.nih.gov/sites/myncbi/kevin.kolahi.1/bibliography/47515692/public/?sort=date&direction=ascending

D. Scholastic Performance

YEAR	COURSE TITLE	GRADE	YEAR	COURSE TITLE	GRADE
	Undergraduate Courses – UCB		2006	Physiology	A
2003	Geography and Physical Sciences	A	2006	Biochemistry/Lab	A+
2003	Integrative Biology	A-	2006	Microbial Genetics/Genomics	A
2003	Reading and Composition 1A	B		**Graduate Courses – UCB/UCSF**	
2003	Calculus	B+	2007	Biomechanics/Lab	A+
2003	Physics: Kinematics/Lab	A+	2007	Aspects of Bioengineering	A
2003	Philosophy: Existential	B	2007	Cell Mechanics/Cytoskeleton	A-
2003	History: The United States	B-	2008	Orthopedic Biomechanics	B+
2004	General Chemistry/Lab	A		**Medical School Courses – OHSU**	
2004	World Regions and Anthropology	A+	2011	Gross Anatomy Imaging	H
2004	Physics: Electromagnetism/Lab	A	2012	Cell Structure & Function	H
2004	General Psychology	A	2012	Systems Processes/Homeostasis	H
2004	General Biology/Lab 1B	B+	2012	Biological Basis of Disease	H
2004	Organic Chemistry/Lab 3A	A+	2012	Principles of Clinical Medicine	NH
2005	Reading and Composition 1B	B	2012	Circulation	H
2004	Musicianship	A-	2013	Metabolism	H
2005	Organic Chemistry/Lab 3B	A+	2013	Neuroscience and Behavior	H
2005	General Biology/Lab 1A	A	2013	Human Growth and Development	H
2005	Human Anatomy	A	2013	Blood	H
2005	Statistics	A	2013	Principles of Clinical Medicine	NH
2005	Art: Drawing	A	2014	Transition to Clerkship	P
2005	Biophysical Chemistry	A	2014-	MD/PhD Longitudinal Clerkship	
2005	Human Nutrition	A		**Graduate School Courses – OHSU**	
2006	Geology: Climate Change	A	2014	The Practice of Ethics and Science	P
2006	Neuropharmacology	A-	2014	Biostatistics	A
2006	Biochemistry: Pathways	A+			

Undergraduate and Graduate Grading: A-F; Medical School Grading: Honors (H), Near-honors (NH), Satisfactory (S); Some courses graded Pass (P)/Fail (F)

Standardized Test Scores

US Medical Licensing Exam I (06/2013): **272** (passing 188)

E. Research Support.

Current Support

1F30HD084095-01 **(Kolahi, PI)**

05/19/15 – 05/18/19

NIH/NICHD

Title: Real-Time Assessment of Fatty Acid Transit in The Human Placental Syncytiotrophoblast

Goal: This project seeks to use live-imaging to track fatty acid movements across the human placenta, and define the mechanisms that drive the transport of different types of fats to the developing fetus.

Role: Principal Investigator